

การเตรียมโพลีเอทิลีนแบบแข็งโดยใช้สารประกอบเชิงซ้อนของโลหะผสมและเอทิลีนไดเอมีน
เป็นตัวเร่งปฏิกิริยา

นางสาวจริยาภรณ์ ป้อมสุข

วิทยานิพนธ์นี้เป็นส่วนหนึ่งของการศึกษาตามหลักสูตรปริญญาวิทยาศาสตรมหาบัณฑิต

สาขาวิชาเคมี ภาควิชาเคมี

คณะวิทยาศาสตร์ จุฬาลงกรณ์มหาวิทยาลัย

ปีการศึกษา 2553

ลิขสิทธิ์ของจุฬาลงกรณ์มหาวิทยาลัย

PREPARATION OF RIGID POLYURETHANE FOAM USING MIXED METAL
COMPLEXES AND ETHYLENEDIAMINE AS CATALYSTS

Miss Jariyaporn Pomsook

A Thesis Submitted in Partial Fulfillment of the Requirements
for the Degree of Master of Science Program in Chemistry

Department of Chemistry

Faculty of Science

Chulalongkorn University

Academic Year 2010

Copyright of Chulalongkorn University

Thesis Title PREPARATION OF RIGID POLYURETHANE FOAM
 USING MIXED METAL COMPLEXES AND
 ETHYLENEDIAMINE AS CATALYSTS
By Miss Jariyaporn Pomsook
Field of Study Chemistry
Thesis Advisor Associate Professor Nuanphun Chantarasiri, Ph. D.

Accepted by the Faculty of Science, Chulalongkorn University in
Partial Fulfillment of the Requirements for the Master's Degree

..... Dean of the Faculty of Science
(Professor Supot Hannongbua, Dr.rer.nat.)

THESIS COMMITTEE

..... Chairman
(Assistance Professor Preecha Lertpratchya, Ph. D.)

..... Thesis Advisor
(Associate Professor Nuanphun Chantarasiri, Ph. D.)

..... Examiner
(Professor Thawatchai Tuntulani, Ph. D.)

..... Examiner
(Associate Professor Polkit Sangvanich, Ph. D.)

..... External Examiner
(Duangruthai Sridaeng, Ph.D.)

จรรยาภรณ์ ป้อมสุข : การเตรียมโฟมพอลิยูรีเทนแบบแข็งโดยใช้สารประกอบเชิงซ้อนของโลหะผสมและเอทิลีนไดเอมีนเป็นตัวเร่งปฏิกิริยา. (PREPARATION OF RIGID POLYURETHANE FOAM USING MIXED METAL COMPLEXES AND ETHYLENEDIAMINE AS CATALYSTS) อาจารย์ที่ปรึกษาวิทยานิพนธ์หลัก: รศ.ดร. นवलพรรณ จันทร์ศิริ, 144 หน้า.

งานวิจัยนี้ได้พัฒนาตัวเร่งปฏิกิริยาสำหรับเตรียมโฟมพอลิยูรีเทนแบบแข็ง โดยใช้สารประกอบเชิงซ้อนของโลหะผสมสองชนิด $[M_1(OAc)_2(en)_2:M_2(OAc)_2(en)_2]$ ที่สังเคราะห์ได้จากเกลือแอกซีเตทของโลหะ $[M(OAc)_2]$ ซึ่ง $M = Ca, Ba, Mn, Co, Ni, Cu$ และ Zn กับเอทิลีนไดเอมีน (en) เป็นตัวเร่งปฏิกิริยา พิสูจน์เอกลักษณ์ของตัวเร่งปฏิกิริยาด้วยเทคนิคอินฟราเรดสเปกโทรสโกปี ยูวี-วิสทิเบิลสเปกโทรสโกปี และวิเคราะห์หาธาตุองค์ประกอบ การเตรียมโฟมพอลิยูรีเทนแบบแข็งใช้ปฏิกิริยาระหว่างพอลิเมอร์ 4,4' มิเทนไดฟีนิลไดไอโซไซยานาตและพอลิอีเทอร์พอลิออลที่ดัชนีไอโซไซยานาต (NCO index) เท่ากับ 100 และ 150 โดยใช้สารประกอบเชิงซ้อนโลหะผสมและเอมีนเป็นตัวเร่งปฏิกิริยาและเปรียบเทียบกับตัวเร่งปฏิกิริยาทางการค้าคือ เอ็น,เอ็น-ไดเมทิลไซโคลเฮกซิลเอมีน (DMCHA) ศึกษาผลทางด้านเวลาของการเกิดปฏิกิริยา สมบัติทางกายภาพ และสมบัติเชิงกลของโฟมพอลิยูรีเทนแบบแข็ง เอทีอาร์-อินฟราเรดสเปกโทรสโกปี เป็นเทคนิคที่ใช้เพื่อหาการเปลี่ยนแปลงของหมู่ไอโซไซยานาต (NCO conversion) ในการเตรียมโฟมพอลิยูรีเทน จากสารประกอบเชิงซ้อนของโลหะผสมทั้งหมด พบว่าตัวเร่งปฏิกิริยาที่ดีที่สุดคือ $Cu(OAc)_2(en)_2:Zn(OAc)_2(en)_2$ ซึ่งเทียบเท่ากับไดเมทิลไซโคลเฮกซิลเอมีน (DMCHA) โดยความหนาแน่นและความสามารถทนทานต่อแรงกดอัด (compressive strength) ของโฟมที่เตรียมจาก $Cu(OAc)_2(en)_2:Zn(OAc)_2(en)_2$ ในดัชนีไอโซไซยานาต 150 เท่ากับ 44.1 kg/m^3 และ 258.5 kPa ตามลำดับ

ภาควิชา.....เคมี..... ลายมือชื่อนิสิต.....
 สาขาวิชา.....เคมี..... ลายมือชื่อ อ.ที่ปรึกษาวิทยานิพนธ์หลัก.....
 ปีการศึกษา.....2553.....

5272242023: MAJOR CHEMISTRY

KEYWORDS: MIXED METAL COMPLEXES / RIGID POLYURETHANE
FOAM / CATALYST

JARIYAPORN POMSOOK: PREPARATION OF RIGID
POLYURETHANE FOAM USING MIXED METAL COMPLEXES AND
ETHYLENEDIAMINE AS CATALYSTS. ADVISOR: ASSOC. PROF.
NUANPHUN CHANTARASIRI, Ph. D., 144 pp.

In this research, the catalysts for rigid polyurethane foams were developed by using mixed metal complexes $[M_1(OAc)_2(en)_2:M_2(OAc)_2(en)_2]$ synthesized from metal acetates $[M(OAc)_2]$, where $M = Ca, Ba, Mn, Co, Ni, Cu$ and Zn] and ethylenediamine (en). The mixed metal complexes were characterized by infrared spectroscopy, UV-visible spectroscopy, and elemental analysis. Rigid polyurethane foams were prepared from the reaction between polymeric 4,4' methane diphenyl diisocyanate and polyether polyol at the NCO indexes of 100 and 150. Mixed metal complexes were used as catalysts and their catalytic activities were compared with that of N,N-dimethylcyclohexylamine (DMCHA), which is a commercial catalyst, by investigation of reaction times, physical and mechanical properties of rigid polyurethane foams. ATR-IR spectroscopy was used to determine isocyanate (NCO) conversion of polyurethane foams. Among all mixed metal complexes, $Cu(OAc)_2(en)_2:Zn(OAc)_2(en)_2$ showed the best catalytic activity and was comparable to that of DMCHA. Density and the compressive strength of the foam prepared by $Cu(OAc)_2(en)_2:Zn(OAc)_2(en)_2$ at NCO index of 150 were 44.1 kg/m^3 and 258.5 kPa, respectively.

Department : Chemistry Student's Signature

Field of Study : Chemistry Advisor's Signature

Academic Year : 2010

ACKNOWLEDGEMENTS

The author wishes to express my deep gratitude to my advisor, Associate Professor Dr. Nuanphun Chantarasiri for their generous assistance, benevolent guidance and encouragement throughout the course of this research.

Many thanks to the thesis committees, Assistant Professor Dr. Preecha Lertpratchya, Professor Dr. Thawatchai Tuntulani, Associate Professor Dr. Polkit Sangvanich, Department of chemistry, Faculty of science, Chulalongkorn University and Dr. Duangruthai Sridaeng, Department of chemistry, Faculty of science, Rangsit University, For their invaluable discussion and suggestion.

Definitely, this thesis cannot be completed without kindness and helpful of many people. Firstly, I would like to thank South City Petrochem Co., Ltd. and Huntsman (Thailand) Co., Ltd. The Metallurgy and Materials Science Research Institute for their chemical and SEM support, respectively. In addition, I am grateful to acknowledge the grant and funding supports provided by Center for Petroleum, Petrochemicals, and Advanced Materials, NCE-PPAM. I sincerely thank Department of Chemistry, Chulalongkorn University and Scientific and Technological Research Equipment Center, Chulalongkorn University. In addition, I would like to thank the Asian Development Bank of Chulalongkorn University for supporting scholarship.

This thesis could not have been complete without generous help of the member of Supra molecular Chemistry Research Laboratory, especially Mr. Wittaya Pengjam, for his valuable suggestions. Finally, the author owes a deep debt of gratitude to my family for their continued support, and Mr. Watcharapon Pumgrumarn owes love and encouragement.

CONTENTS

	Page
ABSTRACT (THAI).....	iv
ABSTRACT (ENGLISH).....	v
ACKNOWLEDGEMENTS.....	vi
CONTENTS.....	vii
LIST OF TABLES.....	xii
LIST OF FIGURES.....	xviii
LIST OF SCHEMES.....	xxiv
LIST OF ABBREVIATIONS.....	xxvi
CHAPTER I INTRODUCTION.....	1
1.1 Statement of the problem.....	1
1.2 Research objectives.....	5
1.3 Scope of the research.....	7
CHAPTER II THEORY AND LITERATURE REVIEWS.....	8
Theory.....	8
2.1 Classified of cellular polymers.....	9
2.1.1 Flexible foam.....	9
2.1.2 Rigid foam.....	10
2.2 Raw materials.....	11
2.2.1 Isocyanates.....	11
2.2.2 Polyol.....	14
2.2.3 Blowing agent.....	17

	Page
2.2.4 Catalyst.....	17
2.2.5 Surfactants.....	23
2.3 Basic reactions of isocyanates.....	24
2.4 Formulations.....	29
2.5 Mechanical properties.....	31
Literature reviews.....	34
CHAPTER III EXPERIMENTAL.....	39
3.1 Chemicals.....	39
3.2 Synthetic procedures.....	39
3.2.1 Synthesis of metal-amine complexes in acetone.....	40
3.2.1.1 Synthesis of metal-ethylenediamine complexes $[M(OAc)_2(en)_2]$	40
3.2.1.2 Synthesis of mixed metal-ethylenediamine complexes...	42
3.2.1.3 Synthesis of metal-triethylenetetramine complexes; $M(OAc)_2(trien)$	44
3.2.1.4 Synthesis of mixed metal-triethylenetetramine complexes.....	46
3.2.2 Synthesis of metal complexes in water $(W_M_1(OAc)_2(en)_2:M_2(OAc)_2(en)_2)$	50
3.3 Rigid polyurethane (RPUR) foam preparation.....	51
3.3.1 Preparation of RPUR foams catalyzed by mixed metal complexes.....	51
3.3.2 Preparation of RPUR foams using an aluminum mold.....	52

	Page
3.4 Instrumentation.....	53
CHAPTER IV RESULTS AND DISCUSSION.....	57
4.1 Synthesis of mixed metal-amine complexes	
[M ₁ (OAc) ₂ (en) ₂ :M ₂ (OAc) ₂ (en) ₂] and	
[M ₁ (OAc) ₂ (trien):M ₂ (OAc) ₂ (trien)]	57
4.2 Characterization mixed metal-amine complexes	
[M ₁ (OAc) ₂ (en) ₂ :M ₂ (OAc) ₂ (en) ₂] and	
[M ₁ (OAc) ₂ (trien):M ₂ (OAc) ₂ (trien)]	58
4.2.1 Mn(OAc) ₂ (en) ₂ :M ₂ (OAc) ₂ (en) ₂ complexes.....	59
4.2.2 Ni(OAc) ₂ (en) ₂ :M ₂ (OAc) ₂ (en) ₂ complexes.....	60
4.2.3 Cu(OAc) ₂ (en) ₂ :M ₂ (OAc) ₂ (en) ₂ complexes.....	61
4.2.3.1 FTIR spectroscopy of	
Cu(OAc) ₂ (en) ₂ :M ₂ (OAc) ₂ (en) ₂ complexes.....	62
4.2.3.2 UV-visible spectroscopy of	
Cu(OAc) ₂ (en) ₂ :M ₂ (OAc) ₂ (en) ₂ complexes.....	63
4.2.3.3 Elemental analysis of	
Cu(OAc) ₂ (en) ₂ :M ₂ (OAc) ₂ (en) ₂ complexes.....	65
4.2.3.4 Mass spectrometry of	
Cu(OAc) ₂ (en) ₂ :M ₂ (OAc) ₂ (en) ₂ complexes.....	66
4.2.3.5 Determination of metal amount in	
Cu(OAc) ₂ (en) ₂ :M ₂ (OAc) ₂ (en) ₂ complexes	
by flame atomic spectrometry (FAAS)	69
4.2.4 Cu(OAc) ₂ (trien):M ₂ (OAc) ₂ (trien) complexes.....	72

	Page
4.2.4.1 FTIR spectroscopy of Cu(OAc) ₂ (trien):M ₂ (OAc) ₂ (trien) complexes.....	72
4.2.4.2 UV-visible spectroscopy of Cu(OAc) ₂ (trien):M ₂ (OAc) ₂ (trien) complexes.....	73
4.2.4.3 Elemental analysis of Cu(OAc) ₂ (trien):M(OAc) ₂ (trien) complexes.....	75
4.2.4.4 Mass spectrometry of Cu(OAc) ₂ (trien):Ni(OAc) ₂ (trien).	76
4.2.4.5 Determination of metal amount in Cu(OAc) ₂ (trien):M ₂ (OAc) ₂ (trien) complexes by flame atomic spectrometry (FAAS).....	78
4.3 Preparation of rigid polyurethane (RPUR) foams.....	78
4.3.1 Preparation of RPUR foams catalyzed by mixed metal complexes.....	78
4.3.1.1 Preparation of RPUR foams using an aluminum mold.....	80
4.3.2 Reaction times and rise profile.....	81
4.3.3 Apparent density.....	91
4.3.3.1 Effect of NCO indexes on foam density.....	91
4.3.3.2 Effect of catalyst quantity on foam density.....	94
4.3.4 Foaming temperature.....	95
4.3.5 NCO conversion of RPUR foams.....	98
4.3.6 Compressive properties of RPUR foams.....	102
4.3.7 Cell Morphology Sample Preparation and Testing.....	103
4.3.8 Thermal stability characterization.....	104

	Page
CHAPTER V CONCLUSION	110
5.1 Conclusion.....	110
5.2 Suggestion for future work.....	111
REFERENCES	112
APPENDICES	120
APPENDIX A	121
APPENDIX B	131
APPENDIX C	139
VITAE	144

LIST OF TABLES

		Page
Table 2.1	Specifications of commercial polyols including functionality values.....	15
Table 2.2	Overview of frequently used catalysts in rigid polyurethane foams.....	19
Table 3.1	Composition of starting materials in the preparation of metal complexes $[M(OAc)_2(en)_2$ and $M(OAc)_2(trien)]$	48
Table 3.2	Composition of starting materials in the preparation of mixed metal-amine complexes $[M_1(OAc)_2(en)_2:M_2(OAc)_2(en)_2$ and $M_1(OAc)_2(trien):M_2(OAc)_2(trien)]$	49
Table 3.3	Composition of starting materials in the preparation of mixed metal - mixed amine complexes $[M_1(OAc)_2(en)(trien): M_2(OAc)_2(en)(trien)]$	50
Table 3.4	Formulation used for foam preparation at different NCO indexes (in part by weight unit, pbw).....	51
Table 3.5	Characteristic IR bands of RPUR foam.....	53
Table 4.1	Elemental analysis (CHN) of $Cu(OAc)_2(en)_2:Zn(OAc)_2(en)_2$	65
Table 4.2	Positive ESI mass spectra of $Cu(OAc)_2(en)_2:M_2(OAc)_2(en)_2$ complexes.....	69
Table 4.3	Operating parameters the determination of metal concentration by FAAS.....	70
Table 4.4	Analytical characteristics of the FAAS method.....	70
Table 4.5	Analytical characteristics of the FAAS method.....	71
Table 4.6	Elemental analysis (CHN) of $Cu(OAc)_2(en)_2:Zn(OAc)_2(en)_2$	75

	Page
Table 4.7 Positive ESI mass spectra of Cu(OAc) ₂ (trien):M ₂ (OAc) ₂ (trien) complexes.....	77
Table 4.8 Analytical characteristics of the FAAS method.....	78
Table 4.9 RPUR foam formulation.....	79
Table 4.10 Reaction profiles of RPUR foams prepared at the NCO index of 100 and catalyzed by mixed metal complexes prepared in acetone.....	85
Table 4.11 Reaction profiles of RPUR foams prepared at the NCO index of 100 and catalyzed by mixed metal complexes prepared in water.....	86
Table 4.12 Reaction profiles of RPUR foam catalyzed by M ₁ (OAc) ₂ :M ₂ (OAc) ₂ :ethylenediamine with different M ₁ (OAc) ₂ :M ₂ (OAc) ₂ ratios at index 100.....	89
Table 4.13 Reaction profiles of RPUR foam catalyzed by M ₁ (OAc) ₂ :M ₂ (OAc) ₂ :amine with different M ₁ (OAc) ₂ :amine ratios at index 100.....	90
Table 4.14 Density of RPUR foams prepared at the index 100-200	93
Table 4.15 Maximum core temperature of RPUR foam catalyzed by mixed metal complexes synthesized in acetone at different NCO indexes.....	96
Table 4.16 Maximum core temperature of RPUR foam catalyzed by mixed metal complexes synthesized in water at different NCO indexes.....	97
Table 4.17 Wavenumber of the functional groups used in calculation.....	100

	Page
Table 4.18	NCO conversions and PIR: PUR ratio of RPUR foams catalyzed mixed metal complexes (synthesized in acetone) at different NCO indexes..... 101
Table 4.19	TGA data of RPUR foam catalyst by mixed metal complexes catalysts (synthesized in acetone) at the NCO index of 150..... 105
Table A1	Isocyanate quantity at different NCO indexes in the above formulations..... 123
Table A2	Free NCO absorbance peak area in PMDI (MR-200) from IR-ATR..... 124
Table A3	NCO conversion of RPUR foam catalyzed by DMCHA at different NCO indexes..... 125
Table A4	NCO conversion of RPUR foam catalyzed by $\text{Cu}(\text{OAc})_2(\text{en})_2:\text{Ni}(\text{OAc})_2(\text{en})_2$ at different NCO indexes..... 125
Table A5	NCO conversion of RPUR foam catalyzed by $\text{Cu}(\text{OAc})_2(\text{en})_2:\text{Zn}(\text{OAc})_2(\text{en})_2$ at different NCO indexes..... 125
Table A6	NCO conversion of RPUR foam catalyzed by $\text{Cu}(\text{OAc})_2(\text{trien}):\text{Ni}(\text{OAc})_2(\text{trien})$ at different NCO indexes..... 126
Table A7	NCO conversion of RPUR foam catalyzed by $\text{Cu}(\text{OAc})_2(\text{trien}):\text{Zn}(\text{OAc})_2(\text{trien})$ at different NCO indexes.... 126
Table A8	NCO conversion of RPUR foam catalyzed by $\text{Cu}(\text{Sal})_2(\text{en})_2:\text{Ni}(\text{Sal})_2(\text{en})_2$ at different NCO indexes..... 126
Table A9	NCO conversion of RPUR foam catalyzed by $\text{Cu}(\text{Sal})_2(\text{en})_2:\text{Zn}(\text{Sal})_2(\text{en})_2$ at different NCO indexes..... 127

	Page
Table A10 NCO conversion of RPUR foam catalyzed by Cu(Sal) ₂ (trien):Ni(Sal) ₂ (trien) at different NCO indexes.....	127
Table A11 NCO conversion of RPUR foam catalyzed by Cu(Sal) ₂ (trien):Zn(Sal) ₂ (trien) at different NCO indexes.....	127
Table A12 NCO conversion of RPUR foam catalyzed by DMCHA at different NCO indexes.....	128
Table A13 NCO conversion of RPUR foam catalyzed by Cu(OAc) ₂ (en) ₂ :Ni(OAc) ₂ (en) ₂ at different NCO indexes.....	128
Table A14 NCO conversion of RPUR foam catalyzed by Cu(OAc) ₂ (en) ₂ :Zn(OAc) ₂ (en) ₂ at different NCO indexes.....	128
Table A15 NCO conversion of RPUR foam catalyzed by Cu(OAc) ₂ (trien):Ni(OAc) ₂ (trien) at different NCO indexes.....	129
Table A16 NCO conversion of RPUR foam catalyzed by Cu(OAc) ₂ (trien):Zn(OAc) ₂ (trien) at different NCO indexes....	129
Table A17 NCO conversion of RPUR foam catalyzed by Cu(Sal) ₂ (en) ₂ :Ni(Sal) ₂ (en) ₂ at different NCO indexes.....	129
Table A18 NCO conversion of RPUR foam catalyzed by Cu(Sal) ₂ (en) ₂ :Zn(Sal) ₂ (en) ₂ at different NCO indexes.....	130
Table A19 NCO conversion of RPUR foam catalyzed by Cu(Sal) ₂ (trien):Ni(Sal) ₂ (trien) at different NCO indexes.....	130
Table A20 NCO conversion of RPUR foam catalyzed by Cu(Sal) ₂ (trien):Zn(Sal) ₂ (trien) at different NCO indexes.....	130
Table B1 Reaction profiles of RPUR foam catalyzed by Ni(OAc) ₂ :M ₂ (OAc) ₂ :ethylenediamine at index 100.....	131

	Page	
Table B2	Reaction profiles of RPUR foam catalyzed by $M_1(\text{OAc})_2:M_2(\text{OAc})_2$:amine with different $M_1(\text{OAc})_2$:amine ratios at index 150.....	132
Table B3	Summary of formulations, reaction times, physical and mechanical properties of PUR foams catalyzed by mixed complexes (metal ratio = 0.7:0.3) and amines as catalysts.....	133
Table B4	Summary of formulations, reaction times, physical and mechanical properties of PUR foams catalyzed by mixed transition complexes (metal ratio = 0.5:0.5) and amines as catalysts.	134
Table B5	Summary of formulations, reaction times, physical and mechanical properties of PUR foams catalyzed by mixed transition complexes (metal ratio = 0.3:0.7) and amines as catalysts.....	135
Table B6	Summary of formulations, reaction times, physical and mechanical properties of PUR foams catalyzed by Cu : Zn : amines as catalysts.....	136
Table B7	Summary of formulations, reaction times, physical and mechanical properties of PUR foams catalyzed by mixed transition complexes and amines as catalysts.....	137
Table B8	Summary of formulations, reaction times, physical and mechanical properties of PUR foams catalyzed by mixed metal : amines : salicylic as catalysts.....	138

	Page
Table C1 Natural abundances of common elements and their isotopes.....	139
Table C2 Positive ESI mass spectra of $M(\text{OAc})_2(\text{en})_2$ and $M(\text{OAc})_2(\text{trien})$ complexes.....	143

LIST OF FIGURES

		Page
Figure 1.1	Structure of mixed metal-amine complexes.....	6
Figure 1.2	Structure of mixed metal-amine complexes where: $M_1 = \text{Cu}$; $M_2 = \text{Zn, Ni}$	6
Figure 2.1	Open cell foam and closed cell foam structures.....	10
Figure 2.2	Toluene diisocyanate isomers used for PU foam manufacture...	12
Figure 2.3	Molecular structure of MDI.....	12
Figure 2.4	Benzene to PMDI.....	13
Figure 2.5	Structure of polyether polyol based sorbitol and sucrose used in the PUR foams.....	16
Figure 2.6	Example of aliphatic and aromatic dicarboxylic acids used in the production of polyester polyols.....	16
Figure 2.7	Structure of silicone surfactants used in PUR foams manufacture	23
Figure 2.8	Compression load deflection test rig.....	31
Figure 2.9	Schematic representation of open cell deformation.....	32
Figure 2.10	Schematic representation of closed cell deformation.....	32
Figure 2.11	Typical compression stress-strain curve for rigid foams.....	33
Figure 2.12	Key reactions in polyurethane foam synthesis.....	34
Figure 2.13	An example of mixed metal-amine complex, $\text{Cu}(\text{CH}_3\text{COO})_2(\text{en})_2$: $\text{Zn}(\text{CH}_3\text{COO})_2(\text{en})_2$	38
Figure 2.14	N, N-dimethylcyclohexyl amine (DMCHA)	38
Figure 3.1	IR spectra of RPUR foams catalyzed by $\text{Cu}(\text{OAc})_2(\text{en})_2$: $\text{Zn}(\text{OAc})_2(\text{en})_2$ (synthesized in acetone).....	52

	Page
Figure 4.1	IR spectra of (a) $\text{Mn}(\text{OAc})_2$;
	(b) $\text{Mn}(\text{OAc})_2(\text{en})_2:\text{Ba}(\text{OAc})_2(\text{en})_2$;
	(c) $\text{Mn}(\text{OAc})_2(\text{en})_2:\text{Ca}(\text{OAc})_2(\text{en})_2$;
	(d) $\text{Mn}(\text{OAc})_2(\text{en})_2:\text{Co}(\text{OAc})_2(\text{en})_2$;
	(e) $\text{Mn}(\text{OAc})_2(\text{en})_2:\text{Zn}(\text{OAc})_2(\text{en})_2$ 59
Figure 4.2	IR spectra of (a) $\text{Ni}(\text{OAc})_2$;
	(b) $\text{Ni}(\text{OAc})_2(\text{en})_2:\text{Ba}(\text{OAc})_2(\text{en})_2$;
	(c) $\text{Ni}(\text{OAc})_2(\text{en})_2:\text{Ca}(\text{OAc})_2(\text{en})_2$;
	(d) $\text{Ni}(\text{OAc})_2(\text{en})_2:\text{Co}(\text{OAc})_2(\text{en})_2$;
	(e) $\text{Ni}(\text{OAc})_2(\text{en})_2:\text{Mn}(\text{OAc})_2(\text{en})_2$;
	(f) $\text{Ni}(\text{OAc})_2(\text{en})_2:\text{Zn}(\text{OAc})_2(\text{en})_2$ 60
Figure 4.3	IR spectra of (a) $\text{Cu}(\text{OAc})_2$; (b) ethylenediamine (en);
	(c) $\text{Cu}(\text{OAc})_2(\text{en})_2$ 62
Figure 4.4	IR spectra of (a) $\text{Cu}(\text{OAc})_2$; (b) $\text{Cu}(\text{OAc})_2(\text{en})_2:\text{Ba}(\text{OAc})_2(\text{en})_2$;
	(c) $\text{Cu}(\text{OAc})_2(\text{en})_2:\text{Ca}(\text{OAc})_2(\text{en})_2$;
	(d) $\text{Cu}(\text{OAc})_2(\text{en})_2:\text{Co}(\text{OAc})_2(\text{en})_2$;
	(e) $\text{Cu}(\text{OAc})_2(\text{en})_2:\text{Mn}(\text{OAc})_2(\text{en})_2$;
	(f) $\text{Cu}(\text{OAc})_2(\text{en})_2:\text{Ni}(\text{OAc})_2(\text{en})_2$;
	(g) $\text{Cu}(\text{OAc})_2(\text{en})_2:\text{Zn}(\text{OAc})_2(\text{en})_2$ 63
Figure 4.5	UV spectra of (a) $\text{Ni}(\text{OAc})_2$; (b) $\text{Cu}(\text{OAc})_2$; (c) $\text{Zn}(\text{OAc})_2$;
	(d) $\text{Cu}(\text{OAc})_2(\text{en})_2:\text{Ni}(\text{OAc})_2(\text{en})_2$;
	(e) $\text{Cu}(\text{OAc})_2(\text{en})_2:\text{Zn}(\text{OAc})_2(\text{en})_2$ 64

	Page	
Figure 4.6	UV spectra of (a) Ni(OAc) ₂ ; (b) Cu(OAc) ₂ ; (c) Cu(OAc) ₂ (en) ₂ :Ni(OAc) ₂ (en) ₂ in acetone; (d) Cu(OAc) ₂ (en) ₂ :Ni(OAc) ₂ (en) ₂ in water.....	64
Figure 4.7	UV spectra of (a) Cu(OAc) ₂ ; (b) Zn(OAc) ₂ ; (c) Cu(OAc) ₂ (en) ₂ :Zn(OAc) ₂ (en) ₂ in acetone; (d) Cu(OAc) ₂ (en) ₂ :Zn(OAc) ₂ (en) ₂ in water.....	65
Figure 4.8	ESI Mass spectrum of (a) Cu(OAc) ₂ (en) ₂ :Zn(OAc) ₂ (en) ₂ and (b) Cu(OAc) ₂ (en) ₂ :Ni(OAc) ₂ (en) ₂	67
Figure 4.9	Estimation of Cu(II), Ni(II) and Zn(II) in metal(II) acetate samples by FAAS.....	71
Figure 4.10	IR spectra of (a) Cu(OAc) ₂ ; (b) Cu(OAc) ₂ (trien):Ni(OAc) ₂ (trien); (c) Cu(OAc) ₂ (trien):Zn(OAc) ₂ (trien)	73
Figure 4.11	UV spectra of (a) Ni(OAc) ₂ ; (b) Cu(OAc) ₂ ; (c) Zn(OAc) ₂ ; (d) Cu(OAc) ₂ (trien):Ni(OAc) ₂ (trien); (e) Cu(OAc) ₂ (trien):Zn(OAc) ₂ (trien)	74
Figure 4.12	UV spectra of (a) Ni(OAc) ₂ ; (b) Cu(OAc) ₂ ; (c) Zn(OAc) ₂ ; (d) Cu(OAc) ₂ (trien):Ni(OAc) ₂ (trien) in acetone; (e) Cu(OAc) ₂ (trien):Ni(OAc) ₂ (trien) in water.....	74
Figure 4.13	UV spectra of (a) Ni(OAc) ₂ ; (b) Cu(OAc) ₂ ; (c) Zn(OAc) ₂ ; (d) Cu(OAc) ₂ (trien):Zn(OAc) ₂ (trien) in acetone; (e) Cu(OAc) ₂ (trien):Zn(OAc) ₂ (trien) in water.....	75
Figure 4.14	ESI Mass spectrum of (a) Cu(OAc) ₂ (trien):Zn(OAc) ₂ (trien) and (b) Cu(OAc) ₂ (trien):Ni(OAc) ₂ (trien)	77

	Page
Figure 4.15 RPUR foams catalyzed by $\text{Cu}(\text{OAc})_2(\text{en})_2:\text{Zn}(\text{OAc})_2(\text{en})_2$ at different NCO indexes (a) 100; (b) 150; (c) 200.....	80
Figure 4.16 RPUR foams catalyzed by $\text{Cu}(\text{OAc})_2(\text{en})_2:\text{Ni}(\text{OAc})_2(\text{en})_2$ at different NCO indexes (a) 100; (b) 150; (c) 200.....	80
Figure 4.17 RPUR foams catalyzed by $\text{Cu}(\text{OAc})_2(\text{en})_2:\text{Zn}(\text{OAc})_2(\text{en})_2$ and prepared in an aluminum mold.....	81
Figure 4.18 Reaction times of RPUR foams prepared at the NCO index of 100 and catalyzed by (a) DMCHA; (b) $\text{Cu}(\text{OAc})_2(\text{en})_2:\text{Zn}(\text{OAc})_2(\text{en})_2$; (c) $\text{Cu}(\text{OAc})_2(\text{trien}):\text{Zn}(\text{OAc})_2(\text{trien})$; (d) $\text{Cu}(\text{OAc})_2(\text{en})_2:\text{Ni}(\text{OAc})_2(\text{en})_2$; (e) $\text{Cu}(\text{OAc})_2(\text{trien}):\text{Ni}(\text{OAc})_2(\text{trien})$	83
Figure 4.19 Rise profile of RPUR foams catalyzed by different mixed metal complexes at the NCO index of 100.....	84
Figure 4.20 Maximum rise rates of RPUR foams prepared at the NCO index of 100 and catalyzed by different mixed metal complexes (a) DMCHA (ref.); (b) $\text{Cu}(\text{OAc})_2(\text{en})_2:\text{Ni}(\text{OAc})_2(\text{en})_2$; (c) $\text{Cu}(\text{OAc})_2(\text{trien}):\text{Ni}(\text{OAc})_2(\text{trien})$; (d) $\text{Cu}(\text{OAc})_2(\text{en})_2:\text{Zn}(\text{OAc})_2(\text{en})_2$; (e) $\text{Cu}(\text{OAc})_2(\text{trien}):\text{Zn}(\text{OAc})_2(\text{trien})$	88
Figure 4.21 Samples for foam density measurements.....	91
Figure 4.22 RPUR foam samples for foam density measurements (a) index 100 (b) index 150 (c) index 200.....	92

	Page
Figure 4.23 Effect of catalyst amount on RPUR foams density catalyzed by different catalysts at NCO index of 100.....	94
Figure 4.24 Temperature profiles of RPUR foams catalyzed by different mixed metal complexes.....	95
Figure 4.25 IR spectra of starting materials and RPUR foams catalyzed by mixed metal complexes (synthesized in acetone) (a) PMDI; (b) $\text{Cu}(\text{OAc})_2(\text{en})_2:\text{Ni}(\text{OAc})_2(\text{en})_2$; (c) $\text{Cu}(\text{OAc})_2(\text{en})_2:\text{Ni}(\text{OAc})_2(\text{en})_2$; (d) $\text{Cu}(\text{OAc})_2(\text{trien}):\text{Ni}(\text{OAc})_2(\text{trien})$; (e) $\text{Cu}(\text{trien}):\text{Zn}(\text{trien})$	98
Figure 4.26 IR spectra of RPUR foams catalyzed by $\text{Cu}(\text{OAc})_2(\text{en})_2:\text{Zn}(\text{OAc})_2(\text{en})_2$ (synthesized in acetone) at different NCO indexes (a) 100; (b) 150; (c) 200.....	99
Figure 4.27 Deformation curves for RPUR foams prepared at the NCO index = 150 with density in the range 45-50 kg/m^3	103
Figure 4.28 SEM of RPUR foams (NCO index = 150) catalyzed by (a) DMCHA; (b) $\text{Cu}(\text{OAc})_2(\text{en})_2$; (c) $\text{Ni}(\text{OAc})_2(\text{en})_2$; (d) $\text{Cu}(\text{OAc})_2(\text{en})_2:\text{Ni}(\text{OAc})_2(\text{en})_2$	104
Figure 4.29 TGA thermograms of RPUR foams catalyzed by (a) DMCHA; (b) $\text{Cu}(\text{OAc})_2(\text{en})_2:\text{Zn}(\text{OAc})_2(\text{en})_2$; (c) $\text{Cu}(\text{OAc})_2(\text{trien}):\text{Ni}(\text{OAc})_2(\text{trien})$ (synthesized in acetone, NCO index = 150).....	105

	Page
Figure 4.30 Weight loss rate versus temperature for different heating rates (from DMCHA, $\text{Cu}(\text{OAc})_2(\text{en})_2:\text{Zn}(\text{OAc})_2(\text{en})_2$ and $\text{Cu}(\text{OAc})_2(\text{trien}):\text{Zn}(\text{OAc})_2(\text{trien})$)	106
Figure 4.31 External appearance of RPUR foams catalyzed by (a) non-catalyst, (b) $\text{Cu}(\text{OAc})_2$, (c) DMCHA, (d) $\text{Cu}(\text{OAc})_2(\text{en})_2:\text{Zn}(\text{OAc})_2(\text{en})_2$, (e) $\text{Cu}(\text{OAc})_2(\text{trien}):\text{Zn}(\text{OAc})_2(\text{trien})$, (f) $\text{Cu}(\text{en})(\text{trien}):\text{Zn}(\text{en})(\text{trien})$	107
Figure 4.32 External appearance of RPUR foams catalyzed by metal-ethylenediamine complexes by (a) $\text{Ba}(\text{OAc})_2(\text{en})_2$ (b) $\text{Ca}(\text{OAc})_2(\text{en})_2$ (c) $\text{Mn}(\text{OAc})_2(\text{en})_2$ (d) $\text{Co}(\text{OAc})_2(\text{en})_2$ (e) $\text{Ni}(\text{OAc})_2(\text{en})_2$ (f) $\text{Cu}(\text{OAc})_2(\text{en})_2$ (g) $\text{Zn}(\text{OAc})_2(\text{en})_2$	108
Figure 4.33 External appearance of test piece RPUR foams catalyzed by mixed metal complexes at index 100.....	109
Figure C1 ESI Mass spectrum of $\text{Cu}(\text{OAc})_2(\text{en})_2$	140
Figure C2 ESI Mass spectrum of $\text{Cu}(\text{OAc})_2(\text{trien})$	140
Figure C3 ESI Mass spectrum of $\text{Ni}(\text{OAc})_2(\text{en})_2$	141
Figure C4 ESI Mass spectrum of $\text{Ni}(\text{OAc})_2(\text{trien})$	141
Figure C5 ESI Mass spectrum of $\text{Zn}(\text{OAc})_2(\text{en})_2$	142
Figure C6 ESI Mass spectrum of $\text{Zn}(\text{OAc})_2(\text{trien})$	142

LIST OF SCHEMES

	Page
Scheme 2.1 Baker mechanism amine catalyst.....	20
Scheme 2.2 Farka mechanism amine catalysts.....	20
Scheme 2.3 Mechanism for tin II salts.....	21
Scheme 2.4 Mechanism for tin VI compounds.....	22
Scheme 2.5 Mechanism of tin-amine synergism.....	22
Scheme 3.1 Synthesis of nickel-ethylenediamine complex	40
Scheme 3.2 Synthesis of copper-ethylenediamine complex.....	41
Scheme 3.3 Synthesis of zinc-ethylenediamine complex.....	41
Scheme 3.4 Synthesis of $\text{Cu}(\text{OAc})_2(\text{en})_2:\text{Ni}(\text{OAc})_2(\text{en})_2$ complex.....	42
Scheme 3.5 Synthesis of $\text{Cu}(\text{OAc})_2(\text{en})_2:\text{Zn}(\text{OAc})_2(\text{en})_2$ complex.....	43
Scheme 3.6 Synthesis of nickel-triethylenetetramine complex.....	44
Scheme 3.7 Synthesis of copper-triethylenetetramine complex.....	44
Scheme 3.8 Synthesis of zinc-triethylenetetramine complex.....	45
Scheme 3.9 Synthesis of $\text{Cu}(\text{OAc})_2(\text{trien}):\text{Ni}(\text{OAc})_2(\text{trien})$ complex.....	46
Scheme 3.10 Synthesis of $\text{Cu}(\text{OAc})_2(\text{trien}):\text{Zn}(\text{OAc})_2(\text{trien})$ complex.....	47
Scheme 4.1 Synthesis of mixed metal-ethylenediamine complexes $[\text{M}_1(\text{OAc})_2(\text{en})_2:\text{M}_2(\text{OAc})_2(\text{en})_2]$ and mixed metal-triethylenetetramine complexes $[\text{M}_1(\text{OAc})_2(\text{trien}):\text{M}_2(\text{OAc})_2(\text{trien})]$ When; $\text{M}_1 = \text{Cu}, \text{M}_2 = \text{Ca}, \text{Ba}, \text{Co}, \text{Mn}, \text{Ni}, \text{Zn};$ $\text{M}_1 = \text{Ni}, \text{M}_2 = \text{Ca}, \text{Ba}, \text{Co}, \text{Mn}, \text{Zn};$ $\text{M}_1 = \text{Mn}, \text{M}_2 = \text{Ca}, \text{Ba}, \text{Co}, \text{Zn}$	58

	Page
Scheme 4.2 Proposed structure of $\text{Cu}(\text{OAc})_2(\text{en})_2:\text{Zn}(\text{OAc})_2(\text{en})_2$	68
Scheme 4.3 Activation mechanism of metal-based catalyst on urethane formation reaction	87

LIST OF ABBREVIATIONS

%	percentage
ϵ	Molar absorptivity
cm	centimeter
cm^{-1}	unit of wavenumber
$^{\circ}\text{C}$	degree Celsius (centigrade)
CCA	2-cyano-4-hydroxycinnamic acid
DBTDL	dibutyltin dilaurate
DMCHA	N,N-dimethylcyclohexylamine
EA	Elemental Analysis
en	ethylenediamine
FTIR	Fourier Transform Infrared Spectrophotometer
g	gram
h	hour
IDT	Initial Decomposition Temperature
ATR-IR	Attenuated- Infrared Total Reflectance
KBr	potassium bromide
kg	kilogram
kV	kilovolt
M	metal
m^3	cubic meter
MDI	4,4'-methane diphenyl diisocyanate
mA	milliampere
mg	milligram

min	minute
mL	milliliter
mm	millimeter
mmol	millimole
N	newton unit
NCO	isocyanate
OHV	hydroxyl value
pbw	part by weight
PIR	polyisocyanurate
PMDI	polymeric 4,4'-methane diphenyl diisocyanate
PUR	polyurethane
rpm	round per minute
RPUR	rigid polyurethane
RT	room temperature
s	second
SEM	Scanning Electron Microscope
t	time
TDI	toluene diisocyanate
TGA	Thermogravimetric Analysis
T _{max}	maximum core temperature
trien	triethylenetetramine
UV	ultraviolet

CHAPTER I

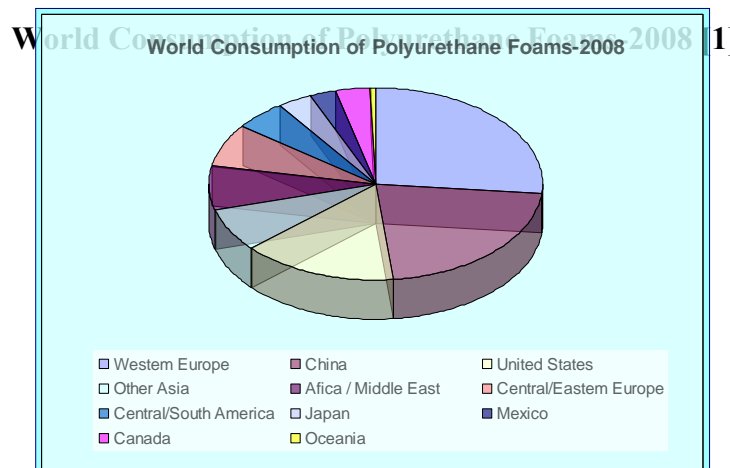
INTRODUCTION

1.1 Statement of the problem

Polyurethane (PU) foams constitute the largest category of cellular polymeric materials. They are produced, for the most part, either in flexible or in rigid forms. Within these major groups, the density and other properties vary depending on the end use. PU foams offer an attractive balance of performance characteristics, namely aging property, mechanical strength, elastic property, chemical resistance, insulating property and cost. Flexible PU foams are used primarily for cushioning and rigid PU foams for insulation. For some applications, foams that have some stiffness and some elasticity are produced; in the trade, they are called semi-flexible or semi-rigid foams.

Flexible polyurethane foam is used primarily as a cushioning material in furniture, transportation and bedding applications. Rigid polyurethane foam is utilized mainly as an insulation material in construction and refrigeration/freezer applications. Flexible polyurethane foams account for 54% of global consumption, but the split with rigid polyurethane foams varies by region. Rigid foams constitute more than 50% of total polyurethane foam consumption in China and Mexico, which are important manufacturing sites for refrigerators and freezers.

The following pie chart shows world consumption of polyurethane foams:



Several thousand producers worldwide manufacture polyurethane foams, frequently at several plant locations. Most foam producers concentrate their efforts on either flexible or rigid foam because the markets and technologies are quite different. In recent years, the industry has witnessed a concentration process, primarily in the United States and Western Europe. Current production capacity for both flexible and rigid polyurethane foams is adequate to meet demand.

Polyurethane foam producers are challenged with manufacturing “greener” products that is, PU foams with improved sustainability and environmental characteristics (for example, polyurethane foams produced with bio-based polyols, rigid foams made with blowing agents with low global warming potential [GWP], and foams not using PBDE [polybrominated diphenylether] fire retardants). Many flexible PU foam producers and automobile seating manufacturers provide products made with bio-based polyols with variable renewable contents.

The global recession of 2008–2009 has significantly reduced demand for polyurethane foams in most countries and regions. Demand in 2009 will be down by 3–35% depending on the product and country or region. Some companies, especially old and/or small production facilities, are expected to shut down permanently and others with multiple manufacturing sites could close some capacity.

For most regions of the world, demand for flexible polyurethane foams is expected to grow at an average annual rate of about 2–4% from 2008 to 2013. Demand for rigid foams will grow at a faster rate. However, assuming that most countries will face drastic drops in 2009 demand (0–5% in the strongest economies to 5–20% in the United States and Western Europe), average annual growth rates of 5–15% are forecast for 2009–2013 [1].

Polyurethane (PU) foams are used in versatile applications such as in automotive interior parts, furniture, insulation, materials for appliances as well as in construction, coatings, adhesives, sealants, and elastomers (CASE) because of their extremely wide range of physical properties and variety in processability of products.

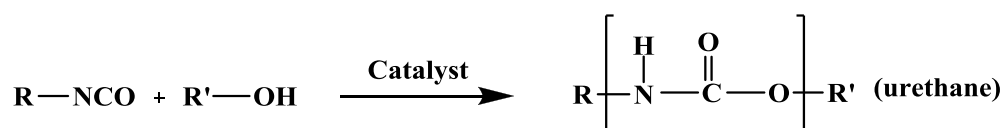
The polyurethane foam formation reaction basically consists of the urethane reaction (gelling) and urea reaction (blowing) accompanied by the generation of CO₂.

There exist, however, many other complex reactions which occur during the production of polyurethane foams simultaneously.

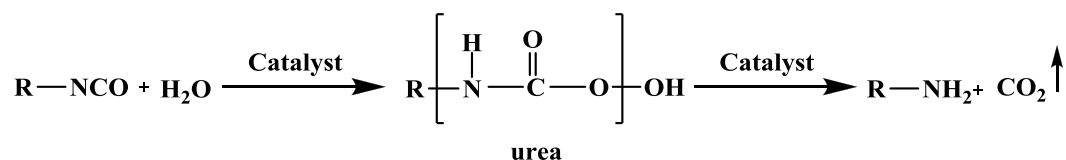
Commercially, polyurethanes are produced by the exothermic reaction of molecules containing two or more isocyanate groups with polyol molecules containing two or more hydroxyl groups. Relatively few basic isocyanates and a far broader range of polyols of different molecular weight and functionalities are used to produce the whole spectrum of polyurethane materials. Additionally, several other chemical reactions of isocyanates are used to modify or extend the range of isocyanate-based polymeric materials. The polymer reaction may be catalyzed, allowing extremely fast cycle times and making high volume production viable.

The foaming can be carried out with physical blowing agent, chemical blowing agent, or mixture of two. There are three main of polyurethane foams leading to polyurethane (PUR) and polyisocyanate (PIR). Polyurethane catalysts are generally classified by their selectivity in catalyzing the main reactions involved in polyurethane formation. Firstly, „gel catalyst“ promotes the isocyanate-alcohol reaction resulting in urethane bonds. Secondly, „blow catalyst“ promotes the isocyanate-water reaction resulting in both urea and carbon dioxide gas. Finally, „trimerization catalyst“ promotes the isocyanurate formation from three isocyanate groups. Catalysts play an important role in the control and balance between the gelling and blowing reactions. In addition to primary reactions, it is considered that the catalytic activity of crosslinking reactions such as allophanate, biuret, and isocyanurate formation have a certain effect on the foaming behavior as well as foam properties [2]. The main reactions are described in Scheme 1.1.

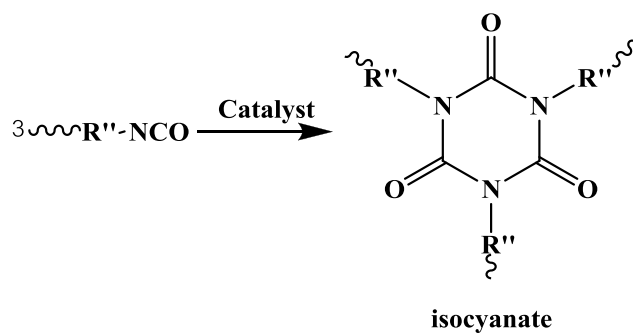
Gelling Reaction:



Blowing Reaction:



Trimerization:



Scheme 1.1 Main reactions involved in polyurethane foam formation

Rigid polyurethane (RPUF) foam demonstrates versatility both through its physical strengths that provides a high level of compression and shear strength, which is further enhanced by bonding with facing materials such as metal or plasterboard and good mechanical properties, low thermal conductivity with a low density and their easy processing that can be performed by one shot or two shot methods. In one shot method, all of materials such as polyol, catalyst, surfactant, blowing agent and isocyanate are put into a mixing cup and mixed homogeneously. In two shot method, isocyanate is added to the mixture of polyol, catalyst, surfactant and blowing agent at the second stage [3].

However, the above reactions cannot be completed without catalysts for catalytic reactions. Practically, catalyst is necessary for the production of polyurethane foams because the reaction between isocyanate with hydroxyl group is

slow [4]. This wide range of products and applications has led to the identification and development of a range of catalyst for rigid foam that can be assigned into four groups:

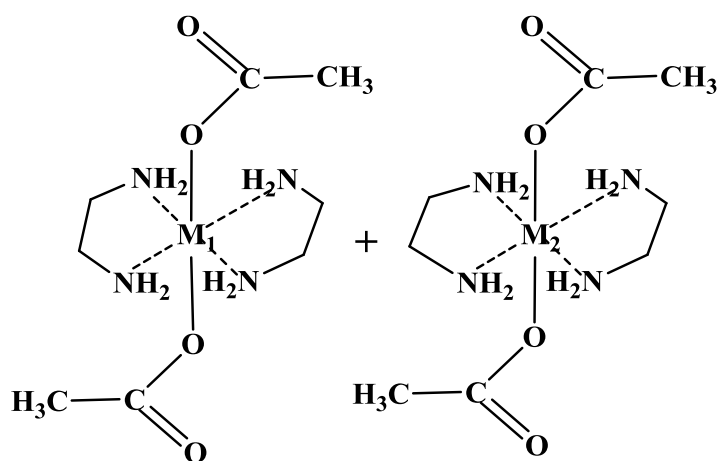
- Aliphatic and aromatic tertiary amines.
- Organometallic compounds; these are normally tin (II) compounds, although lead and bismuth compounds are also used at time.
- Alkali metal salts of carboxylic acids and phenols.
- Miscellaneous compounds such as triazine derivatives.

Tertiary amines and tin compounds are used as catalyst for gelling and blowing reaction; N, N-dimethylcyclohexylamine (DMCHA), Pentamethyldiethylene triamine (PMDETA) and dibutyltin dilaurate (DBTDL). Although conventional catalyst having excellent catalyst activity, they are toxic to human beings and have strong smell. The research in our group involves the development of metal-amine complexes as catalysts for the preparation of rigid polyurethane foams. Metal-amine complexes can be prepared from the reaction between metal acetates, such as copper (II) acetate monohydrate, and aliphatic amine, such as ethylenediamine (en) and triethylenetetramine (trien). It was found that these catalysts showed good catalytic activity; however, their solubility in rigid polyurethane foam starting materials were not good. Moreover, some metal complexes exhibited fast reaction times and caused difficulties in the preparation of rigid polyurethane foams. Therefore, new catalysts were developed in this work.

1.2 Research objectives

The aim of this research focused on the preparation of rigid polyurethane (RPUF) foams catalyzed by mixed metal-ethylenediamine complexes (Figure 1.1) and mixed metal-triethylenetetramine complexes (Figure 1.2). It was expected that the mixed metal complexes showed good solubility and appropriate catalytic activity, which should give the desirable physical and mechanical properties of RPUR foams. The reaction times during foam preparation, the physical and mechanical properties of

RPUR foams were studied by varying catalyst types, the amount of catalysts and isocyanate (NCO) indexes.



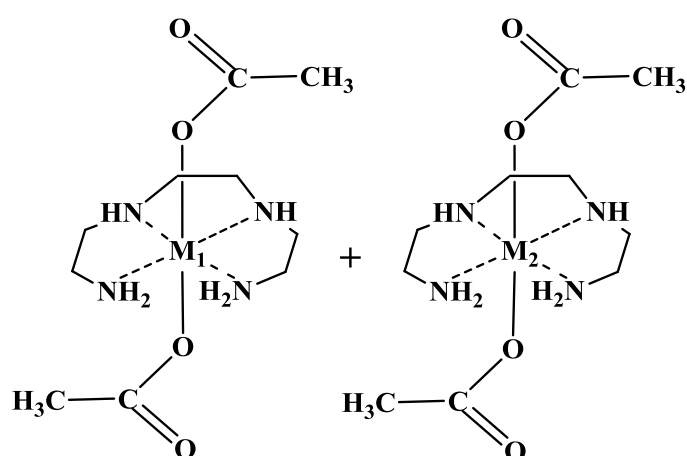
Mixed metal-ethylenediamine complexes
 $M_1(OAc)_2(en)_2:M_2(OAc)_2(en)_2$

Figure 1.1 Structure of mixed metal-amine complexes where:

$M_1 = Cu; M_2 = Zn, Co, Ni, Ba, Ca, Mn$;

$M_1 = Ni; M_2 = Zn, Co, Ba, Ca, Mn$ and

$M_1 = Mn; M_2 = Zn, Co, Ba, Ca$



Mixed metal-triethylenetetramine complexes
 $M_1(OAc)_2(trien):M_2(OAc)_2(trien)$

Figure 1.2 Structure of mixed metal-amine complexes where: $M_1 = Cu; M_2 = Zn, Ni$

1.3 Scope of the research

The scopes of this work were the synthesis of the mixed metal complex-amine catalysts. The characterization techniques employed were ATR-IR spectroscopy, UV-Vis spectroscopy, flame atomic absorption spectroscopy (FAAS), mass spectrometry and elemental analyses. Then, the reaction times during foam preparation were studied, namely gel time, cream time, tack free time and rise time. Afterward, rigid polyurethane foams were characterized by ATR-IR spectroscopy, compression testing, scanning electron microscopy (SEM) and thermogravimetry (TGA).

CHAPTER II

THEORY AND LITERATURE REVIEW

Theory

Although the reaction between isocyanate and hydroxyl compounds was originally identified in the 19th Century, the foundations of the polyurethanes industry were laid in the late 1930s with the discovery, by Otto Bayer, of the chemistry of the polyaddition reaction between diisocyanate and diols to form polyurethane. The first commercially available polyether polyol, poly(tetramethylene ether) glycol, was introduced by DuPont in 1956 by polymerizing tetrahydrofuran [5]. In 1960 Rigid foams based on polymeric MDI (PMDI) offered better thermal stability and combustion characteristics than those based on TDI. In 1967, urethane modified polyisocyanurate rigid foams were introduced, offering even better thermal stability and flammability resistance compared to low-density insulation products. During the 1960s, automotive interior safety components such as instrument and door panels were produced by back-filling thermoplastic skins with semi-rigid foam.

Starting in the early 1980s, water-blown microcellular flexible foam was used to mold gaskets for panel and radial seal air filters in the automotive industry. Since then, increasing energy prices and the desire to eliminate PVC plastic from automotive applications have greatly increased market share. Costlier raw materials are offset by a significant decrease in part weight and in some cases, the elimination of metal end caps and filter housings. Highly filled polyurethane elastomers, and more recently unfilled polyurethane foams are now used in high-temperature oil filter applications [6].

Of the 2.7 million tones of MDI produced globally in 2000 rigid polyurethane foams accounted for 45 percent, mainly for thermal insulation, and with energy-saving regulations tightening the volume is expected to increase. The major use of rigid polyurethane foam is in the construction industry, where its superior long-term

thermal insulation properties combined with good dimensional stability offer many benefits.

The demand for rigid polyurethane foam, whilst being mainly dependent on its low thermal conductivity, is also due to other factors such as good adhesion to facing materials and excellent mechanical strength at low density. Rigid foams can be made at densities from 10 to 1,100 kg/m³, but most are used in the range 28 to 50 kg/m³. Key developments in the past decade have focused on the introduction of environmentally acceptable blowing agents and improvements in catalyst performance.

2.1 Classified of cellular polymers

Foamed plastics have important, ever since man began to use wood, itself a cellular form of the polymer cellulose. Cellulose is the most abundant of all naturally occurring organic compounds [7]. Cellular polymers can also be classified according to their stiffness, the two extremes being rigid and flexible depending on the chemical composition, the rigidity of the polymer backbone, the degree of crystallinity and the degree of crosslinking (if any). Skochdopole and Rubens [8] have defined each term as follows;

2.1.1 Flexible foam

Open cell structured foams contain pores that are connected to each other and form an interconnected network which is relatively soft. The voids (gas cells) coalesce so that the combined solid and gaseous phases are continuous shown in Figure 2.1. Flexible foam densities range from the soft, cozy lounge chair in our living rooms to the durable, yet comfortable seat of our bicycles. The automotive industry uses flexible foam for arm rests, crash pads, side panels, dashboards, and seat cushions. Flexible foam is used as padding for the trucking industry, to protect produce from being damaged in transit. The medical industry uses flexible foam for airless wheelchair tires as well as for various prosthetic devices.

2.1.2 Rigid foam

Closed cell foams do not have interconnected pores. Normally the closed cell foams have higher compressive strength due to their structures. However, closed cell foams are also generally denser, require more material, and consequentially are more expensive to produce. The closed cells can be filled with a specialized gas to provide improved insulation. The gas is dispersed in the form of discrete gas bubbles shown in Figure 2.1. The closed cell structure foams have higher dimensional stability, low moisture absorption coefficients and higher strength compared to open cell structured foams. All types of foam are widely used as core material in sandwich structured composite materials.

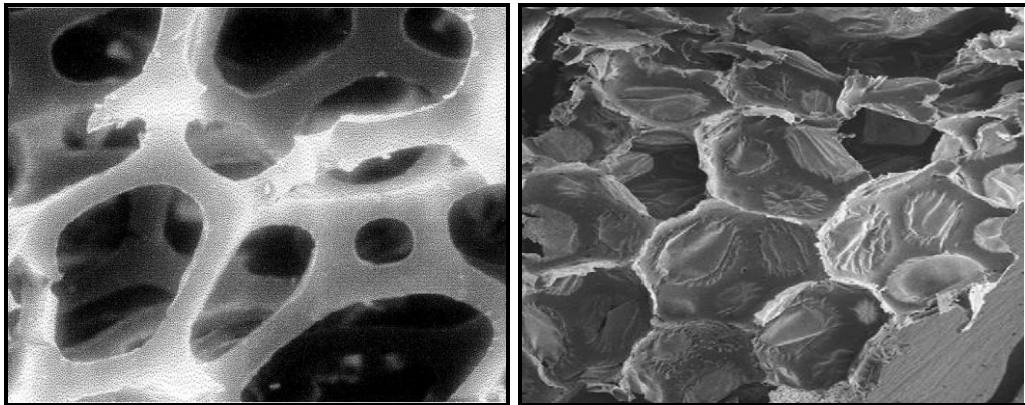


Figure 2.1 Open cell foam and closed cell foam structures [9]

Semi-rigid foams have compression hardness value between those of flexible and rigid foams, but are normally closer to flexible foams. Like flexible foams, they have: an open cell structure, hydrophobicity, flexibility at low temperatures and high temperatures and high temperature stability. The main differences lie in their higher compression hardness and slower recovery rates after compression. This makes them particularly suitable for applications where energy absorption is a key requirement such as interior and exterior automotive applications. Typical examples are instrument panels, knee bolsters, side-impact protection pads, headliners and bumper infill.

2.2 Raw materials

The properties of polyurethane foams can be modified within wide limits depending on the raw material used. The density, flow ability, compressive, tensile or shearing strength, the thermal and dimensional stability, combustibility and other properties can be adjusted to suit the requirements of a given application. The polyols and isocyanates have a major impact on the properties of the foams [4]. In addition, additive such as catalysts, surfactants and blowing agents are used to control and modify the reaction process and performance characteristics of the polymer.

2.2.1 Isocyanates

Isocyanates in general can be prepared in many ways. Besides some well-known laboratory scale methods, among them Curtius, Hofmann, and Lossen rearrangement via nitrene intermediates, there is a number of very special syntheses available to the chemist [10, 11]. Most of these methods, however, were not at all satisfactory for large-scale operation. It is almost exclusively the reaction of phosgene with amines or amine salts which is established commercially. The world's leading isocyanate producers for polyurethane applications are BASF, Bayer, Dow, Enichem, Huntsman ICI, Lyondell Chem. Technologie, and Mitsui. TDI and MDI/PMDI are manufactured via similar processes featuring exclusively phosgenation of the appropriate primary amine isomer mixtures (Figure 2.3), TDA and MDA [12].

In polyurethane chemistry the major focus is on the reactions of isocyanates with compounds that contain active hydrogen groups such as hydroxyl, water, amines, urea and urethane, but also the reactions of isocyanates with other isocyanates needs to be considered [13].

2.2.1.1 Toluene diisocyanate

Toluene diisocyanate (TDI) (liquid, bpt 120°C) TDI is most commonly available as a mixture of 80:20 and 65:35 of the 2,4 and 2,6 isomers, respectively. Toluene diisocyanate isomers were shown in Figure 2.2.

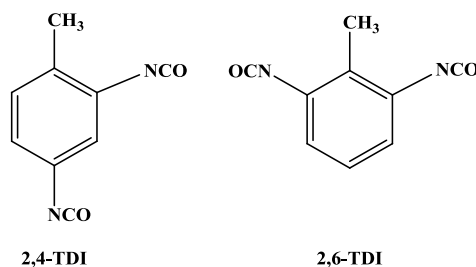


Figure 2.2 Toluene diisocyanate isomers used for PU foam manufacture

2.2.1.2 Methylene diphenylene diisocyanate (MDI)

4,4'-Diphenylmethane diisocyanate (solid, m.p. 38°C, b.p. 195°C) Pure MDI is a crystalline solid at room temperature, so it must be heated slightly in order to convert it into a more manageable form, i.e. a fairly high viscosity liquid. Molecular structure of MDI was shown in Figure 2.3.

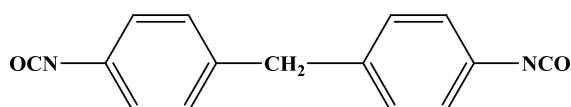


Figure 2.3 Molecular structure of MDI

2.2.1.3 Polymeric MDI

This is a complex mixture of molecules. It contains both 4,4'-MDI and 2,4'-MDI and different grades may have different ratios of these two. The production of isocyanate is based 99.9% on first synthesizing the required molecule structure, but with primary amine instead of isocyanate groups, followed by phosgenation of the amine groups to produce high yields of isocyanate shown in Figure 2.4. PMDA is subsequently phosgenated into the corresponding PMDI in the presence of an inert solvent.

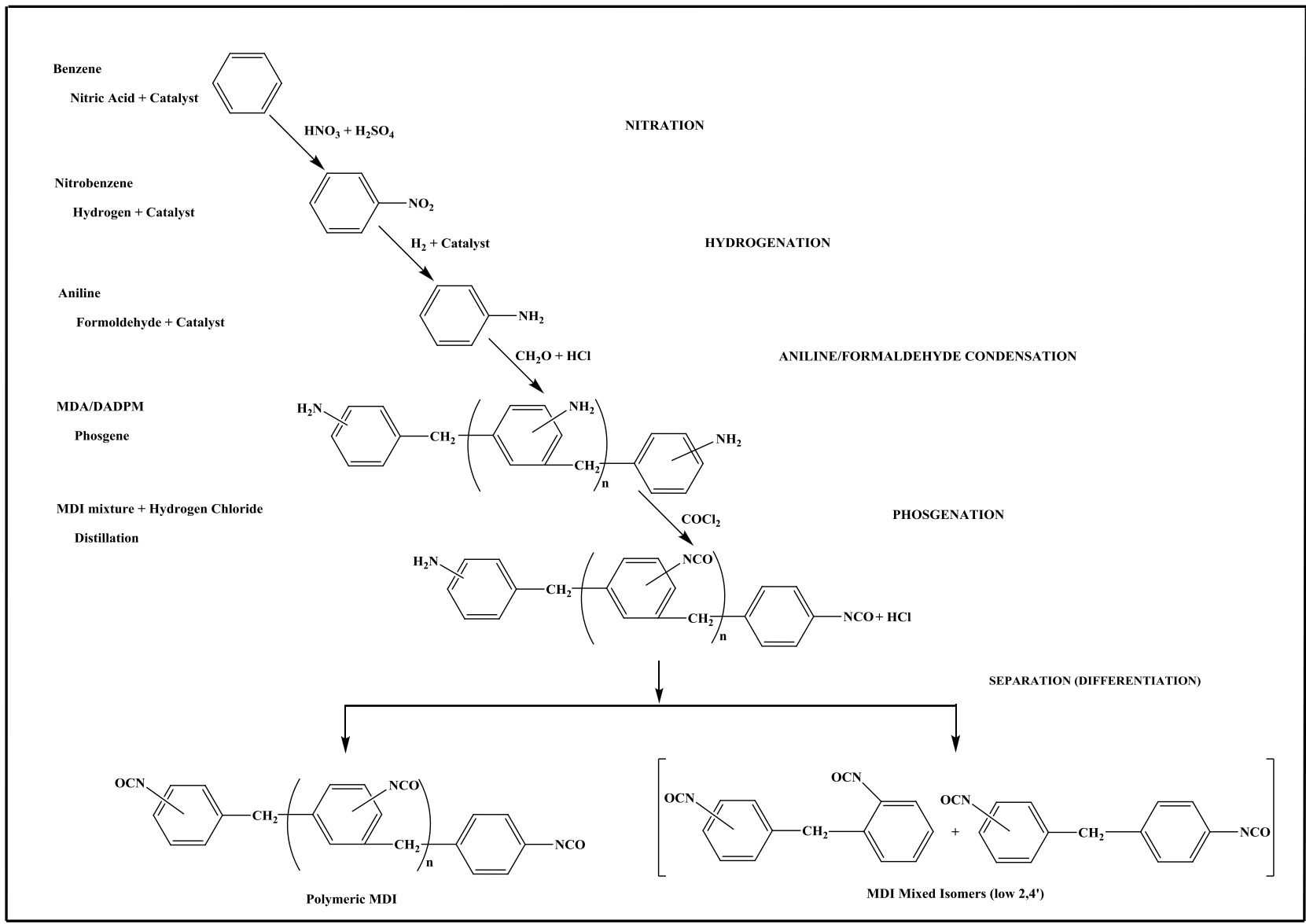


Figure 2.4 Benzene to PMDI [14]

2.2.2 Polyol

For rigid foams, primary and secondary hydroxyl group terminated polyether polyols are most important, followed by polyester polyols, which have the oldest application. The polyol used for the manufacture of PUR foams are usually either polyether or polyester type polyols. Generally, rigid foam polyol have molecular weight of 150-1000 g/mol, functionality 2.5-8.0 and hydroxyl value 250-1000 mgKOH/g. The segment length between junction points this effectively produces more tightly crosslinked networks [15].

The main application of polymeric polyols is as reactants to make other polymers, they can be reacted with isocyanates to make polyurethanes, and this use consumes most polyether polyols [16]. That degree of cross-linking has a dominant effect on the stiffness of the polymer: to obtain the rigid foam there must be a stiff polymer network, and, hence a high degree of cross-linking; for flexible foam a proportionately lesser degree of cross-linking is needed. These materials are ultimately used to make elastomeric shoe soles, foam insulation for appliances (refrigerators and freezers), adhesives, mattresses, automotive seats and so on. Although the high reactive isocyanate group is the unique feature of polyurethane technology, it is polyol that in large part determines the properties of the final polyurethane polymer. The extensive ranges of polyol types that are available to the industry explain why polyurethanes have become the most versatile family of plastic materials.

Specifications of commercial polyols include hydroxyl values which are used in stoichiometric formulation calculations. Examples are shown in Table 2.1.

Table 2.1 Specifications of commercial polyols including functionality values [13]

Alcohol	Chemical Structure	Functionality
Ethylene glycol (EG)	$\text{HO}-\text{CH}_2-\text{CH}_2-\text{OH}$	2
Diethylene glycol (DEG)	$\text{HO}-\text{CH}_2-\text{CH}_2-\text{O}-\text{CH}_2-\text{CH}_2-\text{OH}$	2
Glycerol	$\begin{array}{c} \text{CH}_2-\text{OH} \\ \\ \text{CH}-\text{OH} \\ \\ \text{CH}_2-\text{OH} \end{array}$	3
Trimethylol propane (TMP)	$\begin{array}{c} \text{CH}_2-\text{CH}_2-\text{OH} \\ \\ \text{CH}-\text{CH}_2-\text{OH} \\ \\ \text{CH}_2-\text{CH}_2-\text{OH} \end{array}$	3
Pentaerythritol	$\begin{array}{c} \text{CH}_2-\text{OH} \\ \\ \text{HO}-\text{CH}_2-\text{C}-\text{CH}_2-\text{OH} \\ \\ \text{CH}_2-\text{OH} \end{array}$	4
Sorbitol	$\text{HO}-\text{CH}_2-(\text{CHOH})_4-\text{CH}_2-\text{OH}$	6

2.2.2.1 Polyether polyols

Compounds with several hydroxyl groups, known as polyols, are, together with polyisocyanates, essential components in the manufacture of polyurethanes [17-19]. The polyfunctional starter compounds are mainly ethylene glycol, 1,2-propylene glycol, trimethylolpropane, glycerine, pentaerythritol, sorbitol and sugar, as well as the amines used as ethylenediamine and diaminotoluene.

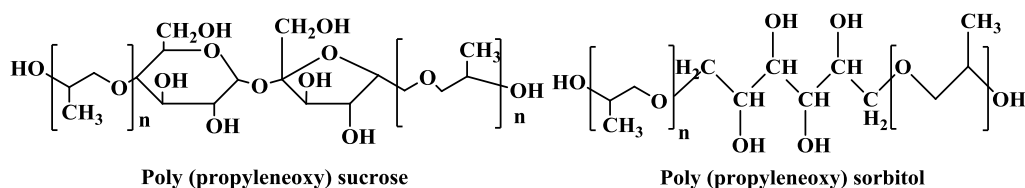
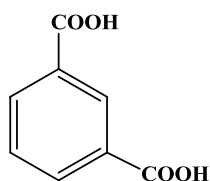
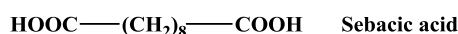
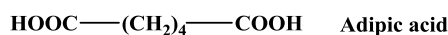


Figure 2.5 Structure of polyether polyol based sorbitol and sucrose used in the PUR foams

2.2.2.2 Polyester polyols

Compared with polyether polyols, polyester polyols tend to be more reactive, produce foams with better mechanical properties, are less susceptible to yellowing in sunlight and are less soluble in organic solvents. However, they are more expensive, more viscous and therefore more difficult to handle. Consequently, they are only used in applications that require their superior properties. Major application is in flexible foams for textile interlinings and shoulder pads (because polyester-based foams have high elongation and good resistance to dry cleaning solvents) and in improved for cushion packaging. Polyester polyols are made by condensation reaction between diols (and triols) and dicarboxylic acids such as:



m-Phthalic acid

Figure 2.6 Example of aliphatic and aromatic dicarboxylic acids used in the production of polyester polyols

2.2.3 Blowing agent

Blowing agents, sometimes referred to as foaming agents, are used to generate cells in polymeric materials. They are generally classified on the mechanism by which gas is created. First classified, physical Blowing Agents (PBAs) are gases or compounds that produce gases as a result of physical processes such as evaporation desorption at elevated temperatures, or reduced pressures. Second classified, chemical blowing Agents (CBAs) are individual compounds or mixtures of compounds that produce gas as a result of a chemical reaction. The chemical change is usually brought about with other decomposition or as a result of chemical reaction with components of the formulation.

Water acts as a blowing agent it produces CO₂ gas by reaction with a diisocyanate. Typical water concentrations are 3–5 parts of water per 100 parts of polyester polyol. The reaction of water with an isocyanate is exothermic and results in the formation of active urea sites which form crosslinks via hydrogen bonding. To reduce the high crosslink density of the foam, auxiliary blowing agents are used to produce low density foams with a softer feel than water-blown (only) foams, and to produce closed cell flexible foams [13].

2.2.4 Catalyst

Catalyst for rigid polyurethane foam include a range of chemical structures, such as tertiary amines, aromatic amine, quaternary ammonium salts, alkali metal carboxylates, and organo-tin compounds. Their catalyst activity is dependent on their basicity, with steric hindrance on the active site playing a secondary role. Catalyst plays a very important role in the reactions of isocyanates. Catalysts exert an influence upon the rates of competing reactions and have a major effect on the ultimate properties of the final foam. A typical catalyst system would consist of a mixture of a tertiary amine and organometallic compounds.

Tertiary amines, organometallics (primarily tin compounds) and carboxylic acid salts are used to catalyse the reaction of isocyanates with water (blowing) and

polyols (polymer gelation). The catalyst controls the relative reaction rates of the isocyanate with polyol and water.

Amine catalysts are generally considered to be predominantly blowing catalysts since they tend to catalyse the isocyanate-water reaction better than the isocyanate-polyol reaction. However, amines do catalyse both reactions, with the relative rates of each reaction being dependant on the specific amine catalyst used.

Organometallic catalysts are mainly seen as gelation catalysts although they do affect the isocyanate-water blowing reaction. Organotin are the most widely used, but organomercury and organolead catalysts are also used. The mercury catalysts are very good for elastomers because they give a long working time with a rapid cure and very good selectivity towards the gelation. The lead catalysts are often used in rigid spray foams. However, both mercury and lead catalysts have unfavourable hazard properties so alternatives are always being sought.

Potassium and sodium carboxylic acid salts and quaternary ammonium carboxylic acid salts are used to catalyze the trimerization reaction and thus are used mainly in isocyanurate foams.

Each catalyst type is specific for a particular chemical reaction. Catalyst mixtures are generally necessary to control the balance of (a) the polymerization: gelling and (b) the gas generation reactions: blowing; both are exothermic reactions. Getting the correct balance of polymerization and foaming is of major importance in the production of closed cell foam. The frequently used catalysts are shown in Table 2.2 [20].

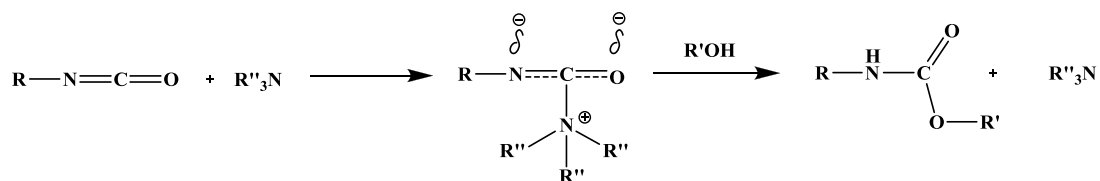
Table 2.2 Overview of frequently used catalysts in rigid polyurethane foams [20]

Catalyst	Code	Catalytic activity
Tertiary amines		
Pentamethyldiethylene triamine	PMDETA	Blowing
Triethylenediamine	TEDA	gelling
Dimethylcyclohexylamine	DMCHA	blowing/gelling
Quaternary ammonium salts		
2-hydroxy propyl trimethyl ammonium	TMR-2	delayed action/ trimer formation
Alkali metal carboxilates		
Potassium acetate	KAc	gelling/ trimer formation
Potassium octoate	KOct	gelling/ trimer formation
Tin complexes		
Stannous octate	SnOct	gelling
Dibutyltin dilaurate	DBTCL	gelling

2.2.4.1 Reaction mechanisms

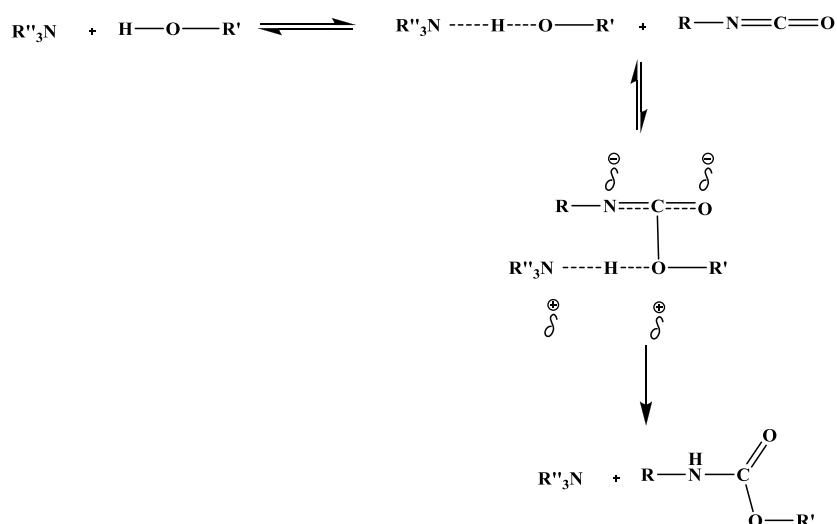
2.2.4.1.1 Amine catalysts

Tertiary amines are the most widely used polyurethane catalysts. Two mechanisms have been proposed for amine catalysis. In the one proposed by Baker (Scheme 2.1), the activation starts by the amine using its lone pair of electrons to coordinate with the carbon of the isocyanate group. This intermediate then reacts with active hydrogen from an alcohol to produce a urethane group.



Scheme 2.1 Baker mechanism amine catalyst [14]

In the second mechanism, proposed by Farka (Scheme 2.2), which is supported in the more recent literature, the activation starts by the amine interacting with the proton source (polyol, water, amine) to form a complex, which then reacts with the isocyanate.

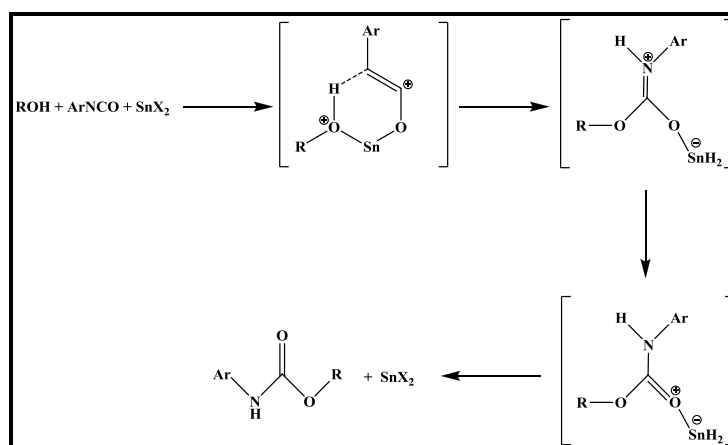


Scheme 2.2 Farka mechanism amine catalysts [14]

Factors that affect the catalytic activity of an amine are nitrogen atom basicity, steric hindrance, spacing of heteroatoms, molecular weight and volatility and end groups. The level of basicity is determined from the pKa value, defined as the pH at which the concentration of unprotonated and protonated forms, of an ionisable group, are equal.

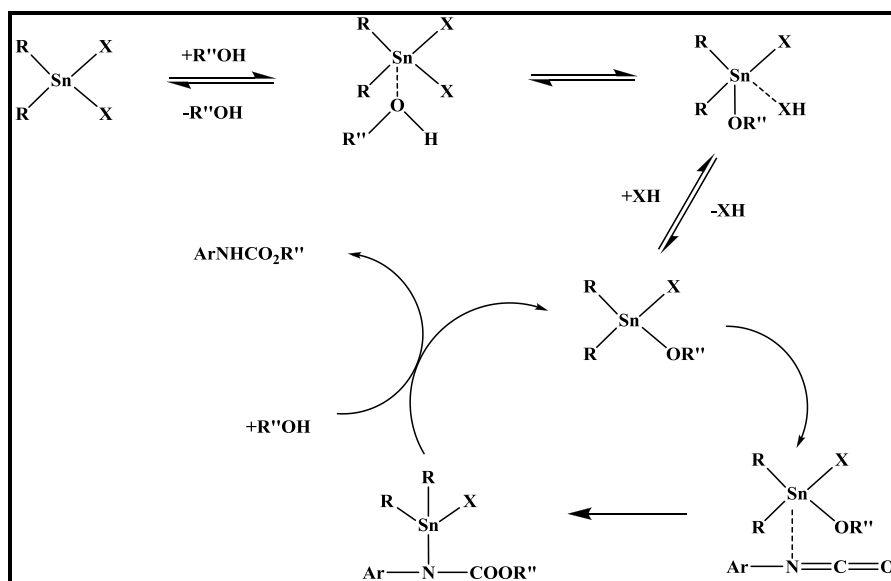
2.2.4.1.2 Organotin catalysts

For the tin II salts the following mechanism has been proposed, Scheme 2.3. The isocyanate, polyol and tin catalyst form a ternary complex, which then gives the urethane product. Two routes, not shown, to the complex have been proposed. In the first one the tin first adds to the polyol then the isocyanate. In the second one the tin adds to the oxygen of the isocyanate then reacts with the polyol.



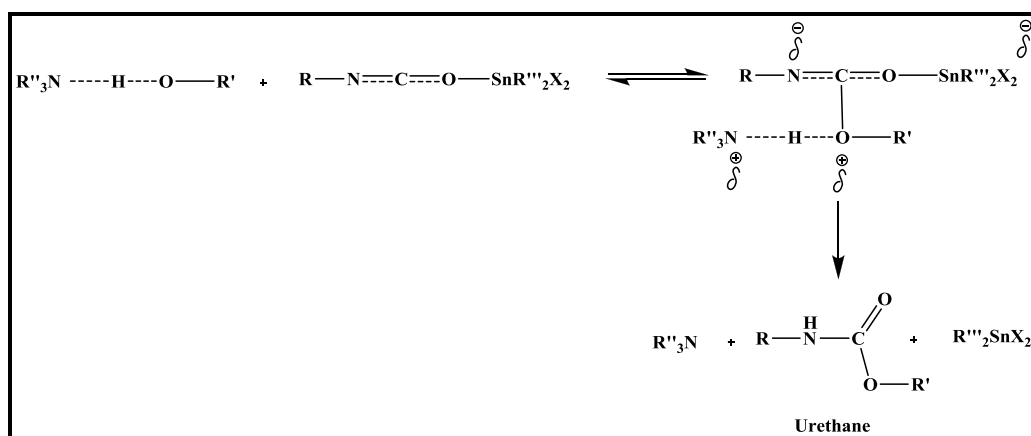
Scheme 2.3 Mechanism for tin II salts [14]

The proposed mechanisms for tin IV catalysts, dialkyltin dicarbonates and dialkyltin dialkylthiolates, is the reaction of the tin with a polyol forming a tin alkoxide, which can then react with the isocyanate to form a complex (Scheme 2.4). Transfer of the alkoxide anion onto the co-ordinated isocyanate affords an N-stannylurethane, which then undergoes alcoholysis to produce the urethane group and the original tin alkoxide.



Scheme 2.4 Mechanism for tin VI compounds [14]

A synergy between tin and amine catalysts is also observed. One of the proposed mechanisms is given in Scheme 2.5.



Scheme 2.5 Mechanism of tin-amine synergism [14]

Tin II compounds are used in flexible slabstock foam with the most common being stannous octoate. These are used because they become inactive during the foaming process, thus do not give any dry heat degradation. When tin IV compounds were used in this application, severe thermal oxidation occurred resulting in foams having much poorer physical properties.

2.2.5 Surfactants

The surfactants most commonly used in the polyurethane industry are polydimethyl siloxane-polyethyl copolymers. Since the late 1950s, these so called “silicone surfactants” almost completely replaced other organic, nonionic surfactants which were previously used before [21]. To obtain the most efficient bubble stability and prevent coalescence the correct balance of foam reactivity and surfactant activity must be obtained. In most polyurethane systems the surfactant must act within a few minutes since if this balance is not optimised the surfactant will not be able to do its job and surface film rupture and defoaming can occur.

Surfactants are used to modify the characteristics of both foam and non-foam polyurethane polymers. In foams, they are used to emulsify the liquid components, regulate cell size, and stabilize the cell structure to prevent collapse and sub-surface voids.

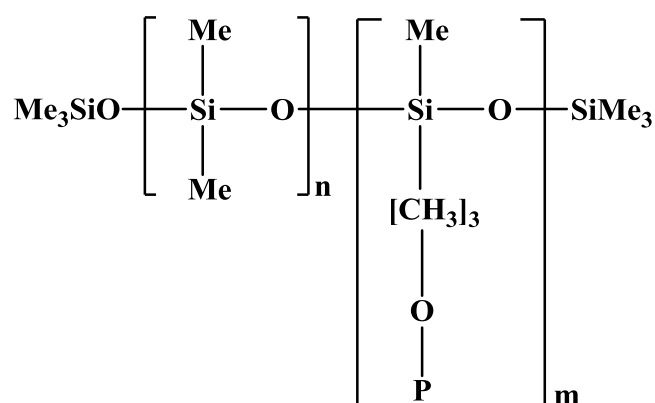


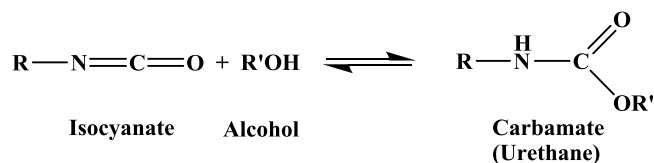
Figure 2.7 Structure of silicone surfactants used in PUR foams manufacture

2.3 Basic reactions of isocyanates

Polyurethanes (IUPAC abbreviation PUR, but commonly abbreviated PU) are in the class of compounds called reaction polymers. A urethane linkage is produced by reacting an isocyanate group, $-N=C=O$ with a hydroxyl (alcohol) group, $-OH$. Polyurethanes are usually made by reacting polyisocyanates with polyols in the presence of a catalyst, whose nature depends on the desired characteristics of the product to be formed [22].

2.3.1 Reactions between isocyanates and hydroxyl groups [14]

The most important reaction in the manufacture of polyurethanes is between isocyanate and hydroxyl groups. The reaction product is a carbamate, which is called a urethane in the case of high molecular weight polymers. The reaction is exothermic and reversible going back to the isocyanate and alcohol.



This reaction is known as the “gelling reaction”. Since it is an exothermic reaction it must be temperature controlled. The rate of polymerization is affected by the chemical structure of the isocyanate and polyol. A catalyst is used to accelerate the reaction rate.

2.3.2 Reactions between isocyanates and water

The reaction of isocyanates with water to produce an amine and carbon dioxide is highly exothermic. The initial reaction product is a carbamic acid, which breaks down into carbon dioxide and a primary amine. The amine will then react immediately with another isocyanate to form a symmetric urea. Due to the formation of carbon dioxide the water reaction is often used as a blowing agent as the level of blow can be tailored, simply by adjusting the amount of water in the formulation.

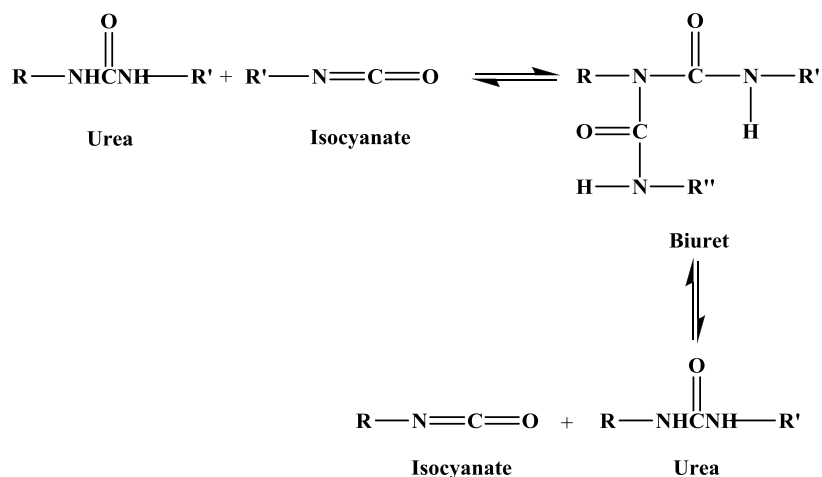
The reaction of unhindered isocyanates with primary amines at room temperature and in the absence of catalyst is 100 to 1,000 times faster than the reaction with primary alcohols. The reactivity of an amine increases with its basicity and consequently, aliphatic amines are much more reactive than aromatic amines. The reactivity of amines can be slowed down by the presence of electron withdrawing groups, another way is to increase the steric hindrance by branching on the carbon next to the nitrogen or introducing substituent in the ortho position of an aromatic amine.

The kinetics of the reaction of amines with isocyanates is complicated by strong product catalysis. Since the product urea is a much weaker base and more hindered than the amine, its catalysis is bi-functional and based on hydrogen bonds between urea and both amine and isocyanate.

2.3.4 Reactions between isocyanates and urea

Biurets are formed from the exothermic reaction of an isocyanate with a urea. With di-substituted urea, mostly formed by the water reaction (see above) a biuret is formed through the active hydrogen.

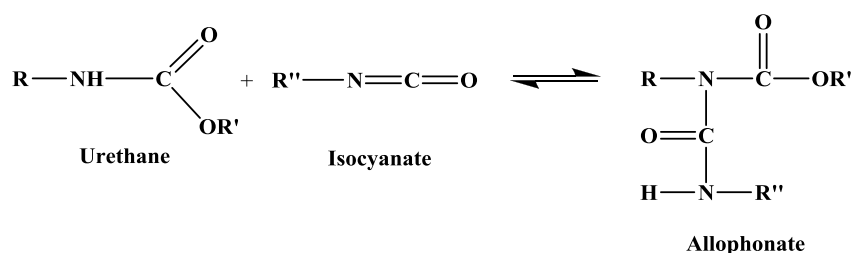
This reaction is significantly faster than the allophanate reaction and occurs at lower temperature, about 100°C compared to 120 to 140°C. In polyurethane systems this reaction, that is reversible upon heating, is often a source for additional cross-linking.



Another important feature of this urea-biuret equilibrium is the potential for redistribution of the biuret across the spectrum of isocyanate species. For instance, if polymeric MDI and a diisocyanate prepolymer are mixed together then the molecules of the di, tri, tetra and higher species are not initially smoothly distributed across the spectrum of derivatives-biuret, allophanate, uretonimine. However, they slowly re-distribute through the various reversible reactions. This redistribution will be faster at higher temperatures, resulting ultimately in a product stable in composition and viscosity.

2.3.5 Reactions between isocyanates and urethanes

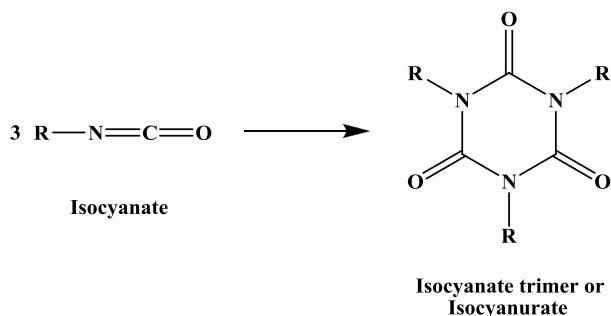
An allophanate group is the result of the exothermic reaction of isocyanate with the active hydrogen on a urethane group



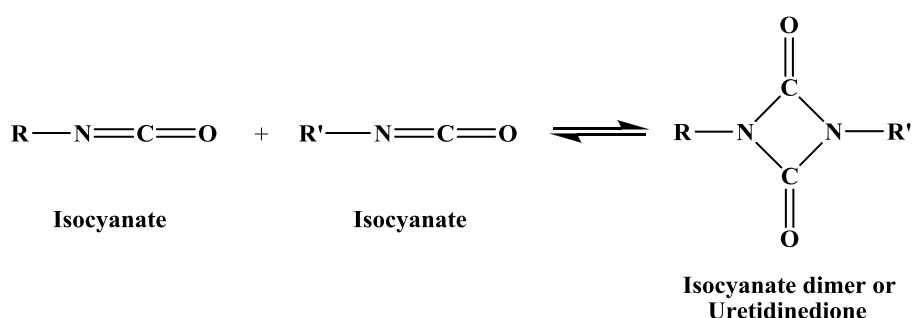
This reaction is slow compared to biuret formation and usually takes place uncatalysed at about 120 to 140°C. The reaction is reversible at temperatures above 150°C so, as with biurets, the reaction increases cross-linking in polyurethane systems. This reverse reaction takes place at lower temperature than with biurets so that the interchange of isocyanate homologues is faster, if the allophanates are heated with a third equivalent of isocyanate, the cyclic triisocyanurate or trimers can be obtained.

2.3.6 Reactions between isocyanates and isocyanates

Thermodynamically, the trimerization of isocyanates is favored. The usual reaction product is the isocyanurate ring.



For aliphatic isocyanates, asymmetric trimerization yielding imino-oxadiazine diones can also be done. Further observable reactions are the formation of dimers (uretidiones) from two isocyanate moieties and the formation of carbodiimides that are formed when two isocyanate groups combine with the simultaneous elimination of carbon dioxide. Carbodiimides further react with isocyanate forming uretone imines [14].



Both aliphatic and aromatic isocyanates readily form trimers. Under more severe conditions, polytrimerisation can occur. In general, trimerisation occurs mainly under the influence of basic catalysts, such as alkali metal alkoxides and carboxylic acid salts in particular. Other catalysts are acetates, carbonates, octoates and N,N-dimethylformamide. Organometallic compounds based on silicon and tin and transition metal elements also act as trimerization catalysts with an insertion reaction being involved in the mechanism. Trimerization can be an undesirable side reaction or a reaction used to introduce branching and cross-linking. It is used in the manufacture of rigid foams, where the cross-linked structure contributes to fire resistance.

Isocyanate trimers are thermally stable and not reversible like dimers, allophanates, biurets and uretonimines and isocyanurate foams of MDI only show significant degradation above 270°C. This is why the polyisocyanurate rigid foams (PIR) more easily meet national fire standards. They are used extensively in building insulation and roofing applications [22].

2.4 Formulations

The amount of isocyanate needed to react with polyol and other reactive components can be calculated to obtain chemically stoichiometric equivalents. This theoretical amount may be adjusted up or down dependent on the PU system, properties required, ambient conditions and scale of production. The adjusted amount of isocyanate used is referred to as the “isocyanate index”,

$$\text{Isocyanate index} = \frac{\text{actual amount of isocyanate}}{\text{theoretical amount of isocyanate}} \times 100$$

The conventional way of calculating the ratio of the components required for PUR manufacture is to calculate the number of part by weight of the isocyanate needed to react with 100 parts by weight of polyol and use proportionate amount of additives. The analytical data require for the calculation are the isocyanate value of the isocyanate and hydroxyl value, residual acid value and water content of the polyol and other reactive additives [4,23].

Isocyanate value (or isocyanate content) is the weight percentage of reactive-NCO groups:

$$\begin{aligned} \text{Isocyanate value} = \% \text{ NCO group} &= \frac{42 \times \text{functionality} \times 100}{\text{molar mass}} \\ &= \frac{4200}{\text{Equivalent weight}} \end{aligned}$$

Hydroxyl value (hydroxyl number; OHV) is expressed in mgKOH/g polyol. This may be defined as the weight of KOH in milligrams that will neutralize the acetyl group produced by acetylation of 1 g of polyol.

$$\begin{aligned}\text{Hydroxyl value} &= \frac{56.1 \times \text{functionality} \times 1000}{\text{molar mass}} \\ &= \frac{56.1 \times 1000}{\text{Equivalent weight}}\end{aligned}$$

Acid value is also expressed as mgKOH/g of polyol and numerically equal to OHV on isocyanate usage.

Water content; water reacts with two –NCO groups and the equivalent weight of water is thus:

$$\text{Equivalent weight} = \frac{\text{molar mass}}{\text{functionality}} = \frac{18}{2}$$

Isocyanate conversion (α), isocyanate conversion can be calculated by FTIR method [24], defined as the ratio between isocyanate peak area at time t and isocyanate peak area at time O:

$$\text{Isocyanate conversion (\%)} = \left[1 - \frac{\text{NCO}^f}{\text{NCO}^i} \right] \times 100$$

Where; NCO^f = the area of isocyanate absorbance peak area at time t
(final isocyanate)

NCO^i = the area of isocyanate absorbance peak area at time O
(initial isocyanate)

2.5 Mechanical properties

The mechanical properties of rigid foams differ markedly from those of flexible foams. The tests used to characterize both types of foam therefore differ, as do their application areas.

Compression load deflection is used to determine the compressive stress-strain behavior, i.e. it is a measure of the load-bearing properties of the material. The test method is somewhat similar to that developed for noncellular plastics. Test on rigid and flexible foams can be determined according to ASTM D1621-04. A universal testing machine fitted with a compression rig (cage) consisting of two parallel flat plates (Figure 2.8) is used for the tests.

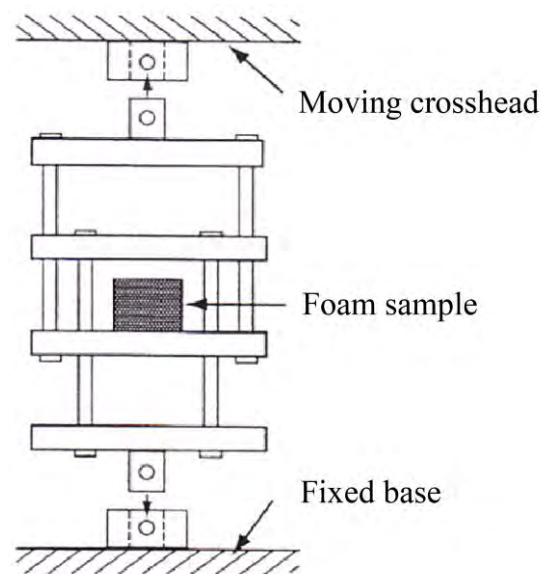


Figure 2.8 Compression load deflection test rig [14]

Compressive properties are perhaps the most important mechanical properties for cellular polymers. Compressive energy absorption characteristics and deformation characteristics of foam depend mainly on density, type of base polymer and the predominance of either open or closed cells. In simple terms, open cell foam (invariably flexible) relies on cell walls bending and bucking, which is essentially a reversible process (Figure 2.8)

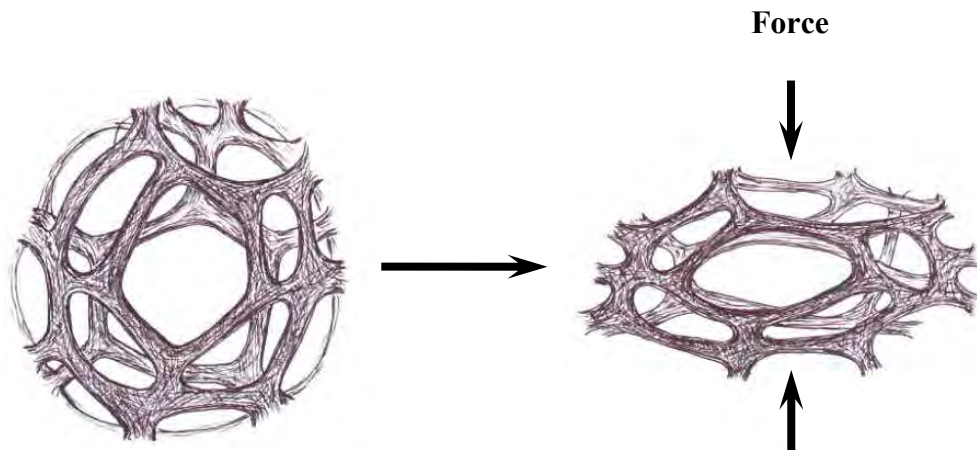


Figure 2.9 Schematic representation of open cell deformation [14]

In addition, as the cell become more compacted during compression, the escape of air through and out of the foam will become increasingly more difficult. The entrapped air will therefore offer some resistance to foam deformation during the final stages of compression. On the other hand, air flow is not a consideration with closed cell foams. In this case (Figure 2.10) deformation involves cell wall bending/buckling (reversible), gas compression, cell wall stretching/yielding (non-reversible). Severe compression causes cell rupture.

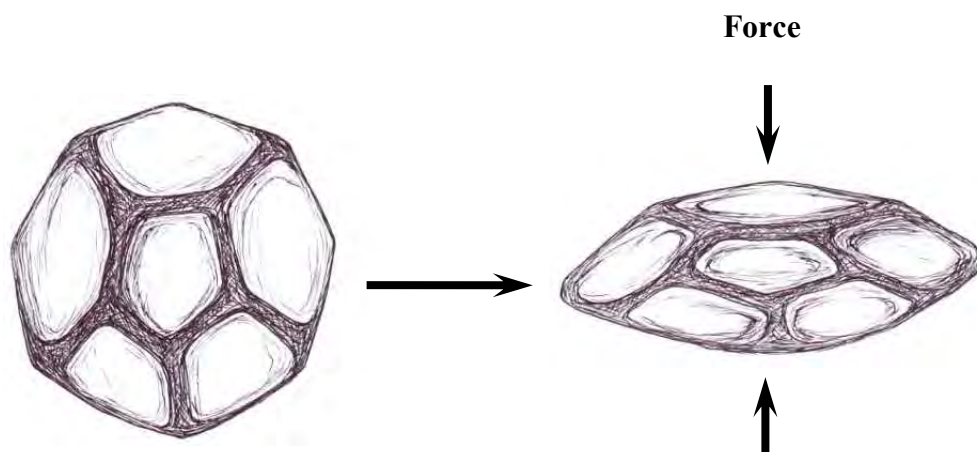


Figure 2.10 Schematic representation of closed cell deformation [14]

Closed cell rigid foams (e.g. PUR foams) exhibit from very limited to no yielding behavior. Consequently, gas compression and matrix strength play important roles during the mechanical deformation of rigid foams. In addition, cell rupture often

occurs during the energy absorption process. The energy absorption characteristics of foam can be represented in term of compression stress-strain curves. Figure 2.10 show typical compression stress-strain curve of rigid cellular polymers.

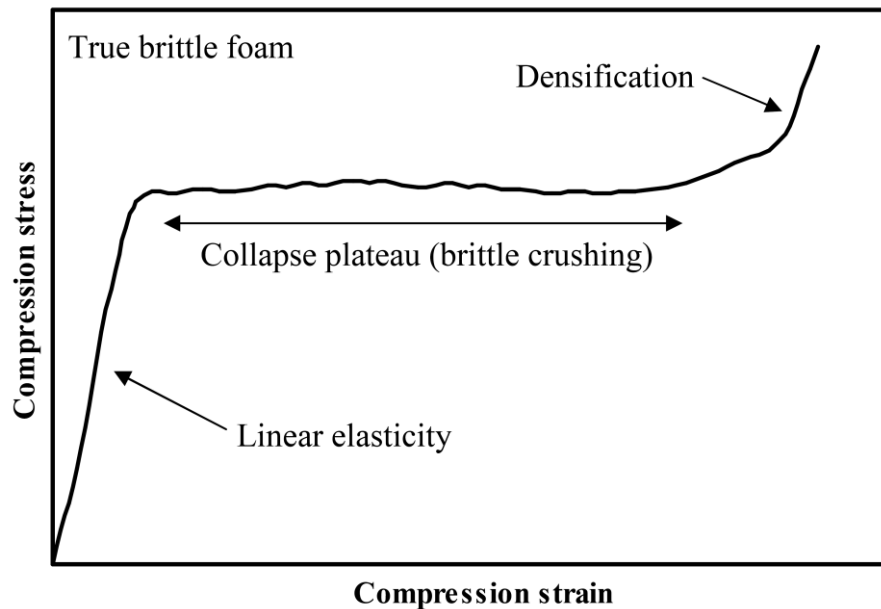


Figure 2.11 Typical compression stress-strain curve for rigid foams

For rigid foams, elements of true brittle crushing are superimposed on the elastic/plastic response. The erratic nature of the collapse plateau corresponds to intermittent rupturing of individual cells. Due to cell rupture in rigid foams, resilience is dramatically affected. Foams can generally withstand only single impacts, for example the liners used inside riding or cycle helmets.

The compressive strength of rigid cellular polymers is usually reported at some definite deformation (5 or 10%). The modulus is then extrapolated to 0% deformation unless otherwise stated. Structural variables that affect the compressive strength and modulus of this foam are, in order of decreasing importance, plastic phase composition, density, cell structure, and gas composition.

Literature reviews

Polyurethane foam has found applications in industry as general use, low-density, insulating materials. Applications include construction panel sandwich structures, cushions and insulation panels for a variety of appliances including refrigerators [25, 26]. Rigid polyurethane foam is widely used as a core material in sandwich structures, yielding lightweight structures [27]. Of course, require the use of a blowing agent to create the foam structure. Most rigid foam, however, is made using physical blowing with volatile liquid chlorofluoromethane, CFM-11. The CFM gas has a much low thermal conductivity than air and, because it is retained within the closed cell structure [28]. Nowadays, the requirement for the development of all water-blown polyurethane foam system is getting higher, because the environmentally friendly blowing agent is carbon dioxide, which is obtained in the reaction between polyisocyanurate and water, but the dimensional stability of the foams of this type is not sufficient [29].

For the polyurethane foam synthesis, two chemical processes are of key importance [30] (Figure 2.11): (1) the “gelation reaction,” in which the alcohol component reacts with the isocyanate component in a polyaddition to form polyurethane; and (2) the “foaming reaction,” which creates gaseous CO₂ (blowing agent in PU foams) by the reaction of isocyanate (NCO) groups with water.

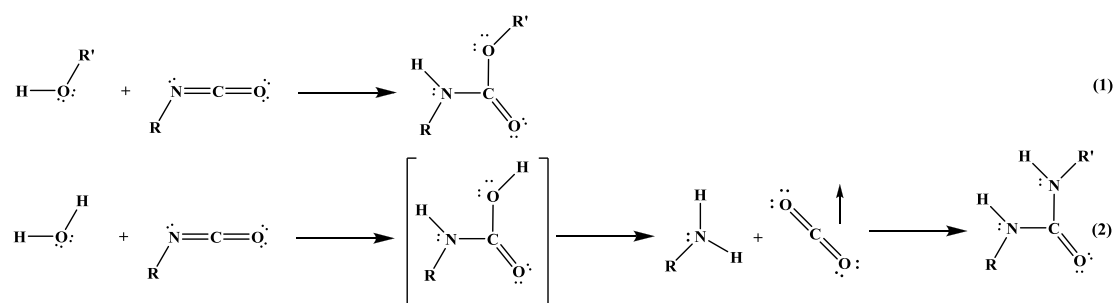


Figure 2.12 Key reactions in polyurethane foam synthesis

Catalysis has been an important field for polyurethane chemistry and many improvements have been accomplished in recent years. Some of the greatest challenges however still remain. Generally, PU catalysts can be divided according to

their function into gel catalysts, blow catalysts, and skin cure catalysts. Such as, in polyurethane foam industry, catalyst is necessary for the production. The catalysis of the isocyanate-hydroxyl reaction has been studied by many authors [31] who found that the reaction of aliphatic isocyanates with hydroxyl groups is catalyzed by many metal carboxylates and organotin compounds. Tertiary amine catalysis of the reaction of aromatic isocyanates with hydroxyl groups has been practiced for some time and is common for the preparation of rigid polyurethane foams [32].

Maris and coworkers [2] studies polyurethane catalysis by tertiary amines. They found that tertiary amines play an important role. In general, the tertiary amine coordinate to the positive electron charged carbon of the NCO group or hydrogen of the OH group and forms a transition state to activate urethane formation reaction. It is said that a tertiary amine can be tuned by maximizing its ability to form a hydrogen bond with alcohol, thereby activating the O–H bond so it can attach to the isocyanate more easily.

Metal-amine complexes have been known due to their applications in polymer synthesis. Their synthesis, characterization and application as crosslinking agents and catalysts are as follows:

Zelevák and coworkers [33] studied three copper acetate complex compounds, namely $\text{Cu}(\text{CH}_3\text{COO})_2(\text{en})_2 \cdot 2\text{H}_2\text{O}$, $\text{Cu}(\text{CH}_3\text{COO})_2(\text{tn})_2$ and $\text{Cu}_2(\text{CH}_3\text{COO})_4(\text{pyz})$ (*en*=ethylenediamine, *tn*=1,3-diaminopropane, *pyz*=pyrazine), were prepared and characterized by thermogravimetry (TGA) under argon, differential thermal analysis (DTA) and evolved gas analysis (EGA) using mass spectrometry (MS). The results of infrared spectroscopy (IR) were evaluated to be used as a spectroscopic criterion for the determination of the carboxylate binding mode in the compounds.

Cara and coworkers [34] studied preparation mixed amines and thy physical properties of complexes of the type $[\text{Ni}(\text{trien})(\text{en})]_x$ (*trien* = triethylenetetra-amine; *en* = ethylenediamine; *x* = Cl, Br, I, SCN, NO₃, ,ACO, ClO₄ and BPh₄ and $[\text{Cu}(\text{trien})(\text{en})]_x$ (*x*=ClO₄ and BPh₄) are reported. The results indicate that both in

solution and in the solid state the compounds are octahedral and that in solution the racemic mixture is present.

Copper carboxylates attract research interest in the field of catalysis [35]. Such systems are prepared by reaction of the corresponding carboxylate salt with bidentate amine (e.g. ethylenediamine) followed by the addition of a salt containing non-coordinating anions [36-37] or, by reaction of metal carboxylate with the organic ligand in a low ligand : metal ratio [38, 39]. The formation of mixed metal complexes was studied.

Kurnoskin [40, 41] synthesized metaliferous epoxy chelate polymers (MECPs) by hardening of the diglycidyl ether of bisphenol A (DGEBA) with the chelates of metals (Mn^{4+} , Fe^{3+} , Ni^{2+} , Cu^{2+} , Zn^{2+} and Cd^{2+}) and aliphatic amines (ethylenediamine, diethylenetriamine, triethylenetetramine and cycloethylated diethylenetriamine). The reactivity of the complexes in reactions with DGEBA and its dependence on the structures of the chelates has been investigated. MECPs have been found to possess increased strength and heat resistance.

Inoue and coworkers [42] studied amine-metal complexes as an efficient catalyst for polyurethane syntheses. Since the reaction of aliphatic isocyanates on preparations of polyurethane are very slow compared with aromatic isocyanates. Therefore, tertiary amines and tin compounds having excellent catalytic activity are used mainly as catalysts for polyurethane formation. In particular, dibutyltindilaurate (DBTDL) has been used. However, tin is toxic to human beings. Accordingly, a new catalyst or catalytic system is necessary to replace this catalyst. In this research they prepared the complexes of $M(acac)_n$ [$M = Mn, Fe, Co, Ni$ and Cu] and tertiary amines are used as new catalysts for the reaction between hexamethylene diisocyanate (HDI) and polyols. They found that $Mn(acac)_n$ -TEDA complex (TETA = Triethylenediamine) showed better catalytic activity than other $M(acac)_n$ complexes and showed comparable catalytic activity with DBTDL catalyst.

The researchers in our group, Pengjam [43] and Saengfak [44], synthesized new class of catalyst for the preparation of rigid polyurethane (RPUR) foams. Metal(II)-amine complexes, $M(OAc)_2(en)_2$ and $M(OAc)_2(trien)$ ($M = Cu, Mn, Ni, Co$,

en = ethylenediamine and trien = triethylenetetramine), were synthesized and used as catalysts in the preparation of RPUR foams. The catalytic activity of metal(II)-amine complexes and properties of RPUR foams were investigated and compared to those prepared by *N,N*-dimethylcyclohexylamine (DMCHA), which is a common commercial tertiary amine catalyst used in the preparation of RPUR foams.

In the preparation of rigid polyurethane (RPUF) foams catalyzed by metal-ethylenediamine complexes; $\text{Cu}(\text{OAc})_2(\text{en})_2$, They showed good reaction times, however, the polymerization was fast and difficult to control. Moreover, the obtained foams had dark color which was due to the color of $\text{Cu}(\text{OAc})_2(\text{en})_2$. Therefore, this research focused on the of rigid polyurethane (RPUF) foams catalyzed by mixed metal-ethylenediamine complexes; $\text{M}_1(\text{OAc})_2(\text{en})_2$: $\text{M}_2(\text{OAc})_2(\text{en})_2$. It was expected that the mixed metal complexes showed good solubility and appropriate catalytic activity, which should give the desirable physical and mechanical properties of RPUR foams.

In the manufacture of RPUR foams, the balance of gelling and blowing reactions is critical to obtain the target morphology and physical properties. The desired RPUR foam characteristics are as follows: fast reaction time, its surface rapidly stops to be gluing, displays a regular cell structure, and does not contract (collapse) after the initial volume growth. In this work, mixed metal-amine complexes were used in the preparation of RPUR foams. (Figure 2.13) shows an example of the complex. The results were compared with a commercial amine catalyst, *N,N*-dimethylcyclohexyl amine (DMCHA), which is known to be gelling and blowing catalysts [20] (Figure 2.14) in order to evaluate the catalytic activity of mixed metal-amine complexes.

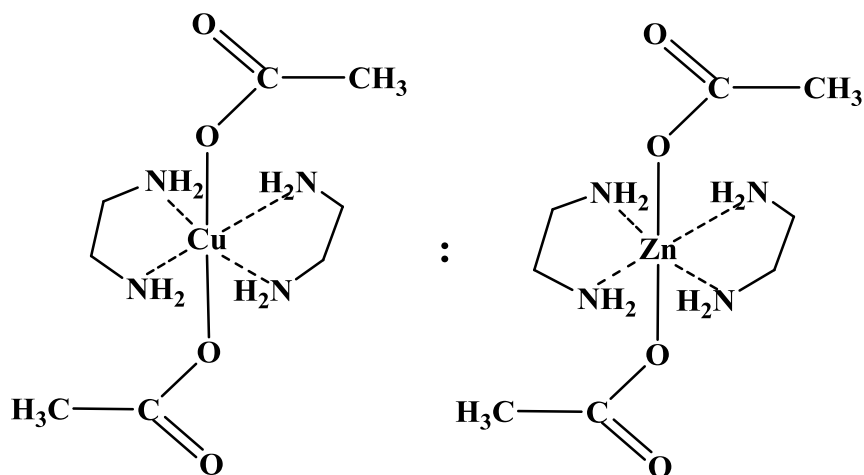


Figure 2.13 An example of mixed metal-amine complex,

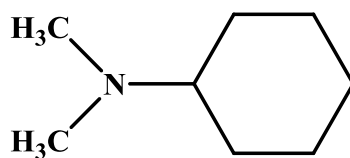
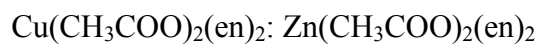


Figure 2.14 N, N-dimethylcyclohexyl amine (DMCHA) [20]

CHAPTER III

EXPERIMENTAL

3.1 Chemicals

Calcium acetate monohydrate [Ca(OAc)₂.H₂O], barium (II) acetate (Ba(OAc)₂), cobalt (II) acetate tetrahydrate [Co(OAc)₂.4H₂O], manganese (II) acetate tetrahydrate [Mn(OAc)₂.4H₂O], nickel (II) acetate tetrahydrate [Ni(OAc)₂.4H₂O], copper (II) acetate monohydrate [Cu(OAc)₂.H₂O], zinc acetate dihydrate [Zn(OAc)₂.2H₂O], salicylic acid [C₆H₄(OH)COOH], ethylenediamine (en) and triethylenetetramine (trien) were obtained from Fluka and Aldrich. Polymeric MDI (4,4' methane diphenyl diisocyanate; PMDI, MR-200): %NCO = 31.0 (%wt.), average functionality = 2.7 and polyol (Raypol[®] 4221, sucrose-based polyether polyol), hydroxyl value (OHV) = 440 mgKOH/g, functionality = 4.3 were supplied by South City Petrochem Co., Ltd. Polysiloxane (TEGOSTAB B8460, Goldschmidt) were obtained from South City Petrochem Co., Ltd. was used as a surfactant. Distilled water was used as a chemical blowing agent. *N,N*-dimethylcyclohexylamine (DMCHA) (South City Petrochem Co., Ltd.) was used as a commercial reference catalyst.

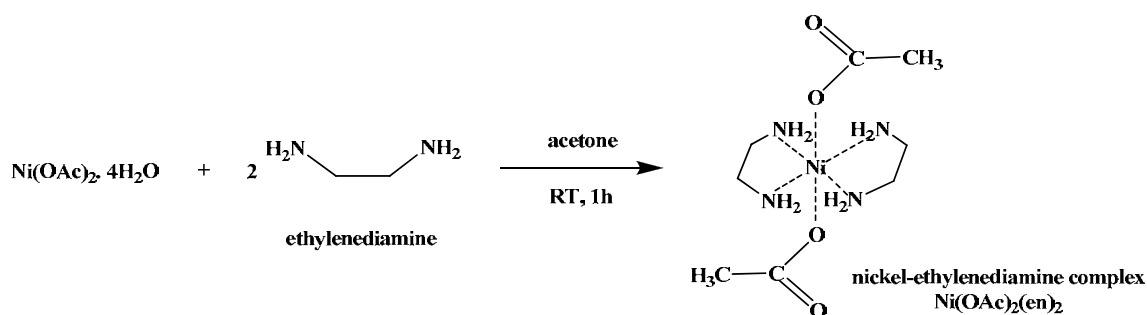
3.2 Synthetic procedures

Metal-amine and mixed metal-amine complexes were synthesized using two methods. In the first method, the metal complex was synthesized using acetone as a solvent [5]. The metal complex was separated from the reaction mixture before using in the preparation of rigid polyurethane foam. In the second method, the preparation of metal complexes was done in water [38] to obtain an aqueous solution containing metal complexes. The metal complex solution was then used in the preparation of rigid polyurethane foam without purification.

3.2.1 Synthesis of metal-amine complexes in acetone

3.2.1.1 Synthesis of metal-ethylenediamine complexes $[M(OAc)_2(en)_2]$

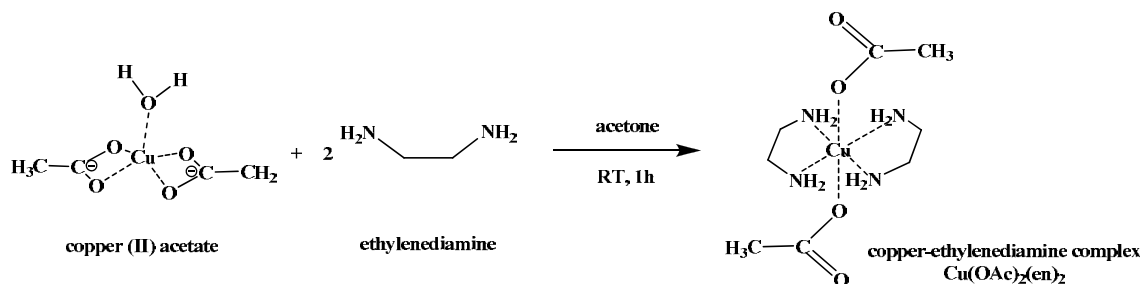
3.2.1.1.1 Synthesis of nickel-ethylenediamine complex



Scheme 3.1 Synthesis of nickel-ethylenediamine complex

The preparation of $Ni(OAc)_2(en)_2$ was performed according to the method reported in the literature [37] as follows: a solution of ethylenediamine (0.33 mL, 5.49 mmol) was stirred in acetone (20 mL) at room temperature for 30 minutes. After that, nickel (II) acetate tetrahydrate (0.59 g, 2.37 mmol) was added and the reaction mixture was stirred at room temperature for 1 hour. Precipitation of $Ni(OAc)_2(en)_2$ complexes was dried under vacuum. $Ni(OAc)_2(en)_2$ was obtained as a purple-red powder (0.57 g, 57%): IR (KBr, cm^{-1}): 3460, 3275 (NH stretching), 2946, 2944, 2890 (CH), 1572 (asymmetric C=O), 1408 (symmetric C=O), 1333 (CN stretching), 1034 (CO stretching). m/z 351.807, UV; λ_{max} (MeOH) = 344 nm, molar absorptivity (ϵ) = 60.

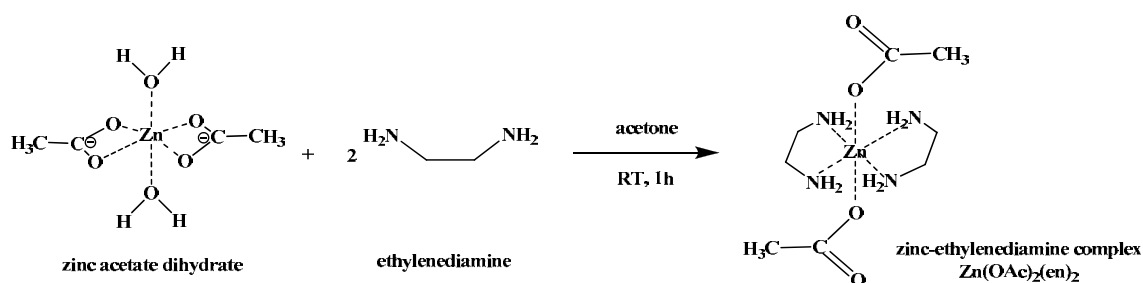
3.2.1.1.2 Synthesis of copper-ethylenediamine complex



Scheme 3.2 Synthesis of copper-ethylenediamine complex

The preparation of $\text{Cu}(\text{OAc})_2(\text{en})_2$ was performed according to the method reported in the literature [5] as follows: a solution of ethylenediamine (0.45 mL, 7.48 mmol) was stirred in acetone (20 mL) at room temperature for 30 minutes. After that, copper (II) acetate monohydrate (0.60 g, 3.02 mmol) was added and the reaction mixture was stirred at room temperature for 1 hour. $\text{Cu}(\text{OAc})_2(\text{en})_2$ precipitated from blue solution and was subsequently isolated by filtration and was dried under vacuum to remove solvent. $\text{Cu}(\text{OAc})_2(\text{en})_2$ was obtained as a purple powder (0.62 g, 62%): IR (KBr, cm^{-1}); 3318, 3269, 3139 (NH), 2986, 2953, 2884 (CH), 1545 (asymmetric C=O), 1396 (symmetric C=O), 1326 (CN), 1039 (CO). m/z 320.876, UV; λ_{max} (MeOH) = 230 nm, molar absorptivity (ϵ) = 4,790.

3.2.1.1.3 Synthesis of zinc-ethylenediamine complex



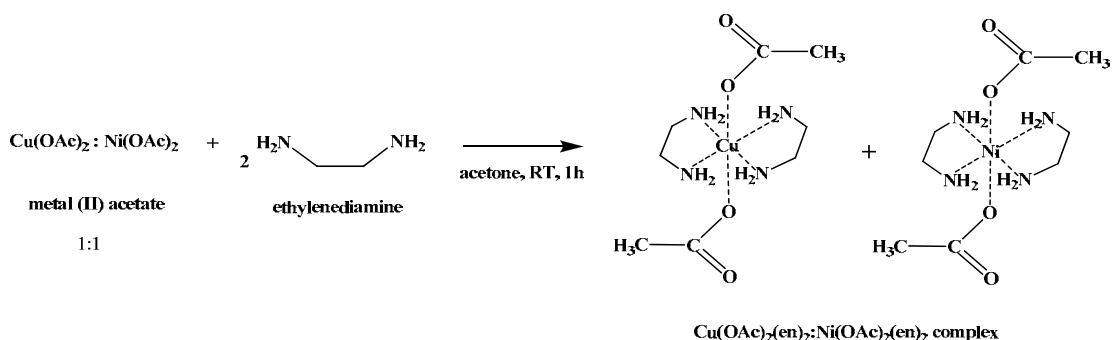
Scheme 3.3 Synthesis of zinc-ethylenediamine complex

The preparation of $\text{Zn}(\text{OAc})_2(\text{en})_2$ was done as follows: a solution of ethylenediamine (0.44 mL, 7.32 mmol) was stirred in acetone (20 mL) at room

temperature for 30 minutes. After that, zinc (II) acetate dihydrate (0.60 g, 2.75 mmol) was added and the reaction mixture was stirred at room temperature for 1 hour. $\text{Zn(OAc)}_2(\text{en})_2$ precipitated from white solution and was subsequently isolated by filtration and was dried under vacuum to remove solvent. $\text{Zn(OAc)}_2(\text{en})_2$ was obtained as a white powder (0.48 g, 48%): IR (KBr, cm^{-1}); 3266, 3165 (NH stretching), 2965, 2929, 2884 (CH stretching), 1553 (asymmetric C=O), 1397 (symmetric C=O), 1335 (CN stretching), 1035 (CO stretching). UV; λ_{max} (MeOH) = 201.0 nm, molar absorptivity (ϵ) = 1,449, m/z 322.785 Anal. Calc. for $\text{ZnC}_5\text{O}_4\text{H}_{12}\text{N}_4$: C 31.64; H 7.31; N 18.45; found C 31.32; H 7.74; N 18.47.

3.2.1.2 Synthesis of mixed metal-ethylenediamine complexes

3.2.1.2.1 Synthesis of $\text{Cu(OAc)}_2(\text{en})_2:\text{Ni(OAc)}_2(\text{en})_2$ complex

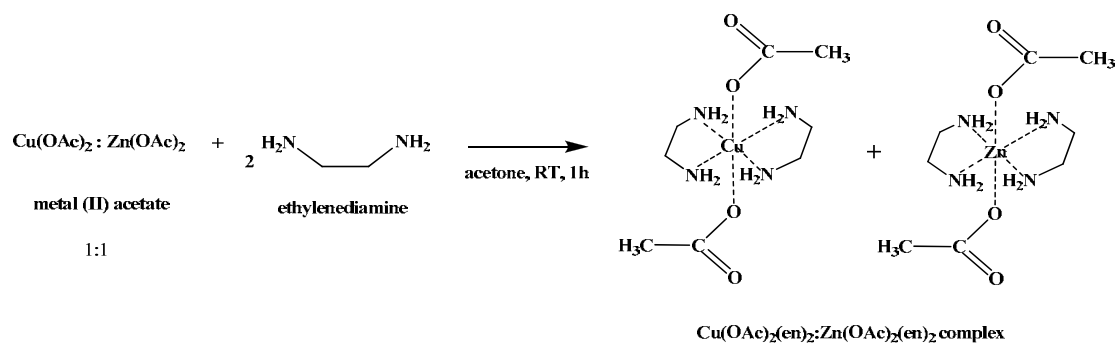


Scheme 3.4 Synthesis of $\text{Cu(OAc)}_2(\text{en})_2:\text{Ni(OAc)}_2(\text{en})_2$ complex

A solution of ethylenediamine (0.45 mL, 3.30 mmol) was stirred in acetone (10 mL) at room temperature for 30 minutes. After that, copper (II) acetate monohydrate (0.30 g, 1.51 mmol) and nickel acetate tetrahydrate (0.29 g, 1.19 mmol) were added and the reaction mixture was stirred at room temperature for 1 hour. $\text{Cu(OAc)}_2(\text{en})_2:\text{Ni(OAc)}_2(\text{en})_2$ precipitated from purple solution and was subsequently isolated by filtration and was dried under vacuum to remove solvent. $\text{Cu(OAc)}_2(\text{en})_2:\text{Ni(OAc)}_2(\text{en})_2$ was obtained as a purple powder. (0.71g, 71%): IR (KBr, cm^{-1}); 3266, 3146 (NH), 2937, 2884 (CH), 1545 (asymmetric C=O), 1396 (symmetric C=O), 1336 (CN), 1011 (CO). $\text{Cu(OAc)}_2(\text{en})_2$ shown m/z 320.876 and

$\text{Ni}(\text{OAc})_2(\text{en})_2$ shown m/z 298.734, UV; λ_{max} (MeOH) = 233 nm, molar absorptivity (ϵ) = 5,236.

3.2.1.2.2 Synthesis of $\text{Cu}(\text{OAc})_2(\text{en})_2:\text{Zn}(\text{OAc})_2(\text{en})_2$ complex

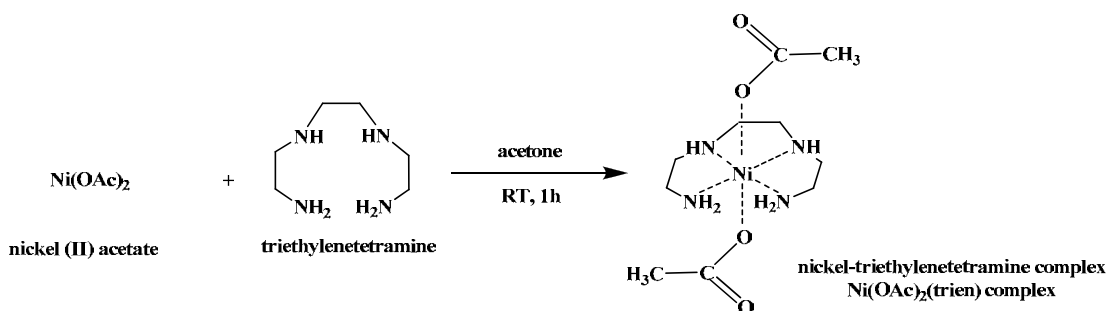


Scheme 3.5 Synthesis of $\text{Cu}(\text{OAc})_2(\text{en})_2:\text{Zn}(\text{OAc})_2(\text{en})_2$ complex

A solution of ethylenediamine (0.45 mL, 3.30 mmol) was stirred in acetone (10 mL) at room temperature for 30 minutes. After that, copper (II) acetate monohydrate (0.29 g, 1.49 mmol) and zinc acetate dihydrate (0.30 g, 1.38 mmol) were added and the reaction mixture was stirred at room temperature for 1 hour. $\text{Cu}(\text{OAc})_2(\text{en})_2:\text{Zn}(\text{OAc})_2(\text{en})_2$ precipitated from purple solution and was subsequently isolated by filtration and was dried under vacuum to remove solvent. $\text{Cu}(\text{OAc})_2(\text{en})_2:\text{Zn}(\text{OAc})_2(\text{en})_2$ was obtained as a purple powder (0.64g, 64%): IR (KBr, cm^{-1}); 3317, 3267, 3139 (NH), 2986, 2953, 2884 (CH), 1545 (asymmetric C=O), 1396 (symmetric C=O), 1326 (CN), 1039 (CO). UV; λ_{max} (MeOH) = 233 nm, molar absorptivity (ϵ) = 6,005. $\text{Cu}(\text{OAc})_2(\text{en})_2$ shown m/z 361.801 and $\text{Zn}(\text{OAc})_2(\text{en})_2$ shown m/z 363.789, Anal. Calc. for $\text{CuZnC}_8\text{O}_4\text{H}_{22}\text{N}_4 \cdot 2\text{H}_2\text{O}$: C 28.35; H 7.75; N 16.54; found C 28.92; H 7.57; N 16.90.

3.2.1.3 Synthesis of metal-triethylenetetramine complexes; $M(\text{OAc})_2(\text{trien})$

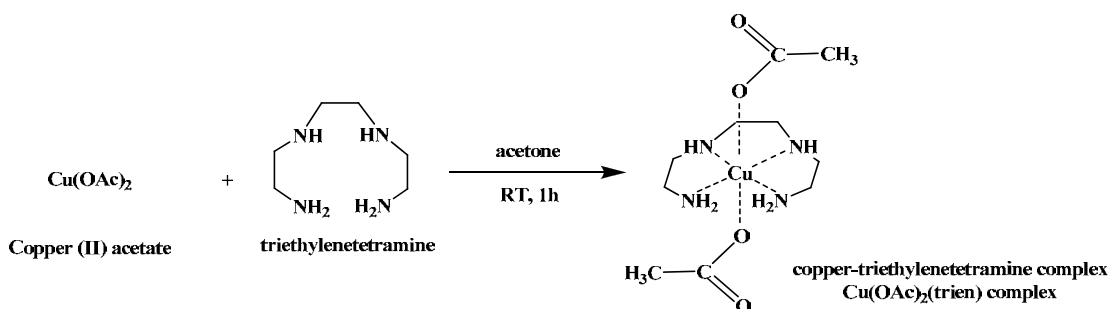
3.2.1.3.1 Synthesis of nickel-triethylenetetramine complex



Scheme 3.6 Synthesis of nickel-triethylenetetramine complex

The preparation of $\text{Ni}(\text{OAc})_2(\text{trien})$ was performed according to the method reported in the literature [5] as follows: a solution of triethylenetetramine (0.37 mL, 2.53 mmol) was stirred in acetone (10 mL) at room temperature for 30 minutes. After that, nickel (II) acetate tetrahydrate (0.63 g, 2.53 mmol) was added and the reaction mixture was stirred at room temperature for 1 hour. The reaction mixture was evaporated and dried under vacuum. $\text{Ni}(\text{OAc})_2(\text{trien})$ was obtained as a purple viscous liquid (0.94 g, 94%): IR (neat, cm^{-1}): 3441, 3409 (NH stretching), 2938 (CH), 1546 (asymmetric C=O), 1466 (symmetric C=O), 1402 (CN stretching), 1024 (CO stretching). $\text{Ni}(\text{OAc})_2(\text{trien}) \cdot 3\text{H}_2\text{O}$ shown m/z 377.09, UV; $\lambda_{\text{max}}(\text{MeOH}) = 348$ nm, molar absorptivity (ϵ) = 46.

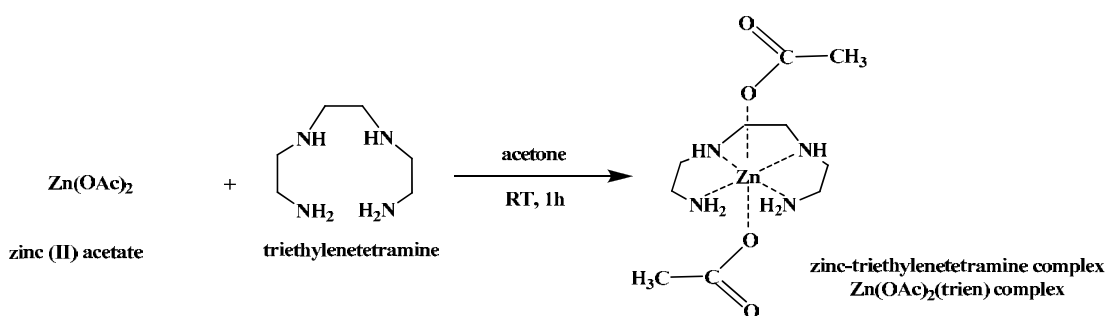
3.2.1.3.2 Synthesis of copper-triethylenetetramine complex



Scheme 3.7 Synthesis of copper-triethylenetetramine complex

The preparation of $\text{Cu}(\text{OAc})_2(\text{trien})$ was performed according to the method reported in the literature [5] as follows: a solution of triethylenetetramine (0.45 ml, 3.07 mmol) was stirred in acetone (10 mL) at room temperature for 30 minutes. After that, copper (II) acetate monohydrate (0.55 g, 2.77 mmol) was added. After the reaction mixture was stirred at room temperature for 1 h, the solution was evaporated and dried under vacuum. $\text{Cu}(\text{OAc})_2(\text{trien})$ was obtained as a blue viscous liquid (0.99 g, 99%): IR (cm^{-1}): 3249 (NH), 2954, 2887 (CH), 1556 (asymmetric C=O), 1401 (symmetric C=O), 1339 (CN), 1019 (CO). $\text{Cu}(\text{OAc})_2(\text{trien})$. shown m/z 328.030, UV; λ_{max} (MeOH) = 258 nm, molar absorptivity (ϵ) = 3,480.

3.2.1.3.3 Synthesis of zinc-triethylenetetramine complex

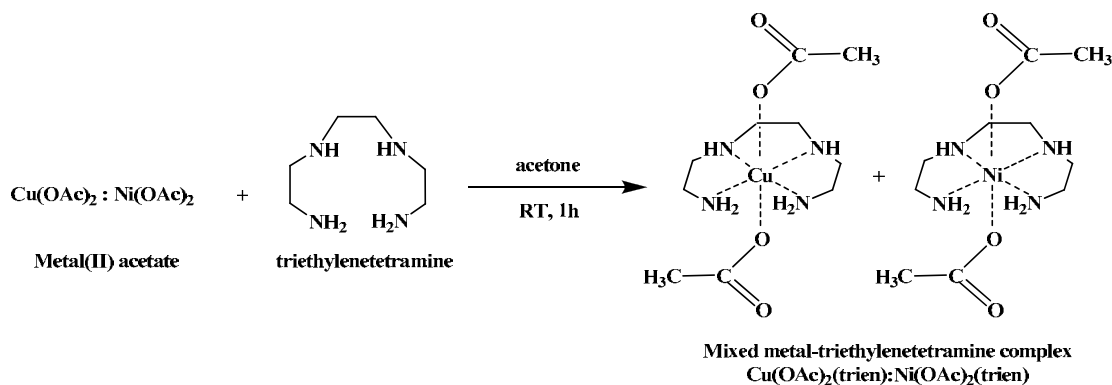


Scheme 3.8 Synthesis of zinc-triethylenetetramine complex

A solution of triethylenetetramine (0.45 mL, 3.08 mmol) was stirred in acetone (10 mL) at room temperature for 30 minutes. After that, zinc (II) acetate dihydrate (0.56 g, 2.53 mmol) was added. After the reaction mixture was stirred at room temperature for 1 h, the solution was evaporated and was dried under vacuum. $\text{Zn}(\text{OAc})_2(\text{trien})$ was obtained as a yellow viscous liquid (0.87 g, 87%): IR (cm^{-1}): 3249 (NH), 2954, 2887 (CH), 1556 (asymmetric C=O), 1401 (symmetric C=O), 1339 (CN), 1019 (CO). UV; λ_{max} (MeOH) = 204 nm, molar absorptivity (ϵ) = 1,573. $\text{Zn}(\text{OAc})_2(\text{trien})\cdot\text{H}_2\text{O}$ shown m/z 348.803, Anal. Calc. for $\text{ZnC}_{10}\text{O}_4\text{H}_{24}\text{N}_4\cdot\text{H}_2\text{O}$: C 34.55; H 7.55; N 16.10; found C 33.12; H 8.24; N 13.96.

3.2.1.4 Synthesis of mixed metal-triethylenetetramine complexes

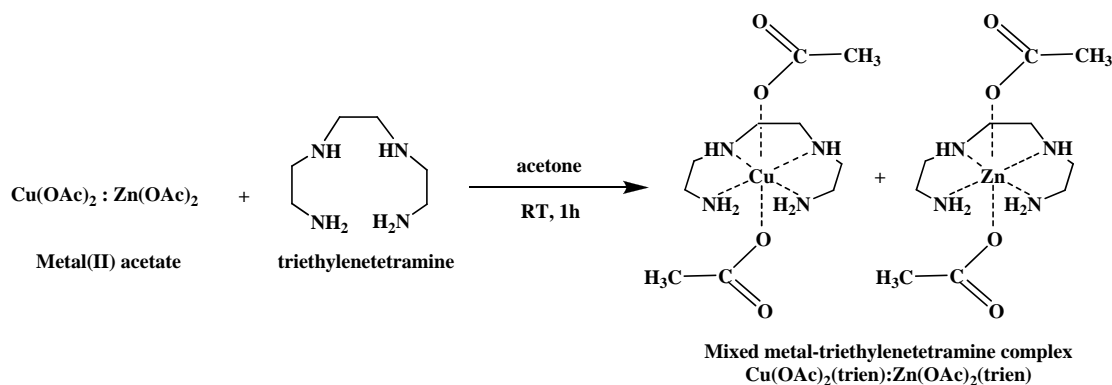
3.2.1.4.1 Synthesis of $\text{Cu}(\text{OAc})_2(\text{trien}):\text{Ni}(\text{OAc})_2(\text{trien})$ complex



Scheme 3.9 Synthesis of $\text{Cu}(\text{OAc})_2(\text{trien}):\text{Ni}(\text{OAc})_2(\text{trien})$ complex

A solution of triethylenetetramine (0.46 mL, 3.15 mmol) was stirred in acetone (10 mL) at room temperature for 30 minutes. After that, copper (II) acetate monohydrate (0.27 g, 1.39 mmol) and nickel acetate tetrahydrate (0.27 g, 1.09 mmol) were added and the reaction mixture was stirred at room temperature for 1 hour. The reaction mixture was dried under vacuum to remove solvent. $\text{Cu}(\text{OAc})_2(\text{trien}):\text{Ni}(\text{OAc})_2(\text{trien})$ was obtained as a blue viscous liquid (0.93g, 93%): IR (cm^{-1}); 3418, 3209 (NH), 2957, 2887 (CH), 1562 (asymmetric C=O), 1409 (symmetric C=O), 1339 (CN), 1024 (CO). UV; λ_{max} (MeOH) = 289 nm, molar absorptivity (ϵ) = 2,963. $\text{Cu}(\text{OAc})_2(\text{trien})$ shown m/z 346.943 and $\text{Ni}(\text{OAc})_2(\text{trien})$ shown m/z 341.961.

3.2.1.4.2 Synthesis of $\text{Cu}(\text{OAc})_2(\text{trien}):\text{Zn}(\text{OAc})_2(\text{trien})$ complex



Scheme 3.10 Synthesis of $\text{Cu}(\text{OAc})_2(\text{trien}):\text{Zn}(\text{OAc})_2(\text{trien})$ complex

A solution of triethylenetetramine (0.45 mL, 3.07 mmol) was stirred in acetone (10 mL) at room temperature for 30 minutes. After that, copper (II) acetate monohydrate (0.27 g, 1.38 mmol) and zinc acetate dihydrate (0.27 g, 1.29 mmol) were added and the reaction mixture was stirred at room temperature for 1 hour. The reaction mixture was dried under vacuum to remove solvent. $\text{Cu}(\text{OAc})_2(\text{trien}):\text{Zn}(\text{OAc})_2(\text{trien})$ was obtained as a purple viscous liquid (0.99g, 99%): IR (KBr, cm^{-1}); 3445, 3285 (NH), 2967, 2890 (CH), 1569 (asymmetric C=O), 1409 (symmetric C=O), 1339 (CN), 1024 (CO). UV; λ_{max} (MeOH) = 258 nm, molar absorptivity (ϵ) = 3,622. $\text{Cu}(\text{OAc})_2(\text{trien})$ shown m/z 350.770 and $\text{Zn}(\text{OAc})_2(\text{trien})\cdot\text{H}_2\text{O}$ shown m/z 347.794, Anal. Calc. for $\text{CuZnC}_{10}\text{O}_4\text{H}_{24}\text{N}_4$: C 32.90; H 7.75; N 15.36; found C 32.70; H 8.15; N 13.07.

Other metal complexes and mixed metal complexes were prepared using similar procedure as described above. Compositions of starting materials in the preparation of all metal complexes in acetone are shown in Tables 3.1-3.3.

Table 3.1 Composition of starting materials in the preparation of metal complexes [M(OAc)₂(en)₂ and M(OAc)₂(trien)]

Metal complexes	Wt. of M(OAc) ₂ (g)	Weight of composition		Yield (%)	Appearance
		en (mL)	trien (mL)		
Ca(OAc)₂(en)₂	0.57	0.48	-	82	White powder
Ba(OAc)₂(en)₂	0.68	0.36	-	90	White powder
Co(OAc)₂(en)₂	0.59	0.45	-	75	Purple-red powder
Mn(OAc)₂(en)₂	0.59	0.46	-	98	Brown viscous liquid
Ni(OAc)₂(en)₂	0.59	0.46	-	57	Purple powder
Cu(OAc)₂(en)₂	0.60	0.45	-	62	Purple powder
Zn(OAc)₂(en)₂	0.60	0.45	-	48	White powder
Ni(OAc)₂(trien)	0.63	-	0.37	94	Purple viscous liquid
Cu(OAc)₂(trien)	0.55	-	0.45	99	Blue viscous liquid
Zn(OAc)₂(trien)	0.56	-	0.45	87	Yellow viscous liquid

en = ethylenediamine, trien = triethylenetetramine

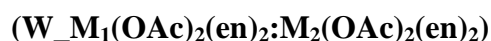
Table 3.2 Composition of starting materials in the preparation of mixed metal-amine complexes [$M_1(OAc)_2(en)_2:M_2(OAc)_2(en)_2$ and $M_1(OAc)_2(trien):M_2(OAc)_2(trien)$]

Metal complexes	Wt. of		Weight of		Yield (%)	Appearance
	M(OAc) ₂ (g)		composition			
	M ₁	M ₂	en (mL)	trien (mL)		
Cu(OAc)₂(en)₂: Ni(OAc)₂(en)₂	0.30	0.29	0.45	-	71	Purple powder
Cu(OAc)₂(en)₂: Zn(OAc)₂(en)₂	0.29	0.30	0.45	-	64	Purple powder
Cu(OAc)₂(en)₂: Ca(OAc)₂(en)₂	0.31	0.27	0.47	-	89	Blue powder
Cu(OAc)₂(en)₂: Ba(OAc)₂(en)₂	0.27	0.38	0.45	-	99	Blue powder
Cu(OAc)₂(en)₂: Co(OAc)₂(en)₂	0.30	0.29	0.45	-	62	Purple-red powder
Cu(OAc)₂(en)₂: Mn(OAc)₂(en)₂	0.30	0.29	0.45	-	98	Brown viscous liquid
Cu(OAc)₂(trien): Ni(OAc)₂(trien)	0.27	0.27	-	0.46	93	Blue viscous liquid
Cu(OAc)₂(trien): Zn(OAc)₂(trien)	0.27	0.27	-	0.45	99	Purple viscous liquid

Table 3.3 Composition of starting materials in the preparation of mixed metal - mixed amine complexes [$M_1(\text{OAc})_2(\text{en})(\text{trien})$: $M_2(\text{OAc})_2(\text{en})(\text{trien})$]

Metal complexes	Wt. of		Weight of		Yield (%)	Appearance
	M(OAc) ₂ (g)		composition			
	M ₁	M ₂	en (mL)	trien (mL)		
Cu(OAc)₂(en)(trien): Ni(OAc)₂(en)(trien)	0.23	0.22	0.16	0.38	98	Blue viscous liquid
Cu(OAc)₂(en)(trien): Zn(OAc)₂(en)(trien)	0.23	0.23	0.15	0.38	95	Blue viscous liquid

3.2.2 Synthesis of metal complexes in water



3.2.2.1 Synthesis of W_Cu(OAc)₂(en)₂:Ni(OAc)₂(en)₂ complex

Copper (II) acetate monohydrate (0.30 g, 1.51 mmol), nickel acetate tetrahydrate (0.29 g, 1.19 mmol) and polysiloxane surfactant (TEGOSTAB B8460) (0.25 ml) were dissolved in 4 mL of distilled water at room temperature and the solution was stirred for 60 minutes. Ethylenediamine (0.45 ml, 3.30 mmol) was then added dropwise and the solution was stirred at room temperature for 30 minutes. W_Cu(OAc)₂(en)₂:Ni(OAc)₂(en)₂ aqueous solution was obtained as a purple solution. UV; λ_{max} (MeOH) = 232 nm, molar absorptivity (ϵ) = 915.

3.2.2.2 Synthesis of W_Cu(OAc)₂(en)₂:Zn(OAc)₂(en)₂ complex

Copper (II) acetate monohydrate (0.29 g, 1.49 mmol), zinc acetate dihydrate (0.30 g, 1.38 mmol) and polysiloxane surfactant (TEGOSTAB B8460) (0.25 ml) were dissolved in 4 mL of distilled water at room temperature and the solution was stirred for 60 minutes. Ethylenediamine (0.45 ml, 3.30 mmol) was then added dropwise and the solution was stirred at room temperature for 30 minutes.

W_Cu(OAc)₂(en)₂:Zn(OAc)₂(en)₂ aqueous solution was obtained as a purple solution. UV; λ_{\max} (MeOH) = 233 nm, molar absorptivity (ϵ) = 4,450.

3.3 Rigid polyurethane (RPUR) foam preparation

3.3.1 Preparation of RPUR foams catalyzed by mixed metal complexes

All of rigid foam samples were synthesized with a two-shot step. The formulation used for foam preparation is presented in Table 3.4. In the first mixing step, the mixture “polyblend” (consisting of polyether polyol, surfactant, catalyst and blowing agent) was weighed into a 700 mL paper cup. The components were mixed for 15 seconds. Then, an appropriate MDI was added to the mixture and vigorously stirred at 2000 rpm for 20 seconds. The foam was allowed to rise and left in the mold for 48 hours at room temperature in order to complete the polymerization reactions before being removed, cut and tested [45-49].

Table 3.4 Formulation used for foam preparation at different isocyanate (NCO) indexes (in parts by weight unit, pbw)

Components (pbw*)	NCO index**		
	100	150	200
Raypol [®] 4221	100	100	100
Catalyst			
- DMCHA (commercial catalyst)	1.0	1.0	1.0
- mixed metal complexes			
Surfactant (B8460)	2.5	2.5	2.5
Blowing agent (H ₂ O)	4.0	4.0	4.0
PMDI (MR-200)	166	249	333

*pbw; parts by weight or gram of components per 100 grams of polyol

$$** \text{ Isocyanate index} = \frac{\text{actual amount of isocyanate}}{\text{theoretical amount of isocyanate}} \times 100$$

3.3.2 Preparation of RPUR foams using an aluminum mold

Polyol, catalyst, blowing agent and surfactant were weighed into a 700 mL paper cup and stirred at 2000 rpm for 15 seconds using a mechanical stirrer. Then, an appropriate MDI was added to the mixture and vigorously stirred at 2000 rpm for 20 seconds. After mixing, the mixture was poured into a 10x10x10 cm aluminum mold to produce free-rise foam. The foam was allowed to rise and left in the mold for 48 hours at room temperature in order to complete the polymerization reactions and finally cut and tested [45, 46].

Since the rigid polyurethane foams obtained from different catalysts have similar IR spectra, therefore, only the IR data RPUR foams obtained from $\text{Cu}(\text{OAc})_2(\text{en})_2:\text{Zn}(\text{OAc})_2(\text{en})_2$ is shown as follows:

RPUR foam catalyzed by $\text{Cu}(\text{OAc})_2(\text{en})_2:\text{Zn}(\text{OAc})_2(\text{en})_2$; IR (IR-ATR); 3392 (N-H), 2975, 2872 (C-H), 2274 (free NCO), 1713 (C=O), 1600 (Ar-H), 1519 (N-H), 1410 (CN isocyanurate), 1312 (CH), 1229, 1085 (C-O urethane), 815, 764 (C-H aromatic ring).

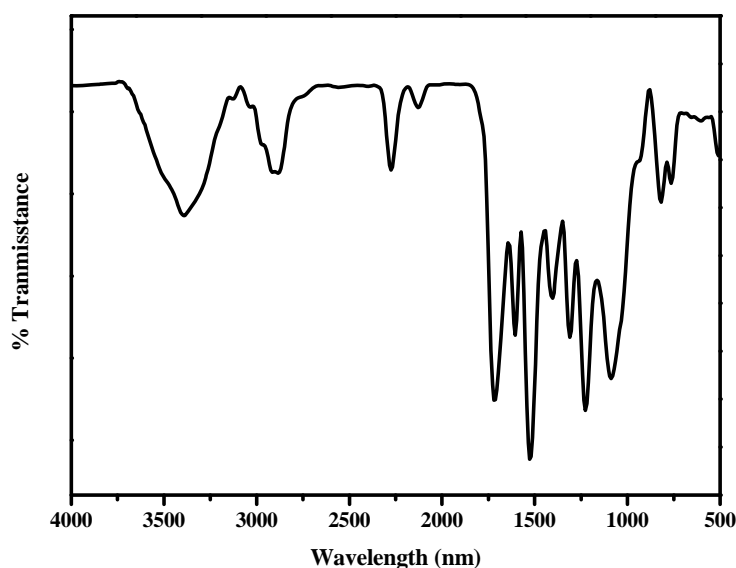


Figure 3.1 IR spectra of RPUR foams catalyzed by $\text{Cu}(\text{OAc})_2(\text{en})_2:\text{Zn}(\text{OAc})_2(\text{en})_2$ (synthesized in acetone)

3.4 Instrumentation

3.4.1 Infrared spectroscopy

FTIR analyses were performed on a Nicolet 6700. FTIR spectrometer was used to study of functional groups on mixed metal complexes as catalyst and foams at room temperature using a Nicolet at a resolution of 4 cm^{-1} and a total of 64 interferograms were signal averaged. It is important that the samples are pressed, reproducibly and with a constant pressure, against the IR-transmitting ATR crystal. The ATR crystal is integrated into the beam of an ATR-IR spectrometer (Nicolet 6700) in such a way that IR light is passed through the crystal by means of total reflection. ATR occurs on the measuring surface that is in contact with the foam sample. The IR bands given in Table 3.5 are used for the analysis. The measurement was controlled by Omnic software.

Table 3.5 Characteristic IR bands of RPUR foam

Functional group	Vibration mode	IR peak (cm^{-1})
NCO	NCO antisymm. Str.	2180-2310
CO	CO str.(urethane, urea, isocyanurate, allophanate, Biuret, etc.	1620-1760
Isocyanurate	Ring deformation and CH_2 -deformation in PMDI	1370-1443
Amide	CN-str. (urethane, urea)	1155-1245
Reference	Non-reaction groups in polyol and isocyanate	935-1050

3.4.2 Ultraviolet–visible spectroscopy

UV/Vis spectroscopy is routinely used in the quantitative determination of solutions of transition metal ions highly conjugated organic compounds. UV-Vis spectra were recorded on ultraviolet and visible spectrophotometer at room temperature. Absorption spectra were obtained on Varian Cary 50 UV-Vis spectrophotometer. The samples were scan over range 200-500 nm and speed was medium.

3.4.3 Mass spectrometry (MS)

Mass spectrometry (MS) is an analytical technique that measures the mass-to-charge ratio of charged particles. Mass spectra were obtained on a micromass Quattro microTM API spectrometer. Electrospray ionization (ESI) was used in this case. ESI can be used for the molecules without any ion sable sites, through the formation of proton, sodium and potassium [50].

3.4.4 Atomic absorption spectrometry (AAS)

Atomic absorption spectroscopy (AAS) is a spectroanalytical procedure for the qualitative and quantitative determination of chemical elements employing the absorption of optical radiation (light) by free atoms in the gaseous state using a flame (Perkin-Elmer : AAnalyst 100)

3.4.5 Elemental analysis

For organic chemists, elemental analysis or "EA" almost always refers to CHN analysis; the determination of the percentage weights of carbon, hydrogen, and nitrogen of a sample. Elemental analyses were carried out using a Perkin-Elmer EP2400 analyzer.

3.4.6 Stopwatch

The foam reaction profile; cream time, gel time, tack free time and rise time were investigated by using a stopwatch.

3.4.7 Thermocouple

Thermocouple is a widely used type of temperature sensor for measurement. The foaming temperatures were recorded by dual thermocouple, Digicon DP-71.

3.4.8 Density

The mass density or density of a material is defined as its mass per unit volume (can change during the ageing process) [14]. The apparent density of foams was measured according to ASTM D 1622-09, the size of specimen was 3.0 x 3.0 x 3.0 cm dimension and the average values of three samples were reported. Density particularly affects the following parameters: modulus, strength (compression), and thermal conductivity.

Foams typically have the following density ranges [14]:

> 600 kg m⁻³ = High density

100-600 kg m⁻³ = Intermediate density

< 100 kg m⁻³ = Low density

3.4.9 Scanning electron microscope (SEM)

Cell size and morphology of rigid foam samples were measured on a Hitachi/S-4800 scanning electron microscope (SEM). A slice of foam about 1.0 mm in thickness was prepared for SEM analysis by coating with gold before scanning in order to provide an electrically conductive surface. The slice was done at an accelerating of 20kV. The sample was observed in the free-rise direction.

3.4.10 Compression testing

The compression testing of foams were performed using universal testing machine (Lloyd/LRX) according to ASTM D1621-09, the specimen size was 3.0 x 3.0 x 3.0 cm dimension, the rate of crosshead movement was fixed at 2.54 mm/min and the preload cell used was 0.100 N.

3.4.11 Thermogravimetric analysis (TGA)

Thermogravimetric analysis (TGA) was examined using a Netzsch STA 409C thermogravimetric analyzer. All samples were heated from 25°C to 600°C at heating rate of 20°C/min under N₂ gas. The result of thermal stability was report in percentage weight residue of foams. Initial decomposition temperature (IDT) was taken at the temperature where 5 wt% loss of foam occurred.

CHAPTER IV

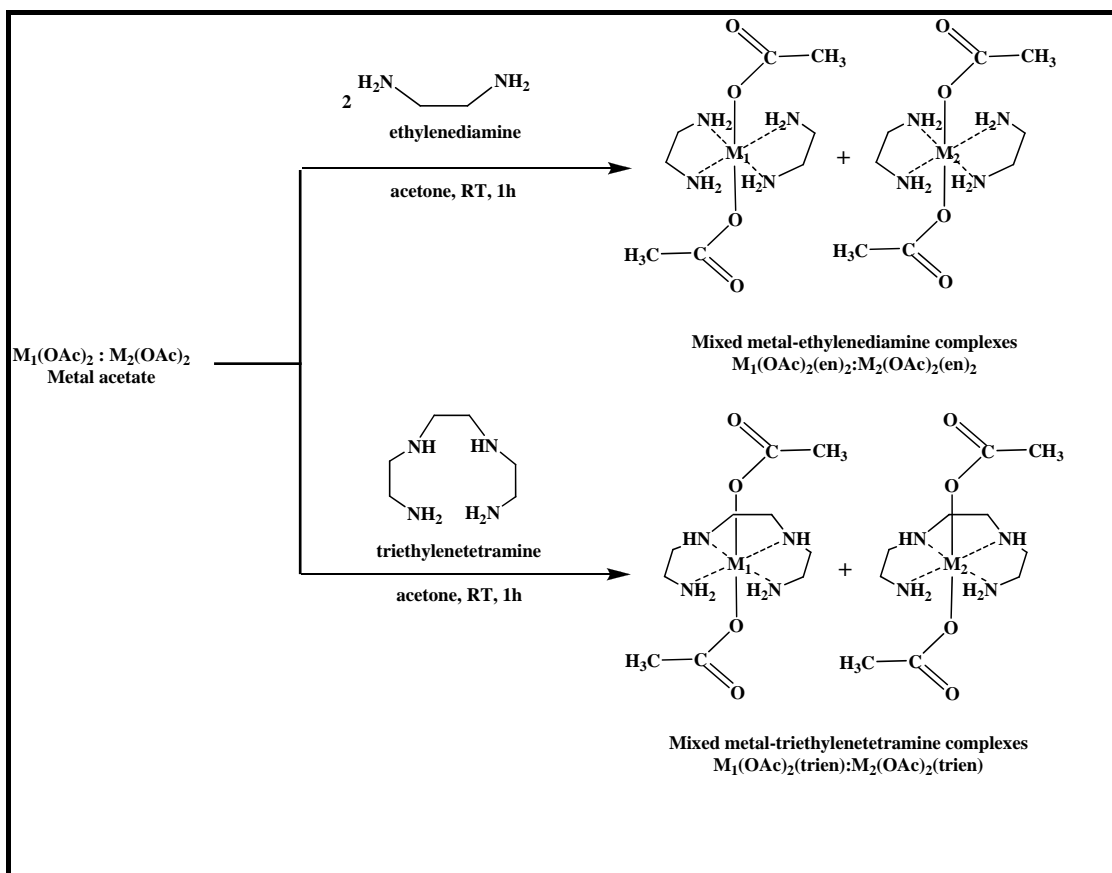
RESULTS AND DISCUSSION

4.1 Synthesis of mixed metal-amine complexes [$M_1(OAc)_2(en)_2:M_2(OAc)_2(en)_2$ and $M_1(OAc)_2(trien):M_2(OAc)_2(trien)$]

The mixed metal complexes were synthesized using two methods. In the first method, mixed metal-ethylenediamine and mixed metal-triethylenetetramine complexes were synthesized from the reaction between the mixture of metal (II) acetate [$M_1(OAc)_2:M_2(OAc)_2$] and aliphatic amine [ethylenediamine (en) or triethylenetetramine (trien)] using acetone as a solvent as shown in Scheme 4.1 [51-53]. The ratio $M_1(OAc)_2:M_2(OAc)_2:en$ and $M_1(OAc)_2:M_2(OAc)_2:trien$ employed in the synthesis of mixed metal complexes was 0.5:0.5:2 and 0.5:0.5:1, respectively. This synthesis was done following the previously reported synthetic procedure for $M(OAc)_2(en)_2$ and $M(OAc)_2(trien)$, where $M = Cu$ and Ni [36, 37]. Acetone was dried under vacuum from the metal complexes before using in the preparation of rigid polyurethane foam.

In the second method, the mixed metal complexes of $M_1(OAc)_2:M_2(OAc)_2$ was stirred in water. Then, a solution of amine was added dropwise followed by addition of polysiloxane surfactant [33, 54]. It was found that the complex formation was obtained in aqueous solution. The solution containing metal complexes could be further used in the preparation of rigid polyurethane foam without purification.

Attempts to prepare metal-ethylenediamine complexes from the mole ratio of $M_1(OAc)_2 : ethylenediamine = 1:1$ using water as a solvent were made. However, the insoluble precipitates in water were obtained.



Scheme 4.1 Synthesis of mixed metal-ethylenediamine complexes

$[M_1(OAc)_2(en)_2 : M_2(OAc)_2(en)_2]$ and mixed metal-triethylenetetramine complexes $[M_1(OAc)_2(trien) : M_2(OAc)_2(trien)]$

When; $M_1 = \text{Cu}, M_2 = \text{Ca}, \text{Ba}, \text{Co}, \text{Mn}, \text{Ni}, \text{Zn};$

$M_1 = \text{Ni}, M_2 = \text{Ca}, \text{Ba}, \text{Co}, \text{Mn}, \text{Zn};$

$M_1 = \text{Mn}, M_2 = \text{Ca}, \text{Ba}, \text{Co}, \text{Zn}$

4.2 Characterization mixed metal-amine complexes

$[M_1(OAc)_2(en)_2 : M_2(OAc)_2(en)_2]$ and $M_1(OAc)_2(trien) : M_2(OAc)_2(trien)$

The mixed metal complexes synthesized using acetone as a solvent were characterized using FTIR, UV-visible spectroscopies and mass spectrometry while those synthesized using water as a solvent could be characterized only by UV-visible spectroscopy. The UV-visible spectra of metal complexes synthesized in acetone and water were compared to confirm the complex formation in water.

4.2.1 Mn(OAc)₂(en)₂:M₂(OAc)₂(en)₂ complexes

IR spectrum of Mn(OAc)₂(en)₂ shows characteristic frequencies of $\nu(\text{NH})$, $\nu(\text{CH})$, $\nu(\text{CN})$ and $\nu(\text{CO})$ at 3281, 2874, 1335 and 1012 cm⁻¹, respectively. The acetate anions in Mn(OAc)₂(en)₂ were characterized by C=O stretching peaks, namely $\nu_{\text{as}}(\text{COO}^-)$ and $\nu_{\text{s}}(\text{COO}^-)$ at 1557 and 1408 cm⁻¹, respectively [55].

4.2.1.1 FTIR spectroscopy of Mn(OAc)₂(en)₂:M₂(OAc)₂(en)₂ complexes

IR spectra of Mn(OAc)₂(en)₂:M₂(OAc)₂(en)₂ (where M₂ = Ba, Ca, Co, Zn) are shown in Figure 4.1. They exhibited absorption band at 3351-3431 cm⁻¹ (N-H stretching), 2932-2983 cm⁻¹ (C-H stretching), 1562-1573 cm⁻¹ (C=O asymmetric stretching), 1416-1420 cm⁻¹ (C=O symmetric stretching), 1340-1344 cm⁻¹ (C-N stretching) and 1019-1059 cm⁻¹ (C-O stretching). The absorption bands of Mn(OAc)₂(en)₂:M₂(OAc)₂(en)₂ exhibited C-O stretching which shifted from typical absorption band of Mn(OAc)₂ at 1027 cm⁻¹. It was found that the IR peak of Mn(OAc)₂(en)₂:M₂(OAc)₂(en)₂ complexes slightly shifted from those of Mn(OAc)₂ which suggested that the complexes were formed. Further characterization using UV-visible spectroscopy could not be done since these metal complexes exhibited weak absorption.

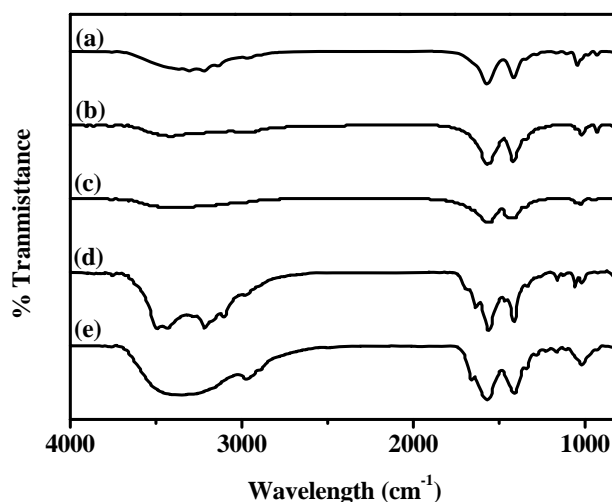


Figure 4.1 IR spectra of (a) Mn(OAc)₂; (b) Mn(OAc)₂(en)₂:Ba(OAc)₂(en)₂; (c) Mn(OAc)₂(en)₂:Ca(OAc)₂(en)₂; (d) Mn(OAc)₂(en)₂:Co(OAc)₂(en)₂; (e) Mn(OAc)₂(en)₂:Zn(OAc)₂(en)₂

4.2.2 Ni(OAc)₂(en)₂:M₂(OAc)₂(en)₂ complexes

IR spectrum of Ni(OAc)₂(en)₂ shows characteristic frequencies of $\nu(\text{NH})$, $\nu(\text{CH})$ and $\nu(\text{CO})$ at 3216, 2890 and 1024 cm⁻¹, respectively. The acetate anions in Ni(OAc)₂(en)₂ were characterized by C=O stretching peaks, namely $\nu_{\text{as}}(\text{COO}^-)$ and $\nu_{\text{s}}(\text{COO}^-)$ at 1568 and 1400 cm⁻¹, respectively [44].

4.2.2.1 FTIR spectroscopy of Ni(OAc)₂(en)₂:M₂(OAc)₂(en)₂ complexes

Ni(OAc)₂(en)₂:M₂(OAc)₂(en)₂ complexes (where M₂ = Ba, Ca, Co, Mn, Zn) showed similar IR spectra as shown in Figure 4.2. Absorption band at 3133-3402 cm⁻¹ (N-H stretching), 2969-2976 cm⁻¹ (C-H stretching), 1548-1588 cm⁻¹ (C=O asymmetric stretching), 1409-1420 cm⁻¹ (C=O symmetric stretching), 1340-1351 cm⁻¹ (C-N stretching) and 1023-1034 cm⁻¹ (C-O stretching). Further characterization using UV-visible spectroscopy could not be done since these metal complexes exhibited weak absorption.

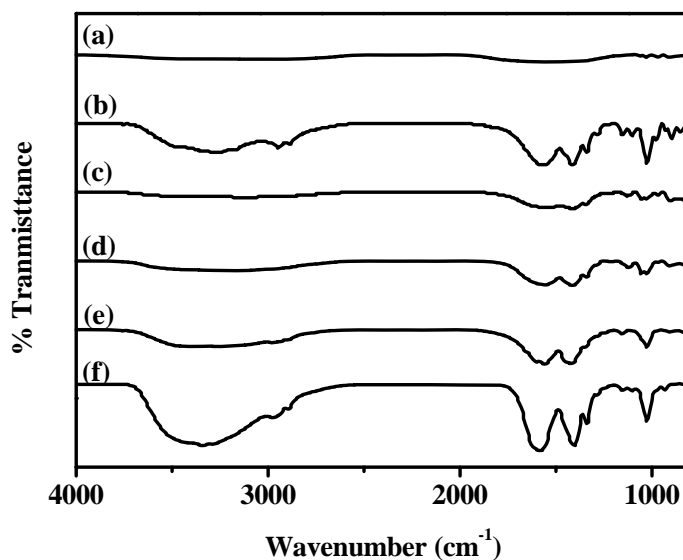


Figure 4.2 IR spectra of (a) Ni(OAc)₂; (b) Ni(OAc)₂(en)₂:Ba(OAc)₂(en)₂; (c) Ni(OAc)₂(en)₂:Ca(OAc)₂(en)₂; (d) Ni(OAc)₂(en)₂:Co(OAc)₂(en)₂; (e) Ni(OAc)₂(en)₂:Mn(OAc)₂(en)₂; (f) Ni(OAc)₂(en)₂:Zn(OAc)₂(en)₂

4.2.3 Cu(OAc)₂(en)₂:M₂(OAc)₂(en)₂ complexes

The preparation and characterization of Cu(OAc)₂(en)₂ were reported in details [36]. IR spectrum of Cu(OAc)₂(en)₂ confirmed the presence of ethylenediamine in the metal complex as shown in Figure 4.3. Four characteristic frequencies, $\nu(\text{NH})$, $\nu(\text{CH})$, $\nu(\text{CN})$ and $\nu(\text{CC})$, can easily be identified at 3140, 2892, 1037 and 987 cm⁻¹, respectively, whereas the $\delta(\text{NH}_2)$ absorption of en is obscured by stretching vibrations of the carboxylate groups.

The acetate anions in Cu(OAc)₂(en)₂ were characterized by C=O stretching peaks, namely $\nu_{\text{as}}(\text{COO}^-)$ and $\nu_{\text{s}}(\text{COO}^-)$ at 1543 and 1393 cm⁻¹. The magnitude of the separation between the stretches ($\Delta = \nu_{\text{as}}(\text{COO}^-) - \nu_{\text{s}}(\text{COO}^-)$) is often used as a spectroscopic criterion for determination of the mode of the carboxylate binding [55–61], including biomolecules. The following order was proposed for Δ values of carboxylate complexes of divalent metal cations [55, 56]:

$$\Delta(\text{monodentate}) > \Delta(\text{ionic}) > \Delta(\text{bridging bidentate}) > \Delta(\text{chelating bidentate})$$

This Δ value is about 170 cm⁻¹ for ionic carboxylate group in acetates, i.e. group which does not interact strongly with the metal ion [55]. In monodentate coordination the redistribution of the electron density takes place, the force field around the metal atom changes and consequently the shift in the frequency of $\nu_{\text{as}}(\text{COO}^-)$ to higher wavenumbers in comparison with ionic group is observed, increasing the value of Δ . On contrary, bidentate coordination shifts the position of the asymmetric carboxylate stretch to lower wavenumbers in comparison with ionic group and thus lowers the value of Δ . In the ‘bridging’ coordination when one divalent metal cation is bound to one of the oxygens in the COO⁻ group and another divalent metal cation to the other oxygen, the $\nu_{\text{as}}(\text{COO}^-)$ band is located at the same position as that of the ‘ionic’ $\nu_{\text{as}}(\text{COO}^-)$ band [62].

Although the difference in wavenumbers, $\Delta = 149 \text{ cm}^{-1}$, between the antisymmetric (1543 cm⁻¹) and symmetric (1393 cm⁻¹) $\nu(\text{CO})$ stretching frequencies is attributable to the existence of bridging acetate ligands.

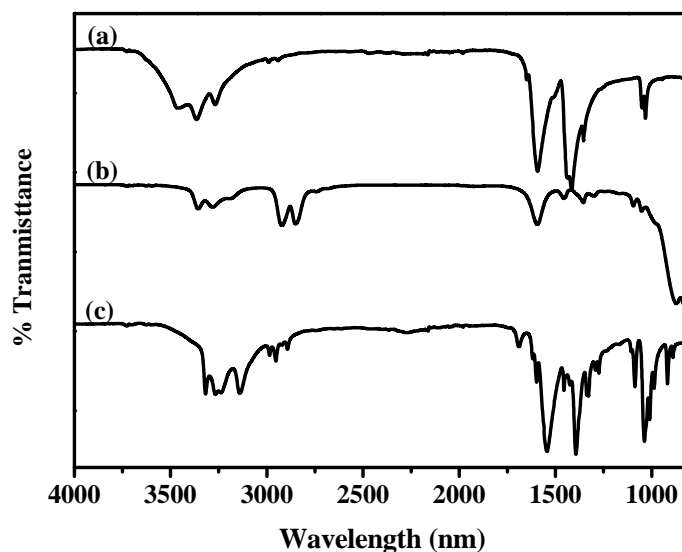


Figure 4.3 IR spectra of (a) $\text{Cu}(\text{OAc})_2$; (b) ethylenediamine (en); (c) $\text{Cu}(\text{OAc})_2(\text{en})_2$

4.2.3.1 FTIR spectroscopy of $\text{Cu}(\text{OAc})_2(\text{en})_2:\text{M}_2(\text{OAc})_2(\text{en})_2$ complexes

IR spectra of $\text{Cu}(\text{OAc})_2(\text{en})_2:\text{M}_2(\text{OAc})_2(\text{en})_2$ (where $\text{M}_2 = \text{Ba}, \text{Ca}, \text{Co}, \text{Mn}, \text{Ni}, \text{Zn}$) are shown in Figure 4.4. They exhibited absorption band at $3310\text{--}3321\text{ cm}^{-1}$ (N-H stretching), $2904\text{--}2966\text{ cm}^{-1}$ (C-H stretching), $1566\text{--}1580\text{ cm}^{-1}$ (C=O asymmetric stretching), $1409\text{--}1435\text{ cm}^{-1}$ (C=O symmetric stretching), $1342\text{--}1343\text{ cm}^{-1}$ (C-N stretching) and $1044\text{--}1051\text{ cm}^{-1}$ (C-O stretching). The C=O stretching of carbonyl group in $\text{Cu}(\text{OAc})_2(\text{en})_2:\text{M}_2(\text{OAc})_2(\text{en})_2$ were different from the typical $\text{Cu}(\text{OAc})_2$ normally appears as absorption band around at 1596 cm^{-1} (C=O asymmetric stretching) and 1443 cm^{-1} (C=O symmetric stretching) [63]. The absorption bands of $\text{Cu}(\text{en})_2:\text{M}_2(\text{en})_2$ exhibited C-O stretching which shifted from typical absorption band of $\text{Cu}(\text{OAc})_2$ at 1033 cm^{-1} . It was found that the IR peak of $\text{Cu}(\text{OAc})_2(\text{en})_2:\text{M}_2(\text{OAc})_2(\text{en})_2$ complexes shifted from those of $\text{Cu}(\text{OAc})_2$ to lower energy because of the influence of amine coordination, which suggested that the complexes were formed.

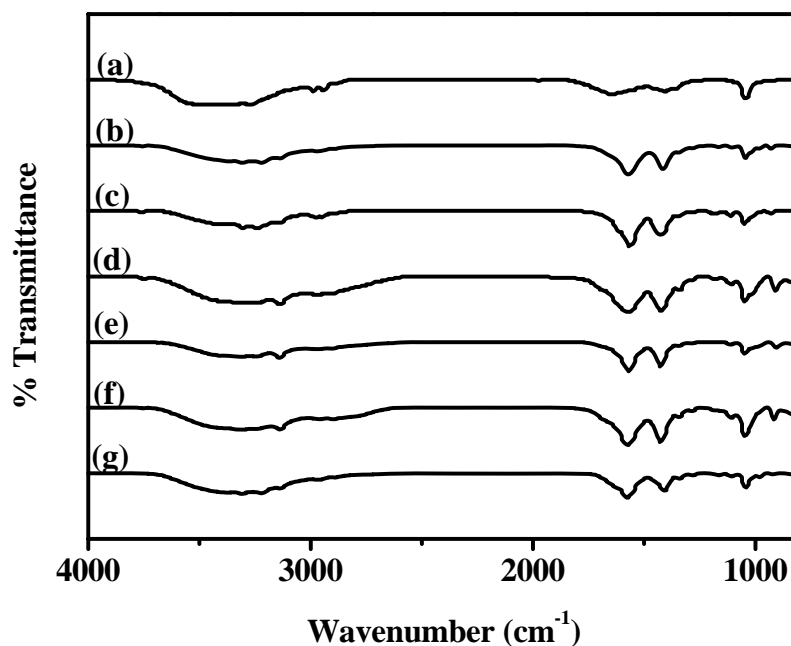


Figure 4.4 IR spectra of (a) $\text{Cu}(\text{OAc})_2$; (b) $\text{Cu}(\text{OAc})_2(\text{en})_2:\text{Ba}(\text{OAc})_2(\text{en})_2$; (c) $\text{Cu}(\text{OAc})_2(\text{en})_2:\text{Ca}(\text{OAc})_2(\text{en})_2$; (d) $\text{Cu}(\text{OAc})_2(\text{en})_2:\text{Co}(\text{OAc})_2(\text{en})_2$; (e) $\text{Cu}(\text{OAc})_2(\text{en})_2:\text{Mn}(\text{OAc})_2(\text{en})_2$; (f) $\text{Cu}(\text{OAc})_2(\text{en})_2:\text{Ni}(\text{OAc})_2(\text{en})_2$; (g) $\text{Cu}(\text{OAc})_2(\text{en})_2:\text{Zn}(\text{OAc})_2(\text{en})_2$

4.2.3.2 UV-visible spectroscopy of $\text{Cu}(\text{OAc})_2(\text{en})_2:\text{M}_2(\text{OAc})_2(\text{en})_2$ complexes

The complex formation was confirmed using UV-visible spectroscopy. $\text{Cu}(\text{OAc})_2(\text{en})_2$ has a strong absorption at 230 nm while $\text{Ni}(\text{OAc})_2(\text{en})_2$ and $\text{Zn}(\text{OAc})_2(\text{en})_2$ show weak absorption. UV-visible spectra of $\text{Cu}(\text{OAc})_2(\text{en})_2:\text{M}_2(\text{OAc})_2(\text{en})_2$ complexes (where $\text{M}_2 = \text{Ni}$ and Zn) are shown in Figure 4.5. The UV absorption spectra of $\text{Cu}(\text{OAc})_2(\text{en})_2:\text{Ni}(\text{OAc})_2(\text{en})_2$ and $\text{Cu}(\text{OAc})_2(\text{en})_2:\text{Zn}(\text{OAc})_2(\text{en})_2$ complexes display a peak at 233.0 nm in methanol, which shifts from the maximum wavelength of $\text{Cu}(\text{OAc})_2$ at 238.9 nm.

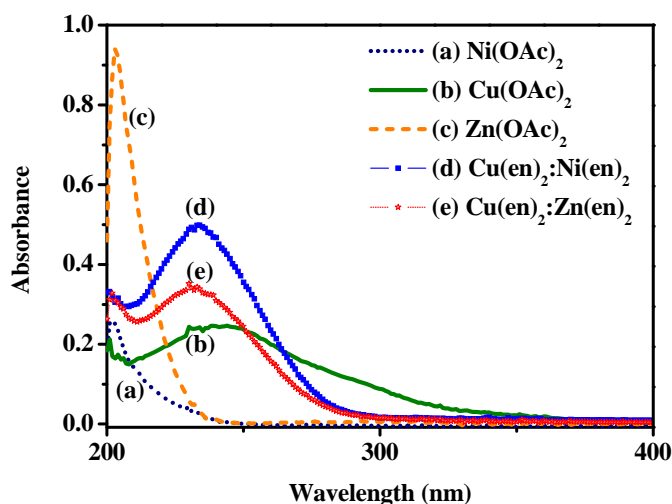


Figure 4.5 UV spectra of (a) $\text{Ni}(\text{OAc})_2$; (b) $\text{Cu}(\text{OAc})_2$; (c) $\text{Zn}(\text{OAc})_2$;
(d) $\text{Cu}(\text{OAc})_2(\text{en})_2:\text{Ni}(\text{OAc})_2(\text{en})_2$; (e) $\text{Cu}(\text{OAc})_2(\text{en})_2:\text{Zn}(\text{OAc})_2(\text{en})_2$

UV spectra of the metal complexes synthesized in water were compared to those synthesized in acetone (Figures 4.6 and 4.7). It was found that the maximum absorption $\text{Cu}(\text{OAc})_2(\text{en})_2:\text{Ni}(\text{OAc})_2(\text{en})_2$ and $\text{Cu}(\text{OAc})_2(\text{en})_2:\text{Zn}(\text{OAc})_2(\text{en})_2$ synthesized in acetone and water appeared at the same position of 232.0 nm.

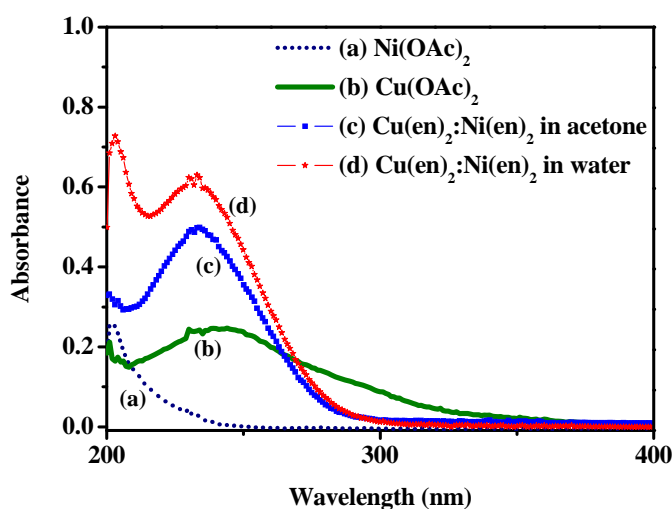


Figure 4.6 UV spectra of (a) $\text{Ni}(\text{OAc})_2$; (b) $\text{Cu}(\text{OAc})_2$;
(c) $\text{Cu}(\text{OAc})_2(\text{en})_2:\text{Ni}(\text{OAc})_2(\text{en})_2$ in acetone;
(d) $\text{Cu}(\text{OAc})_2(\text{en})_2:\text{Ni}(\text{OAc})_2(\text{en})_2$ in water

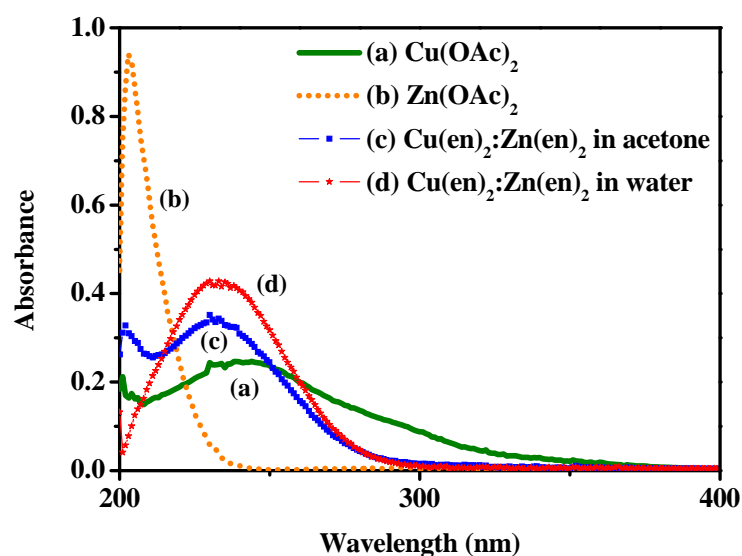


Figure 4.7 UV spectra of (a) $\text{Cu}(\text{OAc})_2$; (b) $\text{Zn}(\text{OAc})_2$;
 (c) $\text{Cu}(\text{OAc})_2(\text{en})_2:\text{Zn}(\text{OAc})_2(\text{en})_2$ in acetone;
 (d) $\text{Cu}(\text{OAc})_2(\text{en})_2:\text{Zn}(\text{OAc})_2(\text{en})_2$ in water

4.2.3.3 Elemental analysis of $\text{Cu}(\text{OAc})_2(\text{en})_2:\text{M}_2(\text{OAc})_2(\text{en})_2$ complexes

Elemental analysis (CHN) of $\text{Cu}(\text{OAc})_2(\text{en})_2:\text{Zn}(\text{OAc})_2(\text{en})_2$ showed the results in agreement with the calculated values (Table 4.1).

Table 4.1 Elemental analysis (CHN) of $\text{Cu}(\text{OAc})_2(\text{en})_2:\text{Zn}(\text{OAc})_2(\text{en})_2$

Sample type	Elements determined	Calculated (%)	Experimental (%)
$\text{Cu}(\text{OAc})_2(\text{en})_2:\text{Zn}(\text{OAc})_2(\text{en})_2 \cdot 2\text{H}_2\text{O}$	%C	28.35	28.92
	%H	7.75	7.57
	%N	16.54	16.90

4.2.3.4 Mass spectrometry of $\text{Cu}(\text{OAc})_2(\text{en})_2:\text{M}_2(\text{OAc})_2(\text{en})_2$ complexes

Mass spectra of copper acetylacetonate $[\text{Cu}(\text{acac})_2]$ have been recorded using a number of ionization techniques including electron and chemical ionization (EI and CI) [63]. Many ions were found such as $[\text{Cu}(\text{acac})_2]^+$, $[\text{Cu}(\text{acac})_2+\text{H}]^+$ and $[\text{Cu}(\text{acac})_2-\text{H}_2\text{O}]^+$.

From the positive-ion ESI mass spectra, $^{63}\text{Cu}(\text{OAc})_2(\text{en})_2$ shows the peak corresponding to $[\text{Cu}(\text{OAc})_2(\text{en})_2]^+$ at m/z of 301.792 (Appendix, Figure C1) and $^{58}\text{Ni}(\text{OAc})_2(\text{en})_2$ shows the peak as $[\text{Ni}(\text{OAc})_2(\text{en})_2\cdot 3\text{H}_2\text{O}+\text{H}]^+$ at m/z of 351.807 (Appendix, Figure C3). $^{64}\text{Zn}(\text{OAc})_2(\text{en})_2$ appeared as $[\text{Zn}(\text{OAc})_2(\text{en})_2\cdot \text{H}_2\text{O}+\text{H}]^+$ at m/z of 322.785 (Appendix, Figure C5).

The positive-ion ESI of $\text{Cu}(\text{OAc})_2(\text{en})_2:\text{Zn}(\text{OAc})_2(\text{en})_2$ (Figure 4.8a and Table 4.2) shows the peaks corresponding to $[\text{Cu}(\text{OAc})_2(\text{en})_2]^+$ and $[\text{Zn}(\text{OAc})_2(\text{en})_2+\text{H}]^+$ at m/z of 301.819 and 303.800, respectively. $[\text{Cu}(\text{OAc})_2(\text{en})_3]^+$ and $[\text{Zn}(\text{OAc})_2(\text{en})_3]^+$ appear at m/z of 361.801 and 363.789, respectively. $[\text{Cu}(\text{OAc})_2(\text{en})_3\cdot 2\text{H}_2\text{O}+\text{Na}]^+$ and $[\text{Zn}(\text{OAc})_2(\text{en})_3\cdot 2\text{H}_2\text{O}+\text{Na}]^+$ appeared at m/z of 421.838 and 423.832, respectively.

The positive-ion ESI of $\text{Cu}(\text{OAc})_2(\text{en})_2:\text{Ni}(\text{OAc})_2(\text{en})_2$ (Figure 4.8b and Table 4.2) shows the peaks of $[\text{Ni}(\text{OAc})_2(\text{en})_2+\text{H}]^+$, $[\text{Ni}(\text{OAc})_2(\text{en})_2+\text{H}]^+$, $[\text{Cu}(\text{OAc})_2(\text{en})_2+\text{H}]^+$ and $[\text{Cu}(\text{OAc})_2(\text{en})_2+\text{H}]^+$ at m/z of 298.734, 300.733, 302.764 and 304.858, respectively.

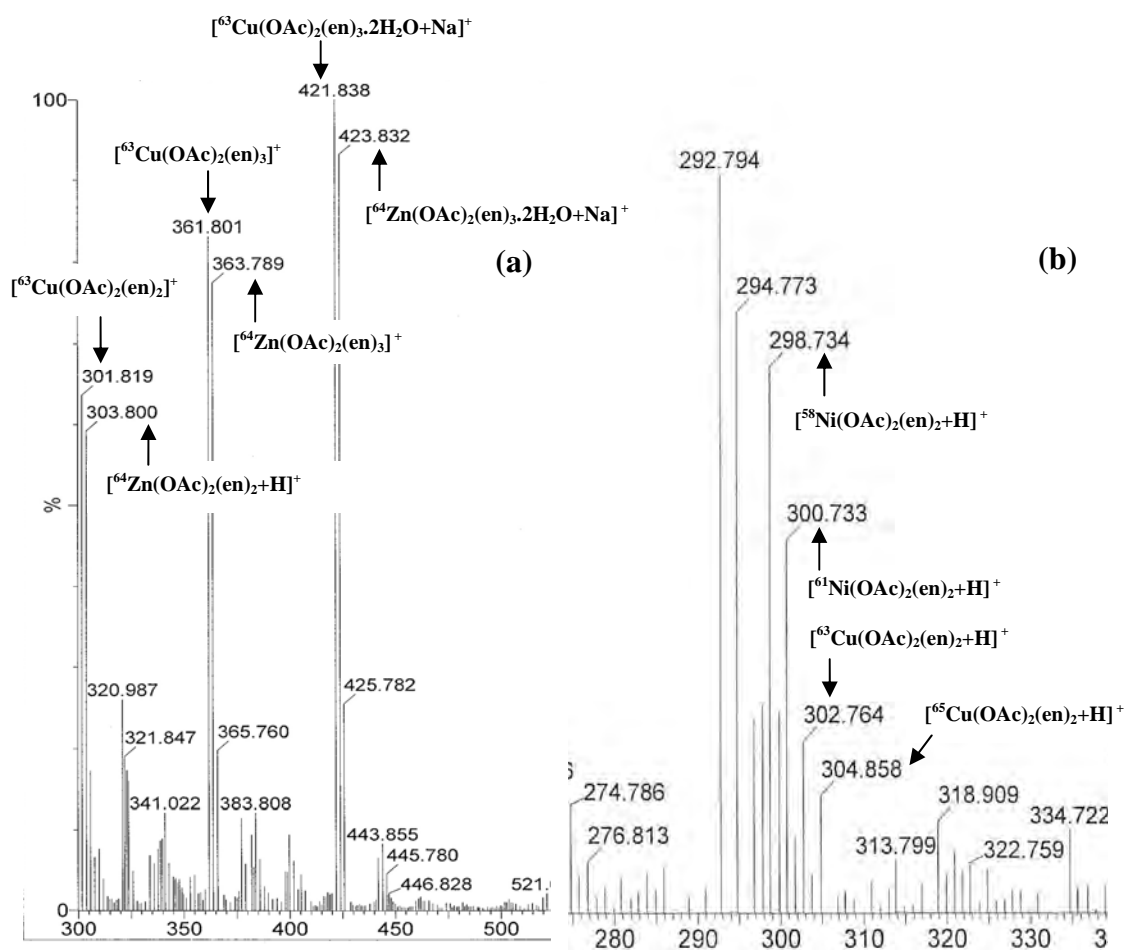
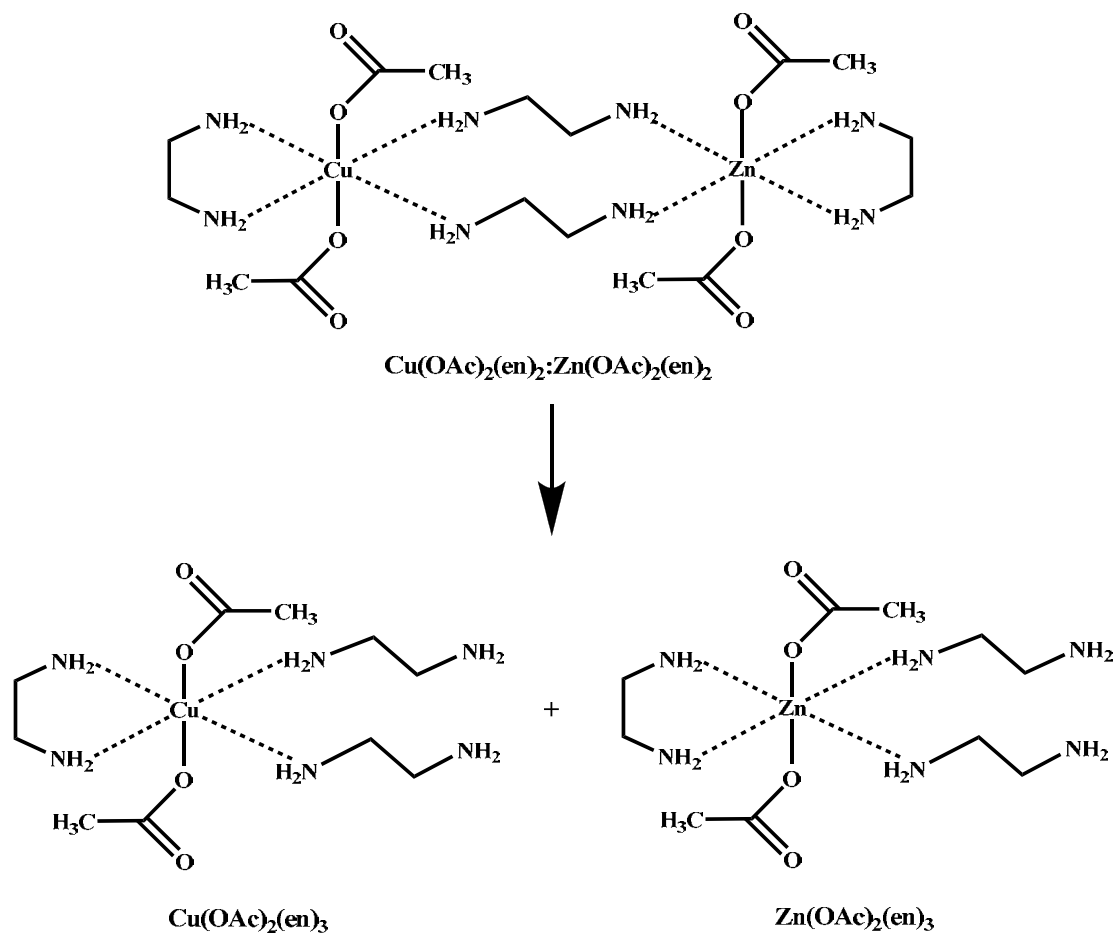


Figure 4.8 ESI Mass spectrum of (a) Cu(OAc)₂(en)₂:Zn(OAc)₂(en)₂ and (b) Cu(OAc)₂(en)₂:Ni(OAc)₂(en)₂

Furthermore, since the positive-ion ESI of Cu(OAc)₂(en)₂:Zn(OAc)₂(en)₂ (Figure 4.8a) showed the molecular ion peak corresponding to [63Cu(OAc)₂(en)₃]⁺, [64Zn(OAc)₂(en)₃]⁺, [63Cu(OAc)₂(en)₃.2H₂O+Na]⁺ and [64Zn(OAc)₂(en)₃.2H₂O+Na]⁺, the structure of Cu(OAc)₂(en)₂:Zn(OAc)₂(en)₂ is proposed as shown in Scheme 4.2. This proposed structure can be ionized by positive-ion ESI to give Cu(OAc)₂(en)₃ and Zn(OAc)₂(en)₃.



Scheme 4.2 Proposed structure of $\text{Cu(OAc)}_2(\text{en})_2:\text{Zn(OAc)}_2(\text{en})_2$

Table 4.2 positive ESI mass spectra of $\text{Cu}(\text{OAc})_2(\text{en})_2:\text{M}_2(\text{OAc})_2(\text{en})_2$ complexes

Molecular ion	Calculated	Found
$\text{Cu}(\text{OAc})_2(\text{en})_2:\text{Zn}(\text{OAc})_2(\text{en})_2$		
$[\text{}^{63}\text{Cu}(\text{OAc})_2(\text{en})_2]^+$	301.214	301.819
$[\text{}^{63}\text{Cu}(\text{OAc})_2(\text{en})_3]^+$	361.312	361.801
$[\text{}^{63}\text{Cu}(\text{OAc})_2(\text{en})_2.2\text{H}_2\text{O}+\text{Na}]^+$	420.333	421.838
$[\text{}^{64}\text{Zn}(\text{OAc})_2(\text{en})_2+\text{H}]^+$	303.221	303.800
$[\text{}^{64}\text{Zn}(\text{OAc})_2(\text{en})_3]^+$	362.311	363.789
$[\text{}^{64}\text{Zn}(\text{OAc})_2(\text{en})_3.2\text{H}_2\text{O}+\text{Na}]^+$	321.332	423.832
$\text{Cu}(\text{OAc})_2(\text{en})_2:\text{Ni}(\text{OAc})_2(\text{en})_2$		
$[\text{}^{63}\text{Cu}(\text{OAc})_2(\text{en})_2+\text{H}]^+$	302.222	302.764
$[\text{}^{65}\text{Cu}(\text{OAc})_2(\text{en})_2+\text{H}]^+$	304.220	304.858
$[\text{}^{58}\text{Ni}(\text{OAc})_2(\text{en})_2+\text{H}]^+$	297.228	298.734
$[\text{}^{61}\text{Ni}(\text{OAc})_2(\text{en})_2+\text{H}]^+$	300.223	300.733

4.2.3.5 Determination of metal amount in $\text{Cu}(\text{OAc})_2(\text{en})_2:\text{M}_2(\text{OAc})_2(\text{en})_2$ complexes by flame atomic spectrometry (FAAS)

The combustion flame is still the most frequently used atomizer in atomic absorption spectrometry (FAAS). The metals were: Ni, Cu and Zn by flame AAS; and C, N and H by flame emission spectrometry. An air-acetylene flame was used for Ni, Cu and Zn. After preparing the samples, the following parameters were optimized for each metal: burner height, acetylene flow rate and impact bead position shown in Table 4.3. Other parameters were according to established operating conditions for this matrix [64]. The calibration curve method was therefore chosen that the calibration curve is shown in Figure 4.9. The stability of the samples analyzed was determined by measuring the absorbance signals periodically which are shown in

Table 4.4. For analytical characteristics of $\text{Cu}(\text{OAc})_2(\text{en})_2$: $\text{M}(\text{OAc})_2(\text{en})_2$ shown in Table 4.5.

Table 4.3 Operating parameters the determination of metal concentration by FAAS

Parameters / Metal	Cu	Ni	Zn
Wavelength (nm)	324.8	232.0	213.9
Slit width (nm)	0.70	0.20	0.70
Read time (sec)	5.0	5.0	5.0
Flame type	Air/C ₂ H ₂	Air/C ₂ H ₂	Air/C ₂ H ₂
Oxidize flow	10.0	10.0	10.0
Fuel flow	3.0	3.0	3.0
Energy	74	55	54
Signal	AA	AA	AA

Table 4.4 Analytical characteristics of the FAAS method

Sample type ^(a)	Elements determined	Regression equation	R²
Cu(OAc)₂	Cu	$A = 0.0119C - 0.0019$	0.9880
Ni(OAc)₂	Ni	$A = 0.0039C - 0.000037$	0.9987
Zn(OAc)₂	Zn	$A = 0.0415C + 0.0024$	0.9984

A, absorbance; C, concentration (ppm)

^(a) Sample treatment: dilution with water

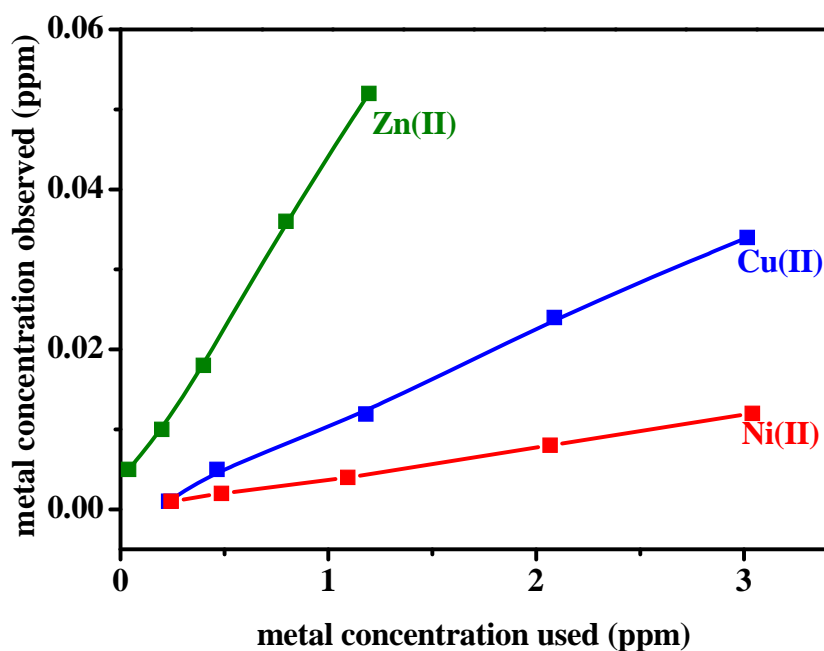


Figure 4.9 Estimation of Cu(II), Ni(II) and Zn(II) in metal(II)acetate samples by FAAS

Table 4.5 Analytical characteristics of the FAAS method

Sample type ^(a)	Elements determined	Concentration (ppm)	Calculated (%)	Experimental (%)
Cu(OAc) ₂ (en) ₂ :Ni(OAc) ₂ (en) ₂	Cu	0.002	10.3	7.29
	Ni	0.002	9.50	11.80
Cu(OAc) ₂ (en) ₂ :Zn(OAc) ₂ (en) ₂	Cu	0.012	10.40	8.29
	Zn	0.003	10.79	11.09

^(a) Sample treatment: dilution with water

It was found that the experimental values did not agree with the calculated value. This might be due to the different sensitivity of each metal.

4.2.4 Cu(OAc)₂(trien):M₂(OAc)₂(trien) complexes

4.2.4.1 FTIR spectroscopy of Cu(OAc)₂(trien):M₂(OAc)₂(trien) complexes

IR spectrum of Cu(OAc)₂(trien) shows the following characteristic frequencies: 3269 (N-H), 1556 $\nu_{\text{as}}(\text{COO}^-)$, 1401 $\nu_{\text{s}}(\text{COO}^-)$ and 1340 (C-N) cm^{-1} . IR spectrum of Ni(OAc)₂(trien) shows characteristic frequencies of $\nu(\text{NH})$, $\nu(\text{CH})$, $\nu(\text{CN})$ and $\nu(\text{CO})$ at 3213, 2986, 1402 and 1024 cm^{-1} , respectively. The acetate anions in Ni(OAc)₂(en)₂ were characterized by C=O stretching peaks, namely $\nu_{\text{as}}(\text{COO}^-)$ and $\nu_{\text{s}}(\text{COO}^-)$ at 1546 and 1409 cm^{-1} , respectively. Furthermore, IR spectrum of Zn(OAc)₂(trien) shows the following characteristic frequencies: 3390 (N-H), 1579 $\nu_{\text{as}}(\text{COO}^-)$, 1410 $\nu_{\text{s}}(\text{COO}^-)$ and 1335 (C-N) cm^{-1} .

IR spectra of Cu(OAc)₂(trien):M₂(OAc)₂(trien) (where M₂ = Ni or Zn) are shown in Figure 4.10. They exhibited absorption band at 3249-3406 cm^{-1} (N-H stretching), 2939-2969 cm^{-1} (C-H stretching), 1566-1591 cm^{-1} (C=O asymmetric stretching), 1406-1413 cm^{-1} (C=O symmetric stretching), 1340-1344 cm^{-1} (C-N stretching) and 1027-1030 cm^{-1} (C-O stretching). The C=O stretching of carbonyl group in Cu(OAc)₂(trien):Ni(OAc)₂(trien) and Cu(OAc)₂(trien):Zn(OAc)₂(trien) appeared as absorption band at 1566 and 1591 cm^{-1} (asymmetric C=O), and absorption band at 1344 and 1340 cm^{-1} (symmetric C=O), respectively, which were different from the typical Cu(OAc)₂ normally appears as absorption band around at 1596 cm^{-1} (C=O asymmetric stretching) and 1443 cm^{-1} (C=O symmetric stretching). The absorption bands of in Cu(OAc)₂(trien):Ni(OAc)₂(trien) and Cu(OAc)₂(trien):Zn(OAc)₂(trien) exhibited C-O stretching at 1027 and 1030 cm^{-1} , respectively, which shifted from typical absorption band of Cu(OAc)₂ at 1033 cm^{-1} . It was found that the IR peak of Cu(OAc)₂(trien):Ni(OAc)₂(trien) and Cu(OAc)₂(trien):Zn(OAc)₂(trien) complexes shifted from those of Cu(OAc)₂ to lower energy because of the influence of amine coordination, which suggested that the complexes were formed.

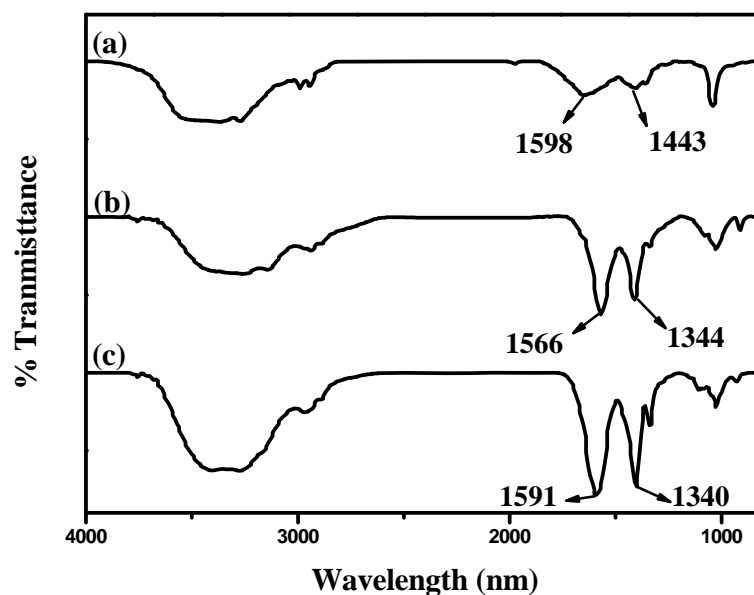


Figure 4.10 IR spectra of (a) $\text{Cu}(\text{OAc})_2$; (b) $\text{Cu}(\text{OAc})_2(\text{trien}):\text{Ni}(\text{OAc})_2(\text{trien})$;
(c) $\text{Cu}(\text{OAc})_2(\text{trien}):\text{Zn}(\text{OAc})_2(\text{trien})$

4.2.4.2 UV-visible spectroscopy of $\text{Cu}(\text{OAc})_2(\text{trien}):\text{M}_2(\text{OAc})_2(\text{trien})$ complexes

$\text{Cu}(\text{OAc})_2(\text{trien})$ has a strong absorption at 258 nm [43] while $\text{Ni}(\text{OAc})_2(\text{trien})$ and $\text{Zn}(\text{OAc})_2(\text{trien})$ show weak absorption. UV-visible spectra of $\text{Cu}(\text{OAc})_2(\text{trien}):\text{M}_2(\text{OAc})_2(\text{trien})$ complexes (where $\text{M}_2 = \text{Ni}$ and Zn) are shown in Figure 4.11. The UV absorption spectra for $\text{Cu}(\text{OAc})_2(\text{trien}):\text{Ni}(\text{OAc})_2(\text{trien})$ and $\text{Cu}(\text{OAc})_2(\text{trien}):\text{Zn}(\text{OAc})_2(\text{trien})$ complexes display a peak at 258.9 nm, which shifted from the maximum absorption of $\text{Cu}(\text{OAc})_2$ at 238.9 nm. This result confirmed the complex formation.

UV spectra of the metal complexes synthesized in water were compared to those synthesized in acetone (Figures 4.12 and 4.13). It was found that the metal complexes synthesized in acetone and water showed absorption at the same wavelength. The maximum absorption of $\text{Cu}(\text{OAc})_2(\text{trien}):\text{Ni}(\text{OAc})_2(\text{trien})$ and $\text{Cu}(\text{OAc})_2(\text{trien}):\text{Zn}(\text{OAc})_2(\text{trien})$ appeared at 258.9 and 257.9 nm, respectively.

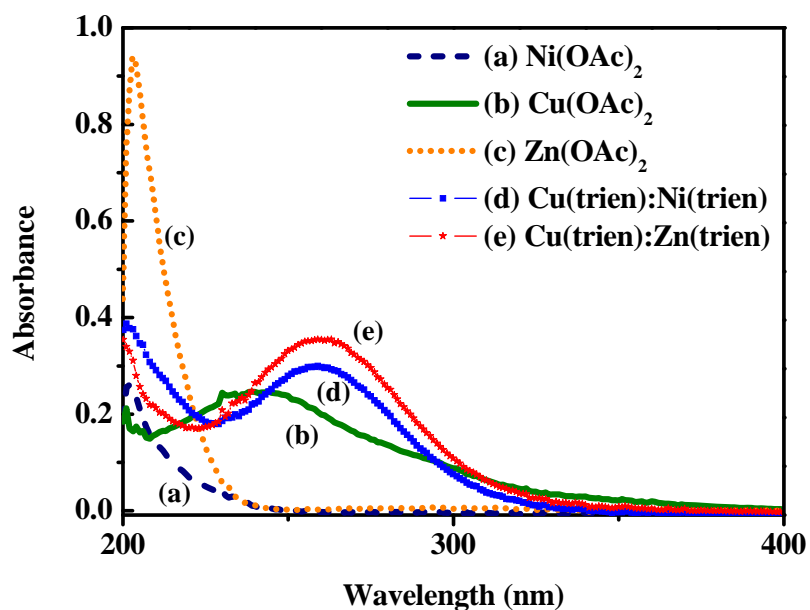


Figure 4.11 UV spectra of (a) $\text{Ni}(\text{OAc})_2$; (b) $\text{Cu}(\text{OAc})_2$; (c) $\text{Zn}(\text{OAc})_2$; (d) $\text{Cu}(\text{OAc})_2(\text{trien}):\text{Ni}(\text{OAc})_2(\text{trien})$; (e) $\text{Cu}(\text{OAc})_2(\text{trien}):\text{Zn}(\text{OAc})_2(\text{trien})$

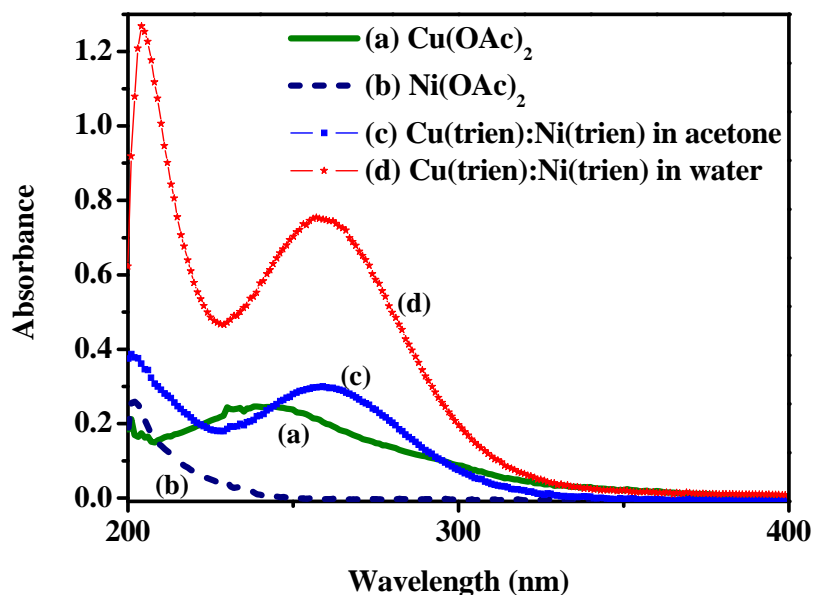


Figure 4.12 UV spectra of (a) $\text{Ni}(\text{OAc})_2$; (b) $\text{Cu}(\text{OAc})_2$; (c) $\text{Zn}(\text{OAc})_2$; (d) $\text{Cu}(\text{OAc})_2(\text{trien}):\text{Ni}(\text{OAc})_2(\text{trien})$ in acetone; (e) $\text{Cu}(\text{OAc})_2(\text{trien}):\text{Ni}(\text{OAc})_2(\text{trien})$ in water

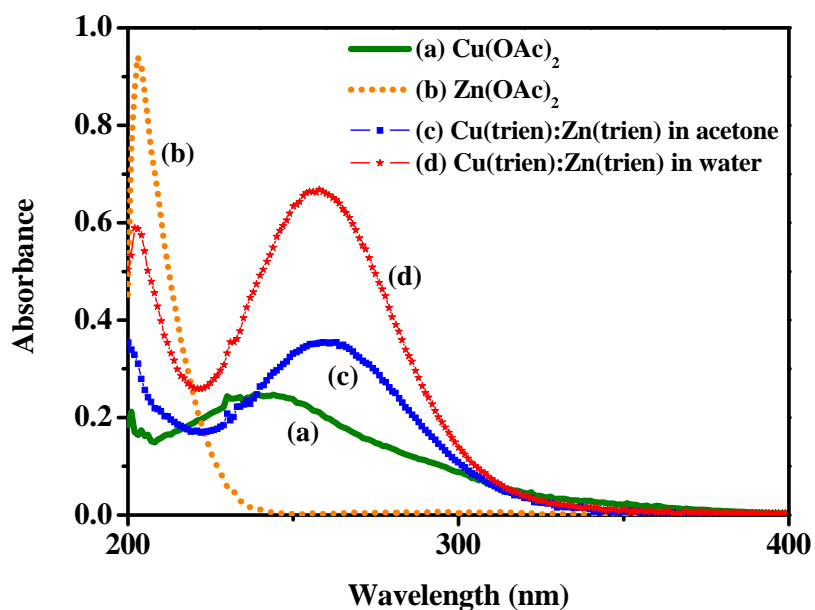


Figure 4.13 UV spectra of (a) Ni(OAc)₂; (b) Cu(OAc)₂; (c) Zn(OAc)₂; (d) Cu(OAc)₂(trien):Zn(OAc)₂(trien) in acetone; (e) Cu(OAc)₂(trien):Zn(OAc)₂(trien) in water

4.2.4.3 Elemental analysis of Cu(OAc)₂(trien):M(OAc)₂(trien) complexes

Elemental analysis (CHN) of Cu(OAc)₂(trien):Zn(OAc)₂(trien) showed the results in agreement with the calculated values (Table 4.6).

Table 4.6 Elemental analysis (CHN) of Cu(OAc)₂(trien):Zn(OAc)₂(trien)

Sample type	Elements determined	Calculated (%)	Experimental (%)
Cu(OAc) ₂ (trien):Zn(OAc) ₂ (trien).2H ₂ O	%C	32.90	32.70
	%H	7.75	8.15
	%N	15.36	13.07

4.2.4.4 Mass spectrometry of Cu(OAc)₂(trien):Ni(OAc)₂(trien)

The positive-ion ESI mass spectrum of ⁶³Cu(OAc)₂(trien) showed the molecular ion peak corresponding as the protonated form at *m/z* of 328.030 and ⁶⁶Zn(OAc)₂(trien).H₂O appears as the protonated form at *m/z* of 348.803. Moreover, ⁵⁸Ni(OAc)₂(trien).3H₂O showed the molecular ion peak as the protonated form at *m/z* of 377.823 (Appendix C).

The positive-ion ESI of Cu(OAc)₂(trien):Zn(OAc)₂(trien) is shown in Figure 4.14. The molecular ion peak corresponding to [⁶³Cu(OAc)₂(trien)+Na]⁺ appears as the Na⁺ form at *m/z* of 350.770 and [⁶⁴Zn(OAc)₂(trien)+H]⁺ appears as the protonated form at *m/z* of 347.794. Moreover, the positive-ion ESI of Cu(OAc)₂(trien):Ni(OAc)₂(trien) is shown up the molecular ion peak corresponding to [⁶³Cu(OAc)₂(trien)+H]⁺ appears as the protonated form at *m/z* of 346.943 and [⁵⁸Ni(OAc)₂(trien).H₂O+H]⁺ appears as the protonated form at *m/z* 341.961 (Table 4.7).

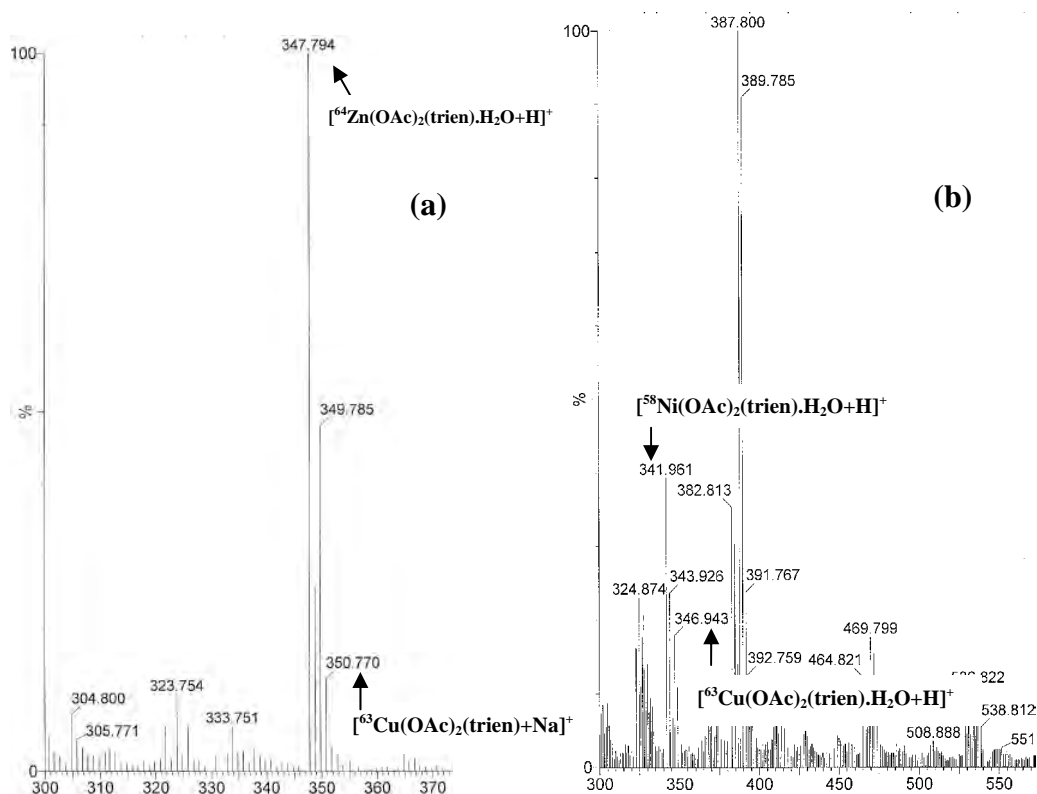


Figure 4.14 ESI Mass spectrum of (a) Cu(OAc)₂(trien):Zn(OAc)₂(trien) and (b) Cu(OAc)₂(trien):Ni(OAc)₂(trien)

Table 4.7 Positive ESI mass spectra of Cu(OAc)₂(trien):M₂(OAc)₂(trien) complexes

Molecular ion	Calculated	Found
Cu(OAc)₂(trien): Zn(OAc)₂(trien)		
[⁶³ Cu(OAc) ₂ (trien) +Na] ⁺	350.241	350.770
[⁶⁴ Zn(OAc) ₂ (trien).H ₂ O+H] ⁺	347.274	347.794
Cu(OAc)₂(trien): Ni(OAc)₂(trien)		
[⁶³ Cu(OAc) ₂ (trien).H ₂ O+H] ⁺	346.274	346.943
[⁵⁸ Ni(OAc) ₂ (trien).H ₂ O+H] ⁺	341.280	341.961

4.2.4.5 Determination of metal amount in $\text{Cu}(\text{OAc})_2(\text{trien})\text{:M}_2(\text{OAc})_2(\text{trien})$ complexes by flame atomic spectrometry (FAAS)

The obtained result was the same as in the case of $\text{Cu}(\text{OAc})_2(\text{trien})\text{:M}_2(\text{OAc})_2(\text{trien})$. It was found that the experimental values did not agree with the calculated values, which might be due to the different sensitivity of each metal. For analytical characteristics of $\text{Cu}(\text{OAc})_2(\text{trien})\text{:Ni}(\text{OAc})_2(\text{trien})$ shown in Table 4.8.

Table 4.8 Analytical characteristics of the FAAS method

Sample type ^(a)	Elements determined	Concentration (ppm)	Calculated (%)	Experimental (%)
$\text{Cu}(\text{OAc})_2(\text{trien})\text{:Ni}(\text{OAc})_2(\text{trien})$	Cu	0.004	9.76	10.07
	Ni	0.030	9.02	6.67
$\text{Cu}(\text{OAc})_2(\text{trien})\text{:Zn}(\text{OAc})_2(\text{trien})$	Cu	0.002	9.70	10.15
	Zn	0.013	9.90	7.88

(a) Sample treatment: dilution with water

4.3 Preparation of rigid polyurethane (RPUR) foams

4.3.1 Preparation of RPUR foams catalyzed by mixed metal complexes

The ratio $\text{M}_1(\text{OAc})_2\text{:M}_2(\text{OAc})_2\text{:en}$ and $\text{M}_1(\text{OAc})_2\text{:M}_2(\text{OAc})_2\text{:trien}$ employed in the synthesis of mixed metal complexes was 0.5:0.5:2 and 0.5:0.5:1, respectively. The rigid polyurethane foams catalyzed by $\text{M}_1(\text{OAc})_2(\text{en})_2\text{:M}_2(\text{OAc})_2(\text{en})_2$, $\text{M}_1(\text{OAc})_2(\text{trien})\text{:M}_2(\text{OAc})_2(\text{trien})$ (when $\text{M}_1 = \text{Cu}$, $\text{M}_2 = \text{Ca}$, Ba , Co , Mn , Ni , Zn ; $\text{M}_1 = \text{Ni}$, $\text{M}_2 = \text{Ca}$, Ba , Co , Mn , Zn and $\text{M}_1 = \text{Mn}$, $\text{M}_2 = \text{Ca}$, Ba , Co , Zn) were prepared by mechanical mixing technique in two step mixing. In the first step, “polyblend” was prepared by mixing polyol, catalysts (mixed metal complexes or DMCHA), surfactant (B8460) and blowing agent (water) in a 700 mL paper cup. In the second step, the isocyanate (polymeric MDI) was added to the “polyblend”, then the mixture were

mixed to obtain homogeneous mixture by mechanical stirrer at 2000 rpm for 20 seconds. During the reaction, cream time, gel time, tack free time and rise time were measured. Cream time is the time of the beginning of blowing reaction. Gel time is the time needed for the mass to reach the gel point (gelling reaction). Tack free time is the time of the foams could not tack with other materials, which is the time when polymerization reaction is completed. Rise time is the time when the foams stop rising, which is the time when CO₂ generation stops. After that, RPUR foams were kept at room temperature for 48 hours before carrying out physical and mechanical characterization. In this work, the amount of polyol, catalyst, surfactant (B8460) and blowing agent (water) were fixed. The polymeric MDI amount was varied to obtain the NCO indexes of 100 and 150 and the amount of catalysts was fixed at 1.0 pbw. RPUR foam formulation is shown in Table 4.9 and their appearances are shown in Figures 4.15-4.16.

Table 4.9 RPUR foam formulation

Components (pbw*)	NCO index**		
	100	150	200
Raypol [®] 4221	100	100	100
Catalyst			
- DMCHA (commercial catalyst)	1.0	1.0	1.0
- mixed metal complexes			
Surfactant (B8460)	2.5	2.5	2.5
Blowing agent (water)	4.0	4.0	4.0
PMDI (MR-200)	166	249	333

*pbw; parts by weight or gram of components per 100 grams of polyol

$$** \text{ Isocyanate index} = \frac{\text{actual amount of isocyanate}}{\text{theoretical amount of isocyanate}} \times 100$$



Figure 4.15 RPUR foams catalyzed by $\text{Cu}(\text{OAc})_2(\text{en})_2:\text{Zn}(\text{OAc})_2(\text{en})_2$ at different NCO indexes (a) 100; (b) 150; (c) 200



Figure 4.16 RPUR foams catalyzed by $\text{Cu}(\text{OAc})_2(\text{en})_2:\text{Ni}(\text{OAc})_2(\text{en})_2$ at different NCO indexes (a) 100; (b) 150; (c) 200

From the results of foam preparation, RPUR foams catalyzed by mixed metal complexes gave good foams in the range of 100-150 NCO indexes. When the foams were prepared with higher NCO indexes, the foams were brittle and not suitable for foam applications.

4.3.1.1 Preparation of RPUR foams using an aluminum mold

In order to test the foam processing ability, RPUR foams were prepared at index 100 using 10x10x10 cm aluminum mold (Figure 4.17) instead of a paper cup. The starting materials were mixed in a paper cup and then poured into the

mold. It was found that an RPUR foam appearance was the same as that prepared in a paper cup [65].

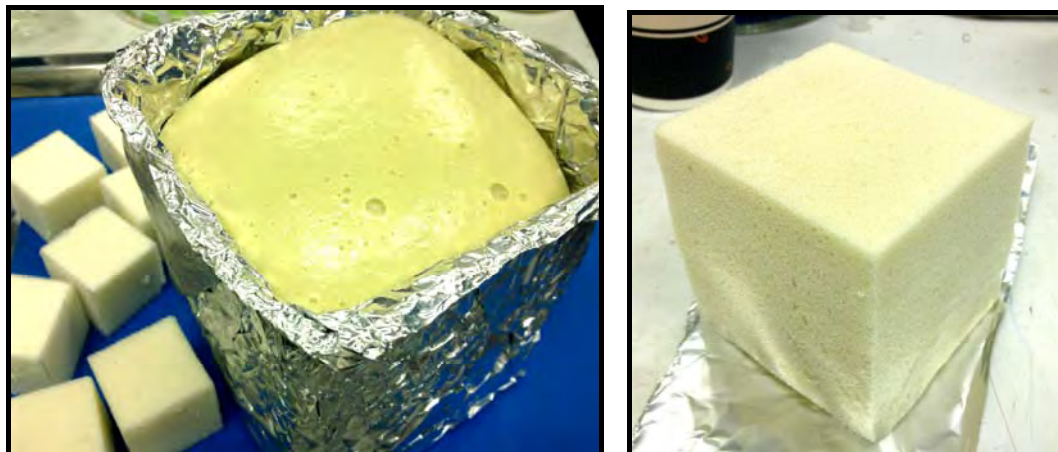


Figure 4.17 RPUR foams catalyzed by $\text{Cu}(\text{OAc})_2(\text{en})_2:\text{Zn}(\text{OAc})_2(\text{en})_2$ and prepared in an aluminum mold

4.3.2 Reaction times and rise profile

The reaction times of RPUR foams catalyzed by mixed metal complexes synthesized in acetone are shown in Table 4.10 and Figure 4.18-4.19 and those synthesized in water are shown in Table 4.11. RPUR foams were prepared at the NCO index of 100. The reaction times measured were cream time (which is the time of the foam start to rise of blowing reaction), gel time (which is the time of foam mixture begin to gel or gelling reaction), tack free time (which is the time of the foam could not tack with other materials or crosslinking reaction) and rise time (which is the foam stop rising).

The obtained results showed that all mixed metal complexes showed comparable catalytic activity to the commercial reference catalyst (DMCHA, dimethylcyclohexylamine). This suggested that catalytic activity of the reaction between isocyanate/hydroxyl groups to give urethane (gelling reaction) and isocyanate group/water to give CO_2 (blowing reaction) of all catalysts were similar. The mixed metal complexes could catalyze RPUR foam polymerization since the metal complexes (Cu-based catalyst) acted as a Lewis acid, throughout copper (II) chemistry, Jahn-Teller distortions are observed as predicted for an octahedral d^9 ion,

although the degree of distortion varies considerably. The complexes with N- donor ligands are Octahedral [45]. The use of an aprotic chelating ligand, such as ethylenediamine promotes the bridging function of the anions in the resulting polymeric structures. The activation starts by coordinated to the oxygen atom of the NCO group and activated the electrophilic nature of the carbon (scheme 4.2). The amine using its lone pair of electrons interacting with the proton source (polyol, water, amine) to form a complex, which then reacts with the isocyanate [66]. Thermal stability of the copper diamine compounds with various counterions (e.g. chloride, sulphate, perchlorate, nitrate) was studied [67-74]. However, the detailed information concerning the thermal properties of the Cu (II) diamine compounds with carboxylates as counterion are scarce [75-76].

The gel time of RPUR foams catalyzed by $\text{Cu}(\text{OAc})_2(\text{trien}):\text{Zn}(\text{OAc})_2(\text{trien})$ indicated that it had comparable catalytic activity to DMCHA. Gel time of $\text{Cu}(\text{OAc})_2(\text{trien}):\text{Zn}(\text{OAc})_2(\text{trien})$ was longer time than that of DMCHA, which resulted in the ease in pouring the starting materials into the mold.

Although mixed metal complexes had comparable catalytic activity than DMCHA catalyst, some complexes gave brittle foams with poor appearance. The complexes which had good catalytic property and gave rigid foams with good appearance were $\text{Cu}(\text{OAc})_2(\text{en})_2:\text{Ni}(\text{OAc})_2(\text{en})_2$, $\text{Cu}(\text{OAc})_2(\text{en})_2:\text{Zn}(\text{OAc})_2(\text{en})_2$, $\text{Cu}(\text{OAc})_2(\text{trien}):\text{Ni}(\text{OAc})_2(\text{trien})$ and $\text{Cu}(\text{OAc})_2(\text{trien}):\text{Zn}(\text{OAc})_2(\text{trien})$.

To investigate, the preparation of mixed metal complexes synthesized in acetone and water that gave a result of reaction profile identically. Therefore, the preparation complexes in water had accurate because foam formulation had water which was blowing agent. Good points: the preparation complexes in water used less time and didn't use to exhausted acetone solvent. Some metal complex absorbs water, example $\text{Cu}(\text{OAc})_2(\text{en})_2$, but didn't decompose that made weight to use incorrect. Some metal complex was soluble in "polyblend" (polyol, catalysts, surfactant and blowing agent) to difficult then the preparation complexes in water were easily dissolved.

Furthermore, rise profile of RPUR foams prepared from $\text{Cu}(\text{OAc})_2(\text{en})_2:\text{Ni}(\text{OAc})_2(\text{en})_2$, $\text{Cu}(\text{OAc})_2(\text{en})_2:\text{Zn}(\text{OAc})_2(\text{en})_2$, $\text{Cu}(\text{OAc})_2(\text{trien}):\text{Ni}(\text{OAc})_2(\text{trien})$ and $\text{Cu}(\text{OAc})_2(\text{trien}):\text{Zn}(\text{OAc})_2(\text{trien})$ showed similar trend to that of DMCHA (Scheme 4.2). DMCHA is a tertiary amine-based catalyst and has strong catalytic activity towards both blowing and gelling reactions [2]. The mixed metal complexes showed longer initial time than DMCHA and exhibited a fast rise curve in the latter stage.

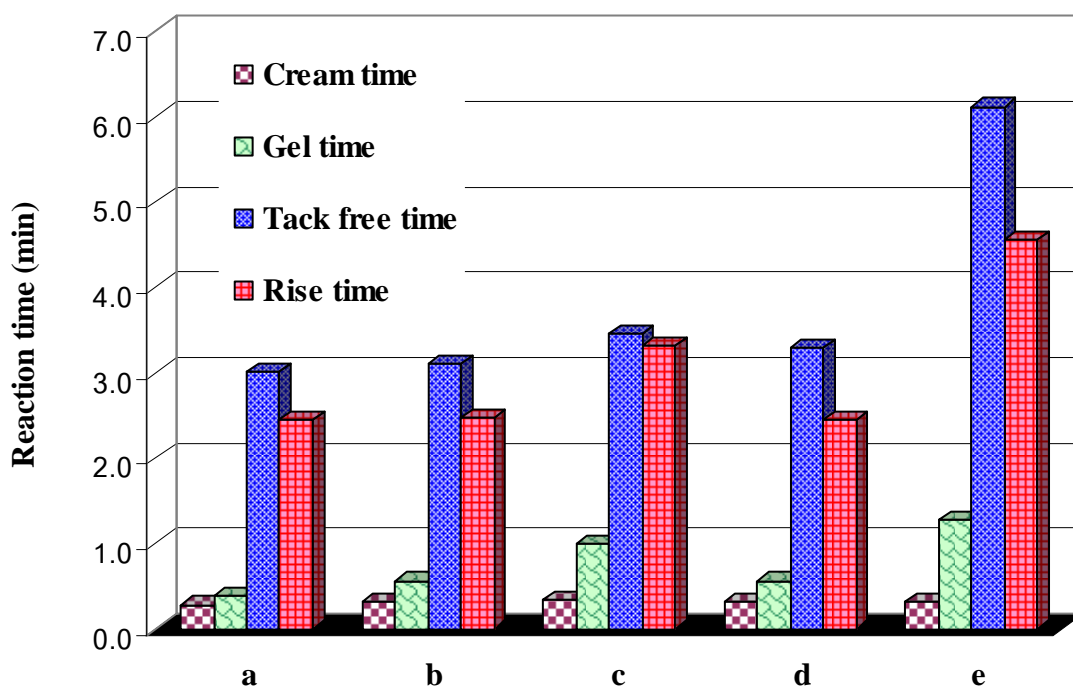


Figure 4.18 Reaction times of RPUR foams prepared at the NCO index of 100 and catalyzed by (a) DMCHA; (b) $\text{Cu}(\text{OAc})_2(\text{en})_2:\text{Zn}(\text{OAc})_2(\text{en})_2$; (c) $\text{Cu}(\text{OAc})_2(\text{trien}):\text{Zn}(\text{OAc})_2(\text{trien})$; (d) $\text{Cu}(\text{OAc})_2(\text{en})_2:\text{Ni}(\text{OAc})_2(\text{en})_2$; (e) $\text{Cu}(\text{OAc})_2(\text{trien}):\text{Ni}(\text{OAc})_2(\text{trien})$

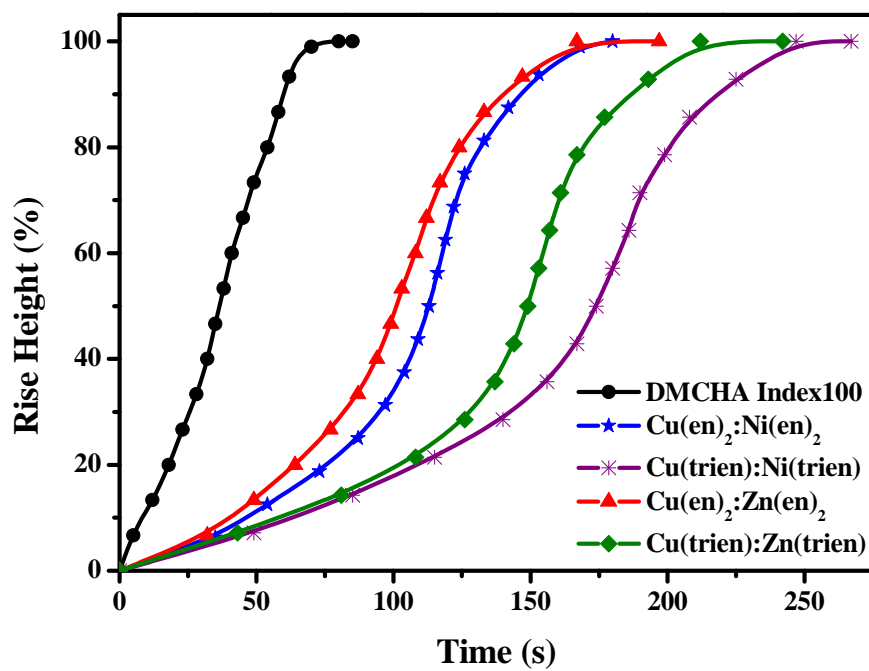


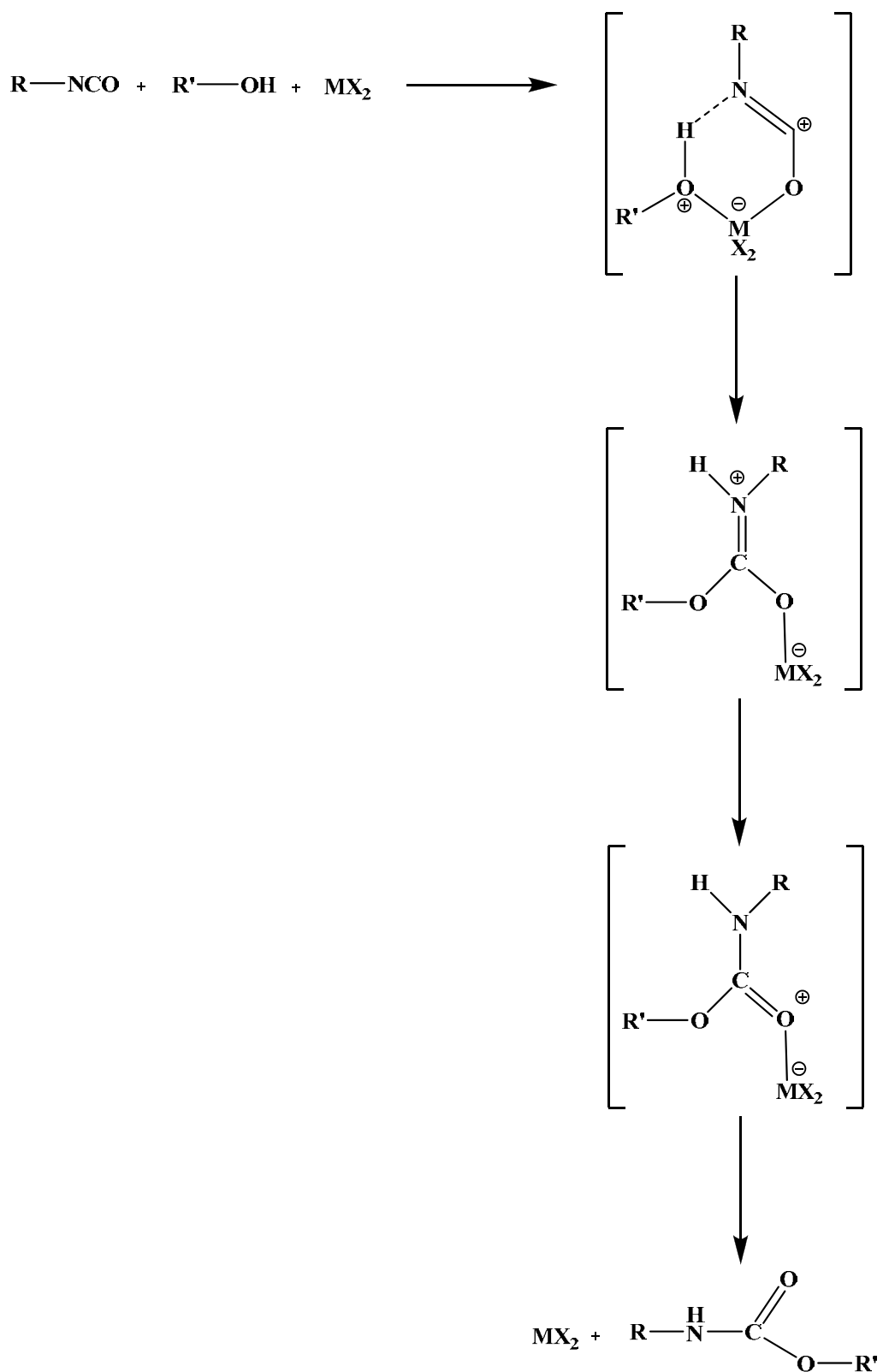
Figure 4.19 Rise profile of RPUR foams catalyzed by different mixed metal complexes at the NCO index of 100

Table 4.10 Reaction profiles of RPUR foams prepared at the NCO index of 100 and catalyzed by mixed metal complexes prepared in acetone

Catalysts	Cream time (min)	Gel time (min)	Tack free time (min)	Rise time (min)	Volume
NCO index 100					
DMCHA	0:22	0:33	3:00	1:20	8/8V
Ni(OAc)₂(en)₂	0:26	0:31	6:09	6:09	6/8V
Cu(OAc)₂(en)₂	0:26	0:39	1:40	2:07	8/8V
Zn(OAc)₂(en)₂	0:22	0:29	3:43	4:11	8/8V
Cu(OAc)₂(en)₂:Ca(OAc)₂(en)₂	0:30	0:42	1:59	1:50	6/8V
Cu(OAc)₂(en)₂:Ba(OAc)₂(en)₂	0:37	0:47	2:11	2:15	7/8V
Cu(OAc)₂(en)₂:Co(OAc)₂(en)₂	0:29	0:51	2:53	2:30	7/8V
Cu(OAc)₂(en)₂:Ni(OAc)₂(en)₂	0:28	0:39	3:01	2:45	8/8V
Cu(OAc)₂(en)₂:Zn(OAc)₂(en)₂	0:29	0:41	1:41	2:12	8/8V
Ni(OAc)₂(trien)	0:26	1:20	8:59	8:59	6/8V
Cu(OAc)₂(trien)	0:30	0:55	2:19	2:44	8/8V
Zn(OAc)₂(trien)	0:25	1:08	3:57	4:17	8/8V
Cu(OAc)₂(trien):Ni(OAc)₂(trien)	0:36	1:28	4:47	4:07	7/8V
Cu(OAc)₂(trien):Zn(OAc)₂(trien)	0:36	1:00	3:45	3:32	8/8V
Cu(en)(trien):Ni(en)(trien)	0:28	1:16	4:43	4:43	7/8V
Cu(en)(trien):Zn(en)(trien)	0:26	0:54	2:59	3:32	8/8V

Table 4.11 Reaction profiles of RPUR foams prepared at the NCO index of 100 and catalyzed by mixed metal complexes prepared in water

Catalysts	Cream time (min)	Gel time (min)	Tack free time (min)	Rise time (min)	Volume
NCO index 100					
DMCHA	0:22	0:33	3:00	1:20	8/8V
W_Ni(OAc)₂(en)₂	0:25	1:24	7:09	7:09	5/8V
W_Cu(OAc)₂(en)₂	0:24	0:49	1:53	2:38	7/8V
W_Zn(OAc)₂(en)₂	0:25	0:29	3:51	4:52	7/8V
W_Cu(OAc)₂(en)₂:Ni(OAc)₂(en)₂	0:28	1:47	5:10	4:38	6/8V
W_Cu(OAc)₂(en)₂:Zn(OAc)₂(en)₂	0:29	1:15	3:24	3:42	7/8V
W_Ni(OAc)₂(trien)	0:28	1:27	7:34	7:34	6/8V
W_Cu(OAc)₂(trien)	0:29	0:55	2:21	2:56	8/8V
W_Zn(OAc)₂(trien)	0:27	1:09	4:11	5:04	8/8V
W_Cu(OAc)₂(trien):Ni(OAc)₂(trien)	0:31	1:41	6:02	7:47	7/8V
W_Cu(OAc)₂(trien):Zn(OAc)₂(trien)	0:31	1:21	4:27	4:56	8/8V



Scheme 4.3 Activation mechanism of metal-based catalyst on urethane formation reaction

The maximum rise rates for RPUR foams prepared at the NCO index of 100 were calculated by differential at secondary stage of rise profile which gives maximum slope as shown in Figure 4.20. It was demonstrated that the RPUR foams catalyzed by $\text{Cu}(\text{OAc})_2(\text{en})_2:\text{Ni}(\text{OAc})_2(\text{en})_2$ and $\text{Cu}(\text{OAc})_2(\text{trien}):\text{Zn}(\text{OAc})_2(\text{trien})$ showed comparable maximum rise rate to those prepared from DMCHA, however, RPUR catalyzed by $\text{Cu}(\text{OAc})_2(\text{en})_2:\text{Ni}(\text{OAc})_2(\text{en})_2$ had poor morphology.

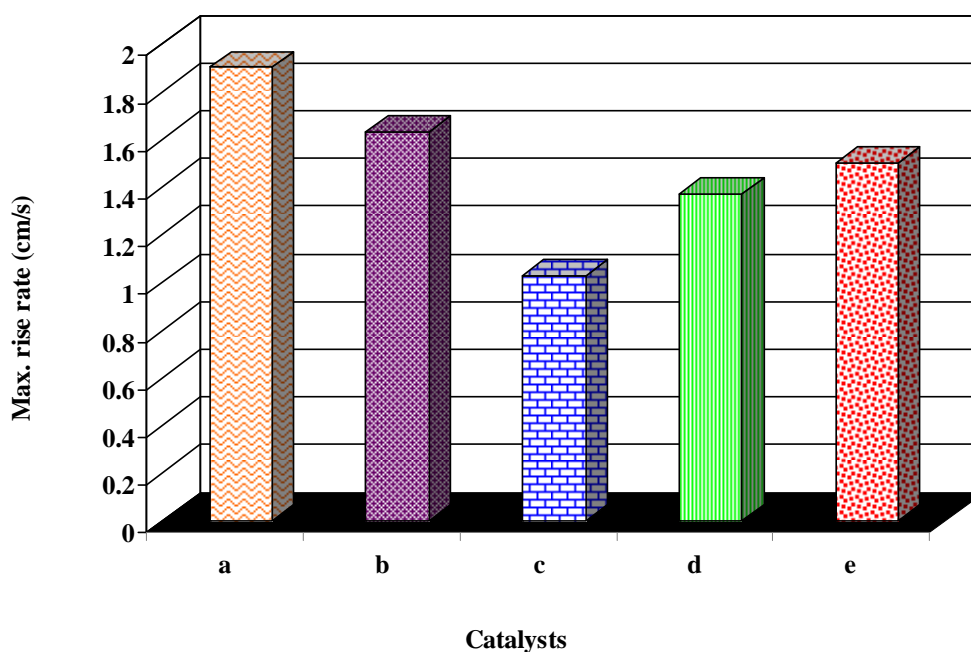


Figure 4.20 Maximum rise rates of RPUR foams prepared at the NCO index of 100 and catalyzed by different mixed metal complexes (a) DMCHA (ref.); (b) $\text{Cu}(\text{OAc})_2(\text{en})_2:\text{Ni}(\text{OAc})_2(\text{en})_2$; (c) $\text{Cu}(\text{OAc})_2(\text{trien}):\text{Ni}(\text{OAc})_2(\text{trien})$; (d) $\text{Cu}(\text{OAc})_2(\text{en})_2:\text{Zn}(\text{OAc})_2(\text{en})_2$; (e) $\text{Cu}(\text{OAc})_2(\text{trien}):\text{Zn}(\text{OAc})_2(\text{trien})$

To further investigate the effect of metals in mixed metal complexes, mixed metal complexes at variable $\text{M}_1(\text{OAc})_2:\text{M}_2(\text{OAc})_2:\text{ethylenediamine}$ ratios of 0.7:0.3:2, 0.5:0.5:2 and 0.3:0.7:2 were synthesized in acetone. The reaction time of RPUR foams catalyzed by these mixed metal complexes are shown in Table 4.12. The data indicated that increasing Cu (II) in $\text{Cu}(\text{OAc})_2(\text{en})_2:\text{Zn}(\text{OAc})_2(\text{en})_2$, resulting in faster reaction times.

Moreover, the rise profile of RPUR foams prepared from mixed metal-amines complexes with variable $M_1(\text{OAc})_2:M_2(\text{OAc})_2$:amine ratios of 0.5:0.5:0.5, 0.5:0.5:1 and 0.5:0.5:2 were investigated as shown in Table 4.13. It was found that variation of ethylenediamine (en) amount showed opposite results to triethylenetetramine (trien). Increase of ethylenediamine resulted in slower reaction time while increase of triethylenetetramine resulted in faster reaction time. This might be due to the completeness of the metal-amine complex formation.

Table 4.12 Reaction profiles of RPUR foam catalyzed by $M_1(\text{OAc})_2:M_2(\text{OAc})_2$: ethylenediamine with different $M_1(\text{OAc})_2:M_2(\text{OAc})_2$ ratios at index 100

Reaction Time (min)	DMCHA	$\text{Cu}(\text{OAc})_2(\text{en})_2:\text{Zn}(\text{OAc})_2(\text{en})_2$		
		0.7:0.3:2	0.5:0.5:2	0.3:0.7:2
Cream time	0:22	0:24	0:31	0:37
Gel time	0:33	0:35	0:48	1:01
Tack free time	3:00	1:40	2:26	2:40
Rise time	1:10	2:24	3:03	2:40
Volume(V)	8/8V	8/8V	8/8V	8/8V

Table 4.13 Reaction profiles of RPUR foam catalyzed by $M_1(\text{OAc})_2:M_2(\text{OAc})_2$:amine with different $M_1(\text{OAc})_2$:amine ratios at index 100

Reaction Time (min)	DMCHA	$\text{Cu}(\text{OAc})_2:\text{Zn}(\text{OAc})_2:(\text{en})_x$			$\text{Cu}(\text{OAc})_2:\text{Zn}(\text{OAc})_2:(\text{trien})_x$		
		0.5:0.5:0.5	0.5:0.5:1	0.5:0.5:2	0.5:0.5:0.5	0.5:0.5:1	0.5:0.5:2
Cream time	0:22	0:33	0:32	0:29	0:30	0:34	0:36
Gel time	0:33	0:57	0:44	0:41	0:57	1:00	1:14
Tack free time	3:00	2:51	2:10	1:41	2:28	3:45	3:58
Rise time	1:10	3:19	2:39	2:12	3:09	3:32	3:52
Volume (V)	8/8V	8/8V	8/8V	8/8V	8/8V	8/8V	8/8V

It could be concluded that the optimum $M_1(\text{OAc})_2:M_2(\text{OAc})_2$:amine ratios of $M_1(\text{OAc})_2:M_2(\text{OAc})_2:\text{en}$ and $M_1(\text{OAc})_2:M_2(\text{OAc})_2:\text{trien}$ were 0.5:0.5:2 and 0.5:0.5:1, respectively. Therefore, more investigations were done on RPUR foams catalyzed by mixed metal complexes prepared at these mole ratios.

4.3.3 Apparent density

The apparent density of RPUR foams were measured according to ASTM D1622. After foam preparation, RPUR foams were kept in room temperature for 48 hours, and then the foams were cut into cubic shape with 3.0 cm x 3.0 cm x 3.0 cm dimensions before apparent density of foams were measured as shown in Figure 4.21.

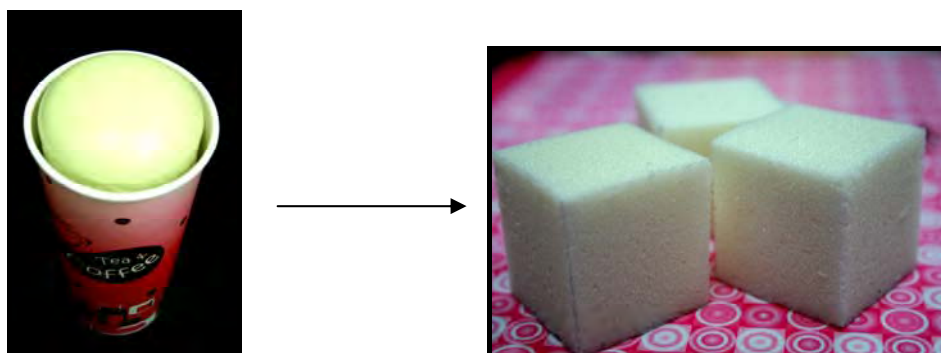


Figure 4.21 Samples for foam density measurements

4.3.3.1 Effect of NCO indexes on foam density

The apparent density of RPUR foams catalyzed by mixed metal complexes at different NCO indexes is shown in Table 4.14. It was found that the apparent density of RPUR foams increased with increasing the content of NCO indexes because the excess of isocyanate in PUR system could undergo further polymerization to give crosslinked structure [77]. RPUR foams prepared from mixed metal complexes had suitable density when prepared at the NCO index 100-150 while the foams prepared at the index 200 were brittle and therefore the density could not be measured (Figure 4.22).

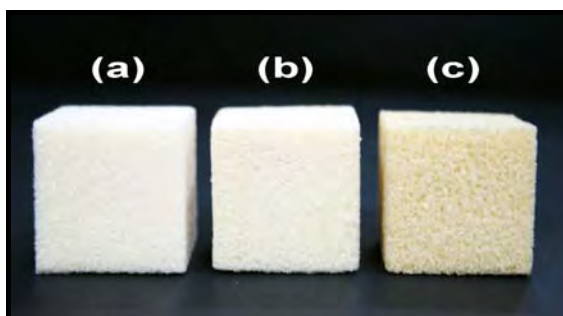


Figure 4.22 RPUR foam samples for foam density measurements (a) NCO index 100 (b) NCO index 150 (c) NCO index 200

In comparison between the densities of RPUR foams prepared from mixed metal complexes and DMCHA, RPUR foams prepared at NCO index = 150 and catalyzed by $\text{Cu}(\text{OAc})_2(\text{en})_2$, $\text{Zn}(\text{OAc})_2(\text{en})_2$ and $\text{Cu}(\text{OAc})_2(\text{en})_2:\text{Zn}(\text{OAc})_2(\text{en})_2$ showed similar density to those prepared from DMCHA. Density of most RPUR foams catalyzed by mixed metal complexes at NCO indexes 100-150 was in the range $40\text{-}50 \text{ kg.m}^3$, which was the desirable density for foam applications [78-79]. It was found that the foams prepared from mixed metal complexes which were synthesized in acetone and water showed similar apparent density and also similar to those prepared from DMCHA.

Table 4.14 Density of RPUR foams prepared at the NCO index 100-200

Catalysts	Catalysts synthesized in water		Catalysts synthesized in acetone		
	NCO index		NCO index		
	W_100	W_150	100	150	200
DMCHA (ref)	34.1	44.7	34.1	44.7	64.3
Ni(OAc)₂(en)₂	51.0	69.4	67.8	70.2	-
Cu(OAc)₂(en)₂	43.3	47.5	39.3	43.6	-
Zn(OAc)₂(en)₂	39.3	44.7	37.0	41.1	-
Cu(OAc)₂(en)₂:Ni(OAc)₂(en)₂	44.9	59.4	39.5	46.7	68.0
Cu(OAc)₂(en)₂:Zn(OAc)₂(en)₂	42.9	48.1	40.3	44.1	72.6
Ni(OAc)₂(trien)	52.0	52.0	44.8	58.9	-
Cu(OAc)₂(trien)	39.4	45.7	41.4	45.3	-
Zn(OAc)₂(trien)	34.4	43.2	36.0	39.8	-
Cu(OAc)₂(trien):Ni(OAc)₂(trien)	41.5	49.6	41.9	52.6	72.3
Cu(OAc)₂(trien):Zn(OAc)₂(trien)	42.9	48.0	40.5	46.7	68.1
Cu(en)(trien):Ni(en)(trien)	-	-	40.7	47.7	-
Cu(en)(trien):Zn(en)(trien)	-	-	38.8	48.5	-

4.3.3.2 Effect of catalyst quantity on foam density

The effect of catalyst quantity on RPUR foam density catalyzed by DMCHA, $\text{Cu}(\text{OAc})_2(\text{en})_2$, $\text{Zn}(\text{OAc})_2(\text{en})_2$, $\text{Cu}(\text{OAc})_2(\text{en})_2:\text{Zn}(\text{OAc})_2(\text{en})_2$ (synthesized in acetone) are shown in Figure 4.23. It was found that the foam density decreased with increasing the content of catalyst in foam formulation since more blowing reactions could occur when increasing amount of catalyst. Furthermore, it was observed that the foam prepared at catalyst quantity of 0.5 part by weight (pbw) showed lower blowing reaction than those prepared from 1.0 and 2.0 pbw of catalyst. Although high catalyst quantities resulted in good blowing reaction, but gel time and tack free time were too short and therefore caused difficult practice in foam process. This resulted in brittle foam which is undesirable foam for applications.

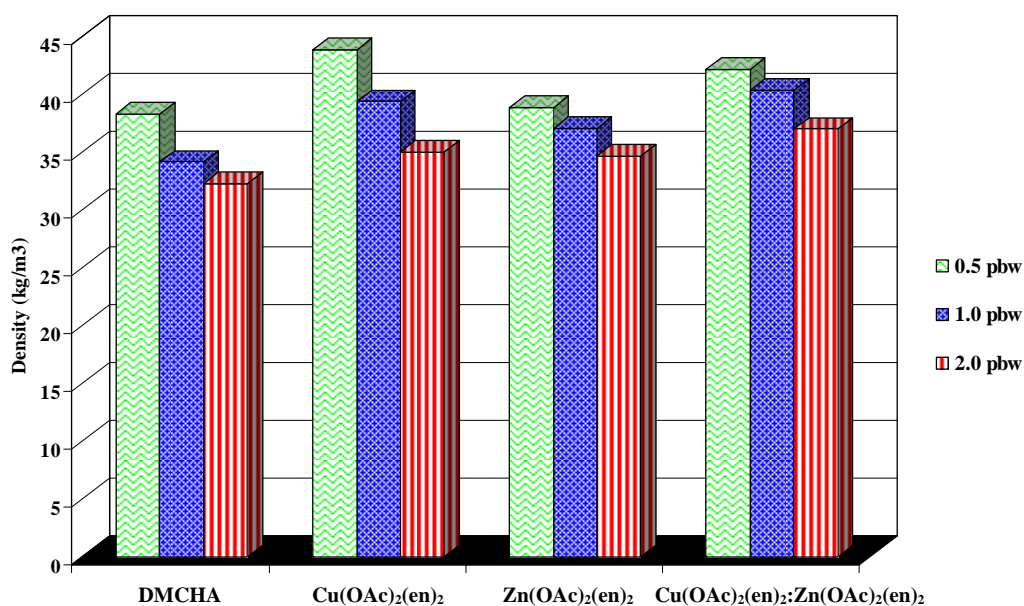


Figure 4.23 Effect of catalyst amount on RPUR foams density catalyzed by different catalysts at NCO index of 100

4.3.4 Foaming temperature

The maximum core temperature of RPUR foams catalyzed by various catalysts (synthesized in acetone) at different NCO indexes is shown in Table 4.15. It was found that the polymerization reaction is exothermic reaction. The maximum core temperature of RPUR foams prepared from metal complexes and mixed metal complexes were in the range 96.2-128.5°C and 102.5-131.3°C, respectively. Moreover, RPUR foams prepared from mixed amine complexes were in the range 104.2-125.1°C. The RPUR foams catalyzed by mixed metal complexes showed higher core temperature than those prepared from metal complexes and DMCHA. The maximum core temperature of RPUR foams prepared from mixed metal complexes synthesized in water were in the range 103.7-123.3°C, which is similar to those synthesized in acetone (Table 4.16).

The temperature profiles of RPUR foams prepared from different catalyst at NCO index of 100 were investigated as shown in Figure 4.24. It was found that the temperature profiles of RPUR foams catalyzed by mixed metal complexes (synthesized in acetone) were the same as those catalyzed by DMCHA.

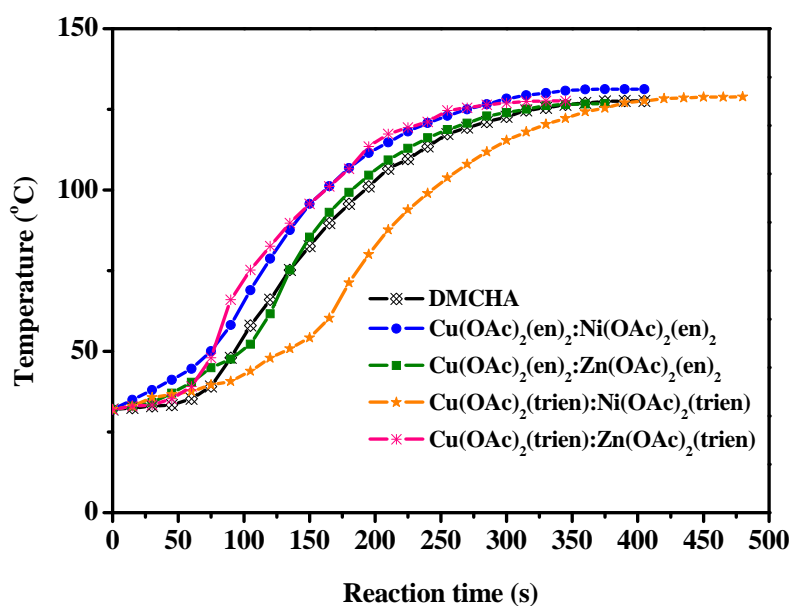


Figure 4.24 Temperature profiles of RPUR foams catalyzed by different mixed metal complexes

Table 4.15 Maximum core temperature of RPUR foam catalyzed by mixed metal complexes synthesized in acetone at different NCO indexes

Catalyst types	NCO Index	Maximum Core Temperature (°C)	Starting time at T_{max} [sec (min)]
DMCHA	100	127.6	390 (6:30)
	150	120.8	420 (7:00)
Ni(OAc)₂(en)₂	100	105.7	705 (11:45)
	150	111.8	840 (14:00)
Cu(OAc)₂(en)₂	100	125.1	390 (6.30)
	150	121.3	465 (7.45)
Zn(OAc)₂(en)₂	100	124.4	435 (7:15)
	150	128.5	540 (9:00)
Cu(OAc)₂(en)₂ :Ni(OAc)₂(en)₂	100	131.3	390 (6:30)
	150	125.8	510 (8:30)
Cu(OAc)₂(en)₂ :Zn(OAc)₂(en)₂	100	126.8	375 (6:15)
	150	123.3	450 (7:30)
Ni(OAc)₂(trien)	100	96.2	855 (14:15)
	150	98.2	1,020 (17:00)
Cu(OAc)₂(trien)	100	122.4	390 (6:30)
	150	114.4	375 (6:15)
Zn(OAc)₂(trien)	100	125.6	465 (7:45)
	150	118.9	600 (10:00)
Cu(OAc)₂(trien) :Ni(OAc)₂(trien)	100	128.9	480 (8:00)
	150	129.8	540 (9:00)
Cu(OAc)₂(trien) :Zn(OAc)₂(trien)	100	127.6	360 (6:00)
	150	111.5	420 (7:00)

Table 4.15 Maximum core temperature of RPUR foam catalyzed by mixed metal complexes synthesized in acetone at different NCO indexes (continued)

Catalyst types	NCO Index	Maximum Core Temperature (°C)	Starting time at T_{max} [sec (min)]
Cu(en)(trien):Ni(en)(trien)	100	104.2	465 (7:45)
	150	106.8	555 (9:15)
Cu(en)(trien):Zn(en)(trien)	100	125.1	375 (6:15)
	150	117.4	435 (7:15)

Table 4.16 Maximum core temperature of RPUR foam catalyzed by mixed metal complexes synthesized in water at different NCO indexes

Catalyst types	NCO Index	Maximum Core Temperature (°C)	Starting time at T_{max} [sec (min)]
DMCHA	100	127.6	390 (6:30)
	150	120.8	420 (7:00)
W_Cu(OAc)₂(en)₂:Zn(OAc)₂(en)₂	100	123.3	390 (6:30)
	150	121.5	465 (7:45)
W_Cu(OAc)₂(trien):Zn(OAc)₂(trien)	100	103.7	570 (9:30)
	150	112.0	555 (9:15)

4.3.5 NCO conversion of RPUR foams

ATR-FTIR spectroscopy was employed to investigate the polymerization of RPUR foam system. IR spectra of polymeric MDI, polyether polyol and RPUR foams prepared from mixed metal complexes synthesized in acetone are shown in Figure 4.25. It was found that the absorption band of isocyanate could be observed at 2275 cm^{-1} . Therefore, the NCO conversion was determined from ATR-FTIR spectra. The ratio of free NCO absorption band increased with the NCO index in the foam formulation as shown in Figure 4.26.

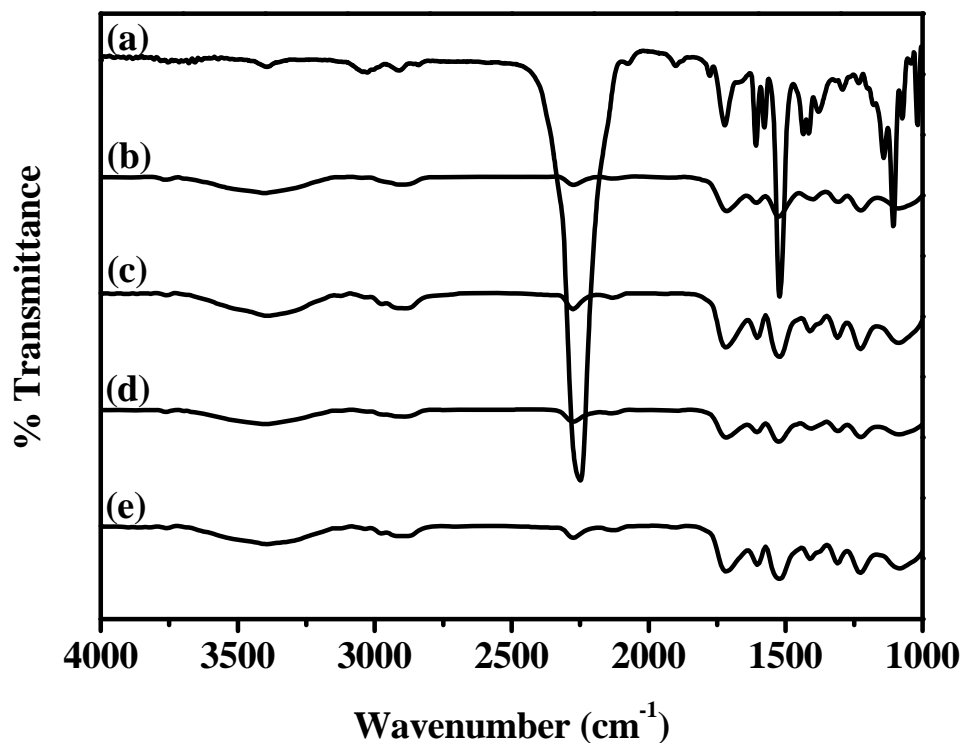


Figure 4.25 IR spectra of starting materials and RPUR foams catalyzed by mixed metal complexes (synthesized in acetone) (a) PMDI; (b) $\text{Cu}(\text{OAc})_2(\text{en})_2:\text{Ni}(\text{OAc})_2(\text{en})_2$; (c) $\text{Cu}(\text{OAc})_2(\text{en})_2:\text{Zn}(\text{OAc})_2(\text{en})_2$; (d) $\text{Cu}(\text{OAc})_2(\text{trien}):\text{Ni}(\text{OAc})_2(\text{trien})$; (e) $\text{Cu}(\text{OAc})_2(\text{trien}):\text{Zn}(\text{OAc})_2(\text{trien})$

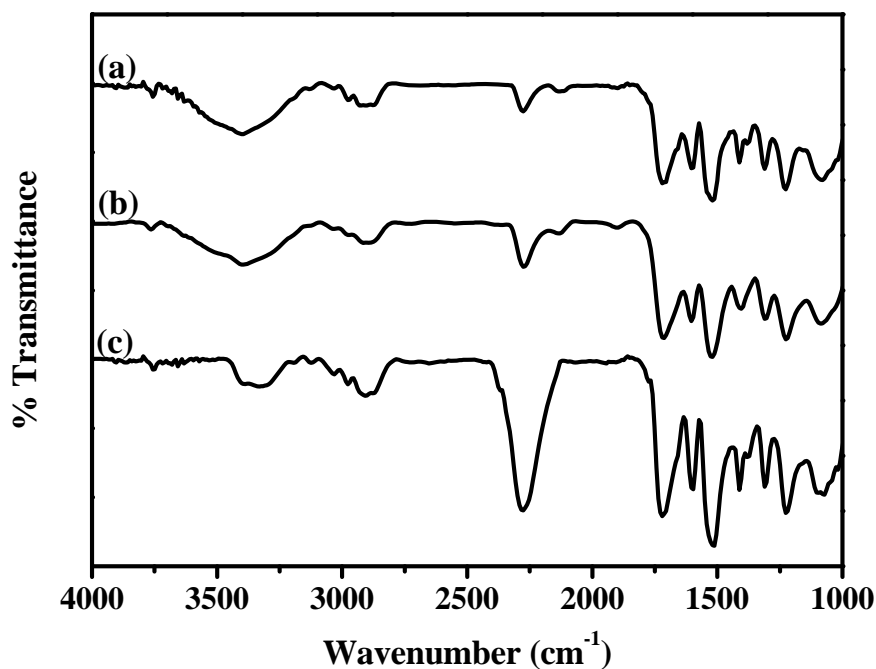


Figure 4.26 IR spectra of RPUR foams catalyzed by $\text{Cu}(\text{OAc})_2(\text{en})_2:\text{Zn}(\text{OAc})_2(\text{en})_2$ (synthesized in acetone) at different NCO indexes
(a) 100; (b) 150; (c) 200

The NCO conversion defined as the ratio between isocyanate peak area at time t and isocyanate peak area at time 0 as shown in following equation [80-85]:

$$\% \text{ conversion of isocyanate } (\alpha) = \left[1 - \frac{\text{NCO}(f)}{\text{NCO}(i)} \right] \times 100$$

where;

NCO(f) is the area of isocyanate absorbance peak area at time t

NCO(i) is the area of isocyanate absorbance peak area at initial time 0 (spectrum (a) in Figure 4.25)

Quantity of free NCO in RPUR foams were normalized by aromatic ring absorption band at 1595 cm^{-1}

Polyisocyanate : polyurethane (PIR/PUR) ratio was calculated from the peak area of isocyanate and urethane at 1415 and 1220 cm^{-1} , respectively (Table 4.17).

Table 4.17 Wavenumber of the functional groups used in calculation [86]

Functional groups	Wave number (cm ⁻¹)	Chemical structure
Isocyanate	2277	N=C=O
Phenyl	1595	Ar-H
Isocyanurate	1415	PIR
Urethane	1220	-C-O-

The results of NCO conversion of RPUR foams catalyzed by mixed metal complexes are shown in Table 4.18. It was found that NCO conversion was 96-99 %. It was found catalyzed by mixed metal complexes that NCO conversion decreased with increasing of the content of NCO indexes. The excess isocyanate could not undergo trimerization to give isocyanurate group since mixed metal complex catalysts were not specific toward of isocyanurate formation. It could be concluded that mixed metal complexes were good catalysts for polyurethane formation and blowing reaction but were unsuitable catalyst for trimerization reaction.

Table 4.18 NCO conversions and PIR: PUR ratio of RPUR foams catalyzed mixed metal complexes (synthesized in acetone) at different NCO indexes

Catalysts	Index	NCO conversion (%)	PIR/PUR
DMCHA (ref.)	100	99.3	0.203
	150	98.9	0.372
Cu(OAc)₂(en)₂:Ni(OAc)₂(en)₂	100	98.9	0.231
	150	99.3	0.228
Cu(OAc)₂(en)₂:Zn(OAc)₂(en)₂	100	99.1	0.207
	150	98.3	0.225
Cu(OAc)₂(trien):Ni(OAc)₂(trien)	100	98.4	0.222
	150	98.1	0.206
Cu(OAc)₂(trien):Zn(OAc)₂(trien)	100	99.0	0.233
	150	98.6	0.238
Cu(en)(trien) : Ni(en)(trien)	100	97.4	0.229
	150	96.2	0.339
Cu(en)(trien):Zn(en)(trien)	100	99.4	0.275
	150	99.3	0.329

4.3.6 Compressive properties of RPUR foams

The compression strength of rigid foam measures the degree of deformation, which will occur when a pressure is applied to the foam and the higher the compression strength, the lower the tendency of the foam to shrink or expand. For applications such as roofs, the foam compression strength should be high enough so that walking on it does no damage. Compression strength is measured on cubic foam samples placed between two parallel plates with a larger area than the specimen and the force required to compress the foam at a constant rate is measured. The test records the applied force and the displacement of the specimen to obtain a stress-strain curve.

The compression testing of foams were performed using universal testing machine (Lloyd/LRX) according to ASTM 1621-09, the specimen size was $3.0 \times 3.0 \times 3.0$ cm dimension, the rate of crosshead movement was fixed at 2.54 mm/min and the preload cell used was 0.100 N. The compression strength of rigid foam is the value of the maximum compressive force divided by the initial surface area of the test specimen, but only if the maximum compressive force is reached before the strain of the sample reaches 10 percent. Otherwise the compressive force is recorded at 10 percent strain. The slope of the initial straight-line part of the stress-strain curve represents the elastic part of the deformation and the ratio between stress and strain is called the elastic or Young's modulus. The compression strength of rigid foam increases with increasing densities and when the foam cells are oriented in the direction of rise, the compression strength parallel to rise will be much higher than the one perpendicular to rise.

Compressive strength of RPUR foams catalyzed by mixed metal complexes at the NCO index = 150 in parallel direction of foam rising are shown in Figure 4.27. Most RPUR foams showed slightly less compressive strength than that catalyzed by DMCHA. Except for RPUR foam catalyzed by $\text{Cu}(\text{OAc})_2(\text{trien}):\text{Zn}(\text{OAc})_2(\text{trien})$, which showed much lower compressive strength than that catalyzed by DMCHA.

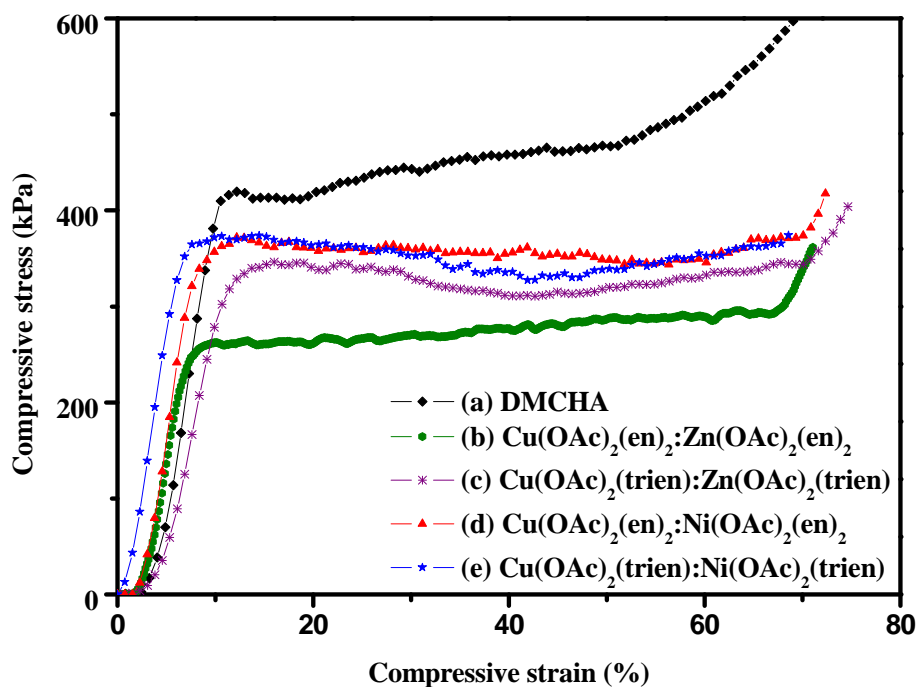


Figure 4.27 Deformation curves for RPUR foams prepared at the NCO index = 150 with density in the range $45\text{-}50\text{ kg/m}^3$.

4.3.7 Cell Morphology Sample Preparation and Testing

Scanning electron microscopy (SEM) using Hitachi/S4800 is performed on the slices of polyurethane foam, which are viewed parallel to the rise direction in the center of the mold. It was found that cell morphology showed spherical cell in parallel direction. SEM micrographs shown in Figure 4.28 showed that both RPUR foams prepared from DMCHA and metal complexes (synthesized in acetone) at the NCO index = 150 had closed cell. The cell size of RPUR foam catalyzed by $\text{Cu}(\text{OAc})_2(\text{en})_2:\text{Ni}(\text{OAc})_2(\text{en})_2$ was smaller and more uniform than that prepared from DMCHA and metal-ethylenediamine complexes, namely $\text{Cu}(\text{OAc})_2(\text{en})_2$ and $\text{Ni}(\text{OAc})_2(\text{en})_2$.

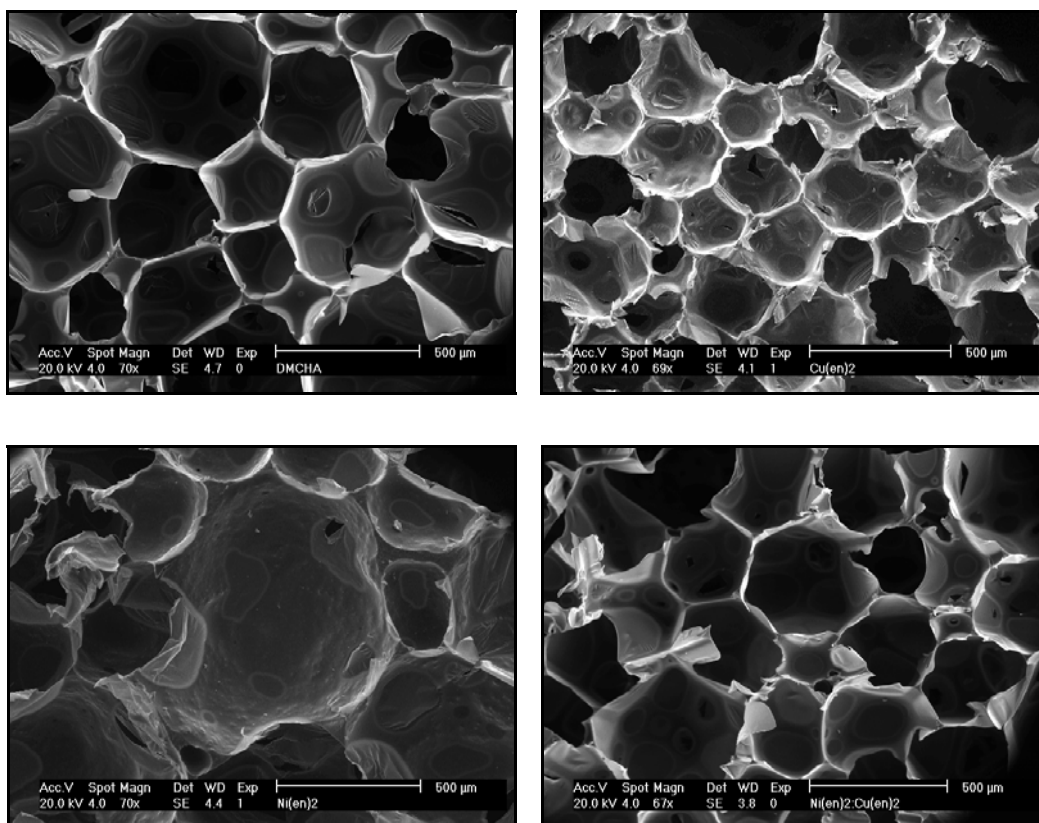


Figure 4.28 SEM of RPUR foams (NCO index = 150) catalyzed by (a) DMCHA; (b) $\text{Cu}(\text{OAc})_2(\text{en})_2$; (c) $\text{Ni}(\text{OAc})_2(\text{en})_2$; (d) $\text{Cu}(\text{OAc})_2(\text{en})_2:\text{Ni}(\text{OAc})_2(\text{en})_2$

4.3.8 Thermal stability characterization

Thermal stability of RPUR foams catalyzed $\text{Cu}(\text{OAc})_2(\text{en})_2:\text{Zn}(\text{OAc})_2(\text{en})_2$ and $\text{Cu}(\text{OAc})_2(\text{trien}):\text{Zn}(\text{OAc})_2(\text{trien})$ (synthesized in acetone) at the NCO index = 150 were analyzed by thermogravimetric analysis (TGA) under nitrogen atmosphere (Figure 4.29 and Table 4.19). TGA thermograms of all RPUR foams showed the decomposition of foams in one step. The initial composition temperature (IDT), which is the temperature at 5% weight loss was found in the range 284.3-287.7°C. The residual weights at 600°C were in the range 41-42 %. RPUR foams catalyzed by mixed metal complexes and DMCHA showed their maximum decomposition temperature (T_{max}) values in the range of 336.1-336.8°C. The foams prepared from all mixed metal complexes catalysts showed similar thermal decomposition with that

prepared from DMCHA catalyst. This indicated that the mixed metal complexes showed similar catalytic reaction to DMCHA.

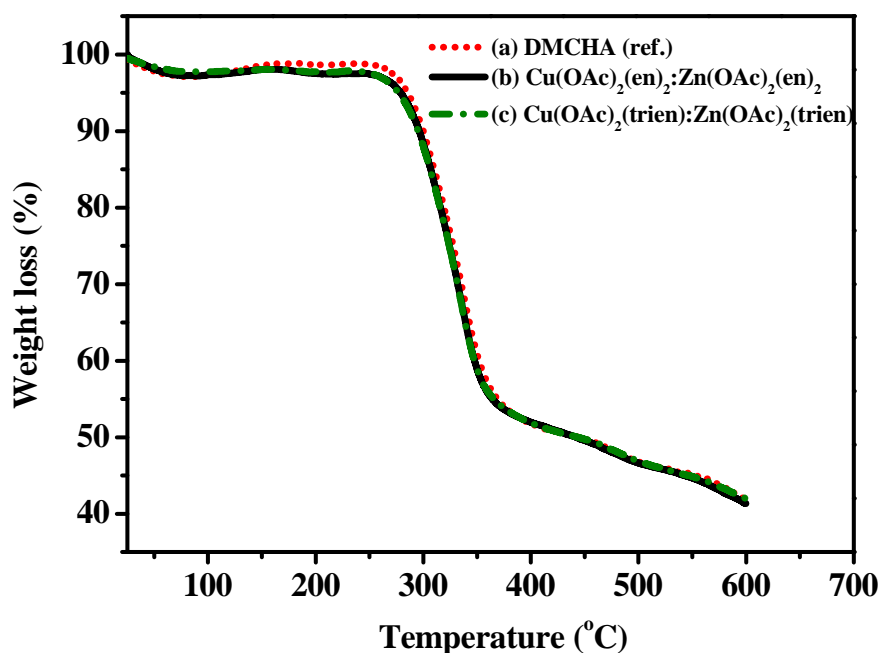


Figure 4.29 TGA thermograms of RPUR foams catalyzed by (a) DMCHA; (b) $\text{Cu}(\text{OAc})_2(\text{en})_2:\text{Zn}(\text{OAc})_2(\text{en})_2$; (c) $\text{Cu}(\text{OAc})_2(\text{trien}):\text{Ni}(\text{OAc})_2(\text{trien})$ (synthesized in acetone, NCO index = 150)

Table 4.19 TGA data of RPUR foam catalyst by mixed metal complexes catalysts (synthesized in acetone) at the NCO index of 150

Catalyst	IDT (°C)	Weight residue (%) at different temperature (°C)					T_{\max} (°C)
		200	300	400	500	600	
		DMCHA (ref.)	287.7	98.6	89.9	51.7	
$\text{Cu}(\text{OAc})_2(\text{en})_2:\text{Zn}(\text{OAc})_2(\text{en})_2$	286.8	98.5	88.4	51.9	46.6	41.3	336.2
$\text{Cu}(\text{OAc})_2(\text{trien}):\text{Zn}(\text{OAc})_2(\text{trien})$	284.3	97.7	87.9	51.8	46.8	41.9	336.1

This slope change can be also clearly seen from the DTG curves of DMCHA, $\text{Cu}(\text{OAc})_2(\text{en})_2:\text{Zn}(\text{OAc})_2(\text{en})_2$ and $\text{Cu}(\text{OAc})_2(\text{trien}):\text{Zn}(\text{OAc})_2(\text{trien})$ as shown in Figure 4.30. The weight loss rates have a rapidly increase and reach a maximum value at about 336.1-336.2°C. This temperature may be a mark of the phase transition. After the phase transition the weight loss rates have a rapid decrease until 412.5-413.0°C and then the weight loss rates are into a range of smooth variation.

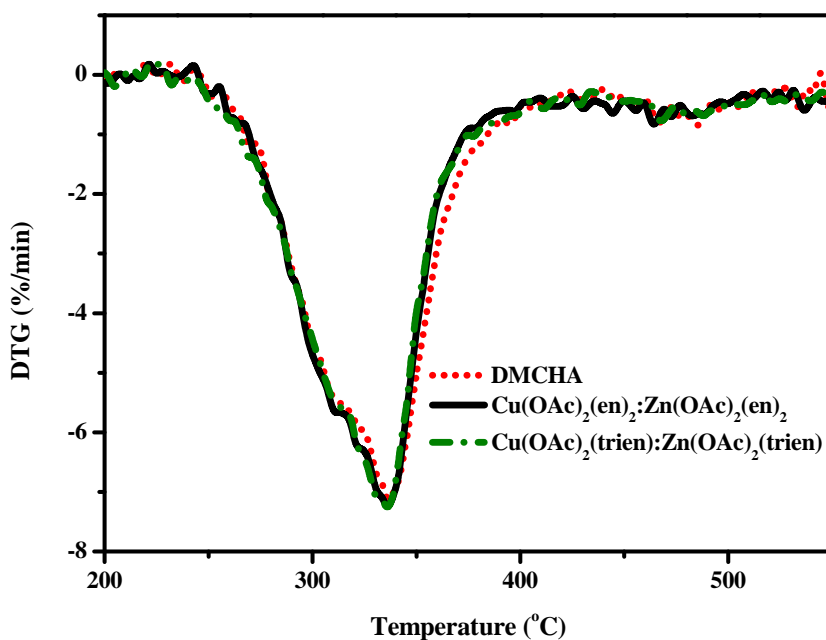


Figure 4.30 Weight loss rate versus temperature for different heating rates (from DMCHA, $\text{Cu}(\text{OAc})_2(\text{en})_2:\text{Zn}(\text{OAc})_2(\text{en})_2$ and $\text{Cu}(\text{OAc})_2(\text{trien}):\text{Zn}(\text{OAc})_2(\text{trien})$)

For comparison, RPUR foams prepared by used of different catalysts and their test specimen in 3.0 x 3.0 x 3.0 cm dimension were shown in Figures 4.31-4.33.

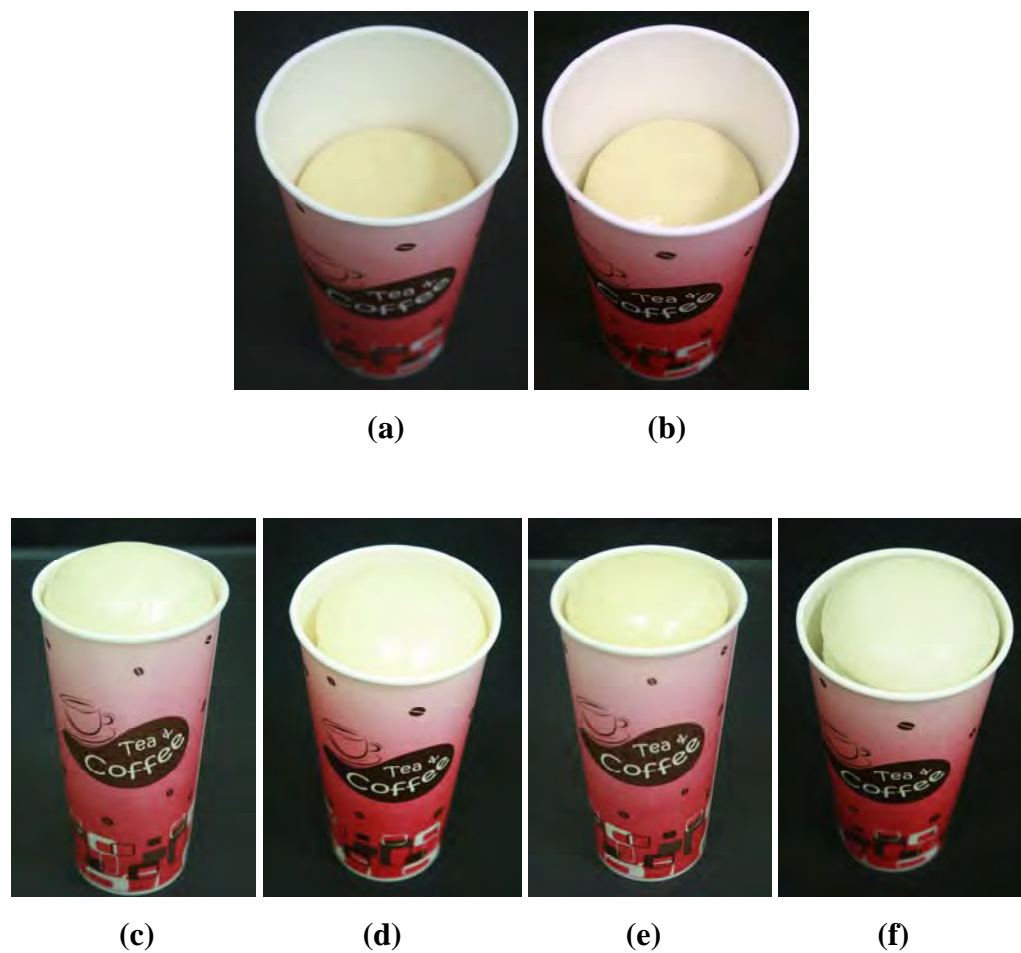


Figure 4.31 External appearance of RPUR foams catalyzed by (a) non-catalyst, (b) $\text{Cu}(\text{OAc})_2$, (c) DMCHA, (d) $\text{Cu}(\text{OAc})_2(\text{en})_2:\text{Zn}(\text{OAc})_2(\text{en})_2$, (e) $\text{Cu}(\text{OAc})_2(\text{trien}):\text{Zn}(\text{OAc})_2(\text{trien})$, (f) $\text{Cu}(\text{en})(\text{trien}):\text{Zn}(\text{en})(\text{trien})$

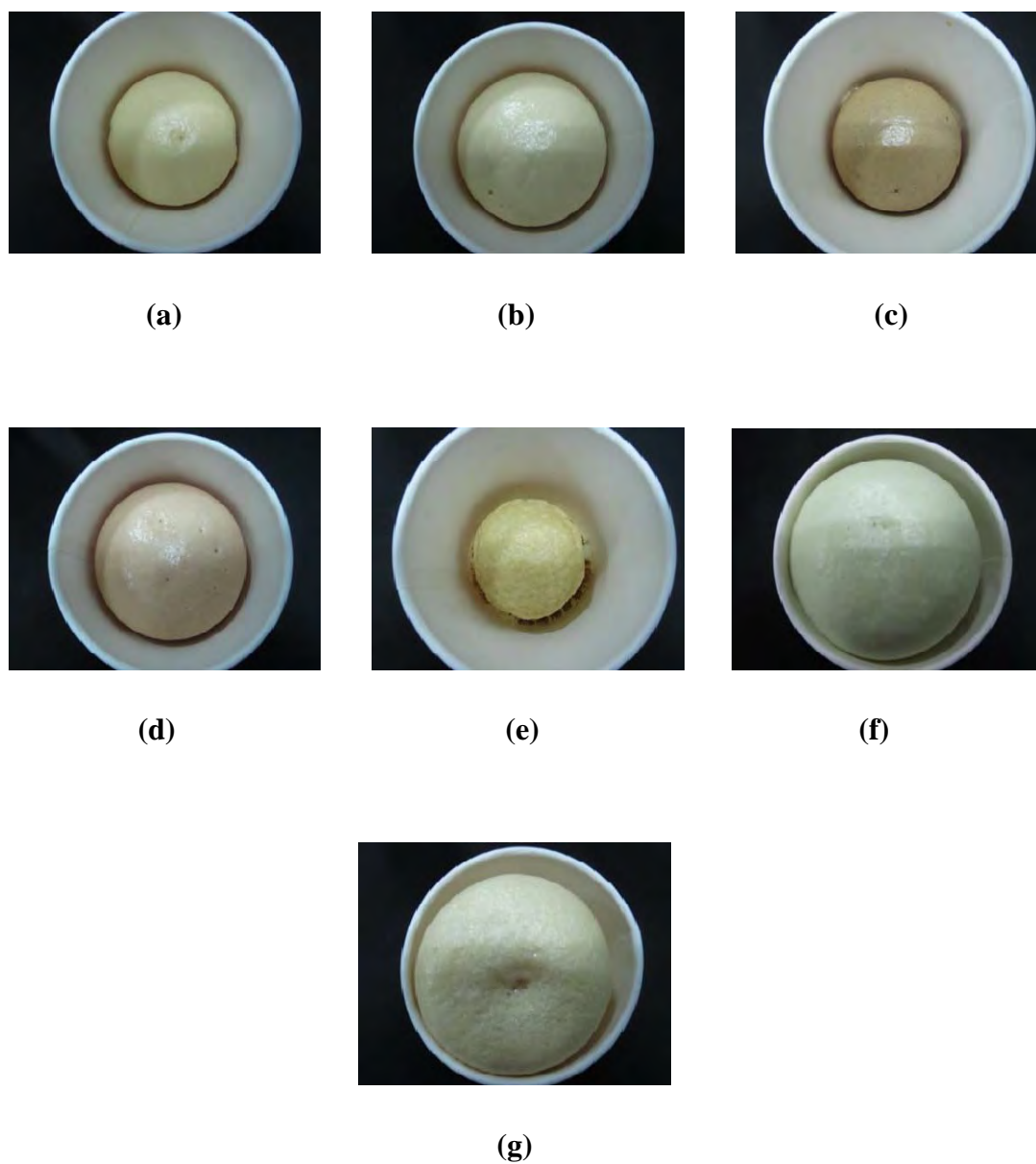


Figure 4.32 External appearance of RPUR foams catalyzed by metal-ethylenediamine complexes by (a) $\text{Ba}(\text{OAc})_2(\text{en})_2$ (b) $\text{Ca}(\text{OAc})_2(\text{en})_2$ (c) $\text{Mn}(\text{OAc})_2(\text{en})_2$ (d) $\text{Co}(\text{OAc})_2(\text{en})_2$ (e) $\text{Ni}(\text{OAc})_2(\text{en})_2$ (f) $\text{Cu}(\text{OAc})_2(\text{en})_2$ (g) $\text{Zn}(\text{OAc})_2(\text{en})_2$

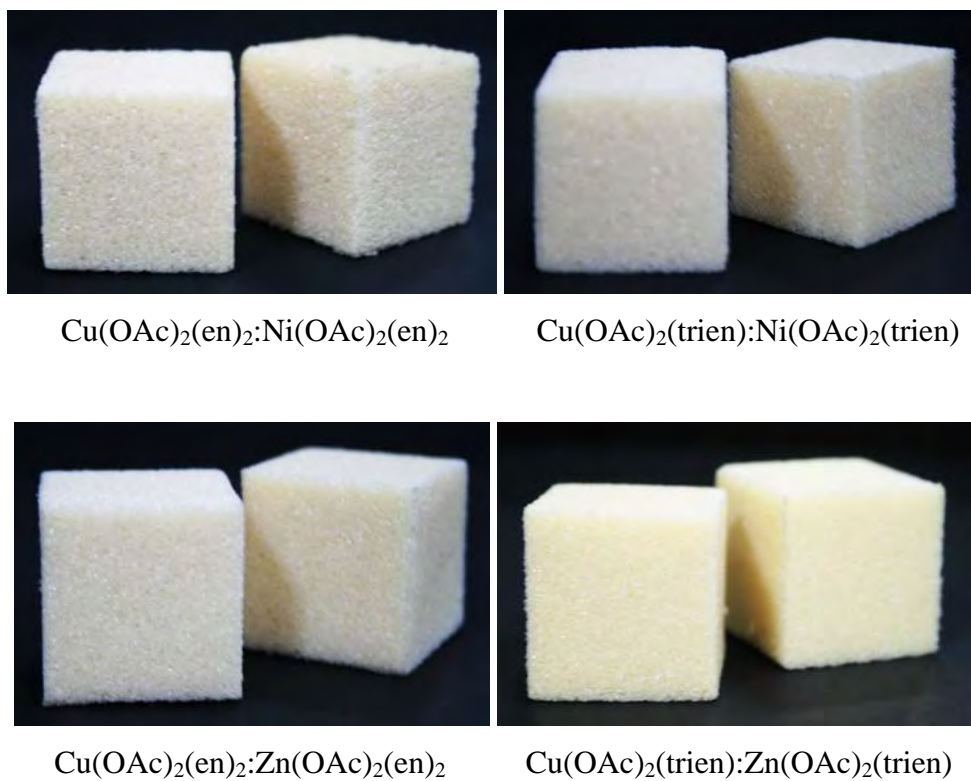


Figure 4.33 External appearance of test piece RPUR foams catalyzed by mixed metal complexes at index 100

CHAPTER V

CONCLUSION

5.1 Conclusion

Metal-amine and mixed metal-amine complexes, namely $M(\text{OAc})_2(\text{en})_2$, $M(\text{OAc})_2(\text{trien})$, $M_1(\text{OAc})_2(\text{en})_2:M_2(\text{OAc})_2(\text{en})_2$, $M_1(\text{OAc})_2(\text{trien}):M_2(\text{OAc})_2(\text{trien})$, were synthesized and used as catalysts for rigid polyurethane foam preparation. They were characterized by means of IR spectroscopy, UV spectroscopy and mass spectrometry.

Rigid polyurethane (RPUR) foam preparations were carried out by one shot and free rise method. RPUR foams catalyzed by mixed metal-amine complexes [$M_1(\text{OAc})_2(\text{en})_2:M_2(\text{OAc})_2(\text{en})_2$ and $M_1(\text{OAc})_2(\text{trien}):M_2(\text{OAc})_2(\text{trien})$ where $M_1 = \text{Cu}$, $M_2 = \text{Ni}$ and Zn] showed better controlled polymerization reaction and foam appearance than those prepared from metal-amine complexes [$M(\text{OAc})_2(\text{en})_2$ and $M(\text{OAc})_2(\text{trien})$]. $\text{Cu}(\text{OAc})_2(\text{en})_2:\text{Zn}(\text{OAc})_2(\text{en})_2$ and $\text{Cu}(\text{OAc})_2(\text{trien}):\text{Zn}(\text{OAc})_2(\text{trien})$ had better solubility in the “polyblend” starting materials than $\text{Cu}(\text{OAc})_2(\text{en})_2$, which resulted in better foam morphology.

From the reaction times, $\text{Cu}(\text{OAc})_2(\text{en})_2:\text{Zn}(\text{OAc})_2(\text{en})_2$ showed better catalytic activity than $\text{Cu}(\text{OAc})_2(\text{en})_2:\text{Ni}(\text{OAc})_2(\text{en})_2$ and a reference commercial catalyst (DMCHA). The reaction time and density decreased as the catalyst content in the foam formulation is increased. Apparent density of RPUR foams increased with increasing of the NCO content. The foams prepared at the NCO indexes of 100 and 150 had the apparent density about of 40 and 50 kg/m^3 , respectively. ATR-IR spectroscopy was used to determine the NCO conversion and polyisocyanurate (PIR): polyurethane (PUR) ratio of RPUR foams catalyzed from various catalysts. It was found that NCO conversion of RPUR foams slightly decreased with increasing of the NCO content.

A critical factor to achieve reproducible data in the preparation of RPUR foams is to mimic the foam processing conditions exactly. The polymerization to give RPUR foams is an exothermic reaction. The maximum core temperature of RPUR foams were in the range of 102.5-131.3°C and increased with increasing of NCO content.

Compressive strength of foam is highly dependent on their apparent density. RPUR foams catalyzed by mixed metal-amine complexes at the NCO index = 150 exhibited compressive strengths in the range 232.4-362.8 kPa, which is comparable to the RPUR foam catalyzed by DMCHA, which had the compressive strength of 415.9 kPa.

Thermogravimetric data showed that RPUR foams catalyzed by mixed metal-amine complexes, $\text{Cu}(\text{OAc})_2(\text{en})_2:\text{Zn}(\text{OAc})_2(\text{en})_2$ and $\text{Cu}(\text{OAc})_2(\text{trien}):\text{Zn}(\text{OAc})_2(\text{trien})$, and DMCHA at the NCO index = 150 showed similar thermal stability to the foam catalyzed by DMCHA.

5.2 Suggestion for future work

The suggestion for future work is to develop the synthesis of mixed metal complexes in water since the aqueous solution of metal complexes can be used in the preparation of water blown RPUR foams without purification.

REFERENCES

- [1] Chinn, H., Löchner, U., and Kishi, A. *Polyurethane Foams*. [Online].
Available from: E-mail: linda.henderson@ihs.com [2009, October]
- [2] Maris, R. V., Tamano, Y., Yoshimura, H., and Gay, K. M. Polyurethane catalysis by tertiary amines. *J. Cell. Plast.* 41 (2005): 305-322.
- [3] Jitrwung, R., Pancharoen, U., and Ngamprompong, s. Effect of parameters on high density flexible polyurethane foam mixing in batch tank. Chemical Engineering. *Chulalongkorn University*, 2000.
- [4] Wood, G. The ICI polyurethane book. 2nd Edition. *John Wiley & Sons*, London, 1990.
- [5] Raymond, B. S., George, B. K. Polyurethanes: A Class of Modern Versatile Materials *J. Chem. Ed.* 69 (1992): 909.
- [6] Feske, B. The Use of Saytex RB-9130/9170 Low Viscosity Brominated Flame Retardant Polyols in HFC-245fa and High Water Formulations, [2004, October]. Las Vegas, NV: *Alliance for the Polyurethane Industry Technical Conference*.
- [7] Mark, H. F., Bikales, N. M., Overberger, C. G., and Menges, G. (eds.). Encyclopedia of Polymer Science and Engineering, *John Wiley & Sons*, New York, 31 (1985): 1-59.
- [8] Randolph, A. F. *Plastics Engineering Handbook*, 3rd Edition. Reinhold, New York, 13, 1963.
- [9] Sarier, N. and Onder, E. Thermal characteristics of polyurethane foams incorporated with phase change materials. *Thermochimica Acta.* 454 (2007) 90–98.
- [10] Ozaki, S. Chemistry and Technology of Isocyanates, *Chem. Rev.* 72 (1972) 457.
- [11] Twitchett, H.J. Synthèse des isocyanates de 2-F-alkyléthyle. *Chem. Soc. Rev.* 3 (1974): 209.

- [12] Ulrich, H. *Chemistry and Technology of Isocyanates*, Wiley, Chichester, 1996, p.385.
- [13] Pentrakoon, D. and Ellis J.W. *An Introduction to Plastic Foams*. *Chulalongkorn university*, Bangkok, 2005.
- [14] Randall, D. and Lee, S. *The polyurethane book*. London: John Wiley & Sons, 2002.
- [15] Landrock, H. *Handbook of plastic foams*. *Noyes Publications*, USA, 1995.
- [16] Chinn; Henry; Akihiro K.; Uwe L. (April 2006). "Polyether Polyols for Urethanes (abstract only without subscription)". SRI Consulting. <http://www.sriconsulting.com/CEH/Public/Reports/688.3000/>.
- [17] Dieterich, D. *Ullmann's Encyclopedia of Industrial Chemistry*, *VCH Weinheim*, New York, Vol. A 21, 1992, p. 665.
- [18] Schauerte, K. and Gupta, P. *Kunststoffhandbuch*. Polyurethane, vol. 7, *Hanser Verlag*, München, 1993, p. 57.
- [19] Friedli, H. *Reaction Polymers*, *Hanser Verlag*, München, 1992, p. 66.
- [20] Oertel, G. *Polyurethane handbook*. *Hanser Publishers*, New York, 1985.
- [21] Lee, S.T. and Ramesh N.S. *Polymeric foams*. *CRC Press*, New York, 2004.
- [22] Schaumstoff, P. Polyurethane rigid foam, a proven thermal insulating material for applications between +130°C and -196°C. *Cryogenics* 38 (1998): 113-117.
- [23] Grimminger, J., and Muha, K. Silicone surfactants for pentane blown rigid foam. *J. Cell. Plast.* 31 (1992): 48-72.
- [24] Modesti, M., and Lorenzetti, A. An experimental method for evaluating isocyanate conversion and trimer formation in polyisocyanurate-polyurethane foams. *Eur. Polymer. J.* 37 (2001): 949-954.
- [25] Szycher, M. and Szycher's *Handbook of Polyurethanes*. New York: CRC Press; 1999.
- [26] Harbron, D. R., Paige, C. J., and Scarrow, R. K. *J Cell plastics*. 37(2001): 43-57.

- [27] Dolomanova, V., Rauhe, J. C. M., and Jensen, L. R. Mechanical properties and morphology of nano-reinforced rigid PU foam. *J. Cell. Plast.* 47 (2011): 81-93.
- [28] Landrock, H. Handbook of plastic foams. *Noyes Publications*, USA, 1995.
- [29] Stirna, U.; Cabulis U. Water-blown polyisocyanurate foams from vegetable oil polyols. *J. Cell. Plast.* 44 (2008): 139-159.
- [30] Saunders, J.H., Frisch, K.C. *Polyurethane Chemistry and Technology, Part I and II*; Wiley Interscience Publishers: New York, 1963, 35, 81-93.
- [31] Squiller, E.P., Rosthauser, J.W. Catalysis in Aliphatic isocyanate-Alcohol Reactions, Water-Borne and Higher Solids Coatings Symposium. *New Orleans*. (1987): 460-477.
- [32] Bechara, I.S., Carroll, F.P. Catalysis of the isocyanate-hydroxyl reaction by non-tin catalysts. *J. Cellular, plastics*. 16 (2) (1980): 89.
- [33] Zeleňák, V., Vargová, Z. Copper (II) acetates with aliphatic/heterocyclic amines coupled TG-CTA-EGA study, IR characterization and structure correlation. *Journal of Thermal Analysis and Calorimetry*, 82 (2005): 747-754.
- [34] Cara, E., Cristini, A., Diaz, A., and Ponticelli, G. Octahedral Complexes of Nickel(II) and Copper(II) with Triethylenetetra-amine. *J.C.S. Dalton*. (1972): 527-530.
- [35] Miller, J. S., Epstein, J. Structures and Magnetic Properties of Novel 1-D Coordination Polymers Containing Both Dicyanamide and Pyridine-Type Ligands, *Chem., Int. Ed. Eng.* 33 (1994) 385.
- [36] Meenakumari, S., Chakravarty, A. R. Incorporation of chelating 2,2'-bipyridine (bipy) ligands at the equatorial sites of $\text{Cu}_2(\mu\text{-O}_2\text{CMe})_4(\text{H}_2\text{O})_2$: an x-ray structure of $[\text{Cu}_2(\mu\text{-O}_2\text{CMe})_2(\text{H}_2\text{O})(\text{bipy})_2](\text{PF}_6)_2$, *Polyhedron*. 12 (1993) 1825.
- [37] Rochon, F. D., Melanson, R., and Andruh, M. The influence of different N-substituted diethylenetriamine ligands on the aggregation of copper(II) monoacetato complexes. *Polyhedron*, 15 (1996): 3075 -3084.

- [38] Meenakumari, S., Tiwari, S. K., Chakravarty, A. R. Synthesis, Crystal Structure, and Magnetic Properties of a Ferromagnetically Coupled Angular Trinuclear Copper(II) Complex $[\text{Cu}_3(\text{O}_2\text{CMe})_4(\text{bpy})_3(\text{H}_2\text{O})](\text{PF}_6)_2$. *J. Chem. Soc., Dalton Trans.* 33 (1994): 2085-2089.
- [39] Perlepes, S., Huffman, J. C., and Christou, G. Synthesis, Structure, and Properties of a Tetrametallic Ferrocenecarboxylato-Bridged Copper(II) Complex. *Polyhedron*, 14 (1995): 1073.
- [40] Kurnoskin, A. V. Metalliferous epoxy chelate polymers: 1. synthesis and properties. *Polymer*, 34 (1993): 1060-1067.
- [41] Kurnoskin, A. V. Metalliferous epoxy chelate polymers: 2. influence of structural fragments on properties. *Polymer*, 34 (1993): 1068-1076.
- [42] Inoue, Sh. I.; Nagai, Y.; Okamoto, H. Amine-manganese complexes as a efficient catalyst for polyurethane syntheses. *Polym. J.* 34 (2002): 298-301.
- [43] Pengjam, W. Preparation of rigid polyurethane foam catalyzed by Cu-amine and Mn-amine complexes. Science Program in Petrochemistry and Polymer Science. *Chulalongkorn University*, 2009.
- [44] Saengfak, B. Preparation of rigid polyurethane foam catalyzed by nickel and cobalt complexes. Science Program in Petrochemistry and Polymer Science. *Chulalongkorn University*, 2009.
- [45] Xiaobin, LI., Hongbin, CAO., and Yi, Zhang. Properties of Water Blown Rigid Polyurethane Foams with Different Functionality. *Wuhan University of Technogy-Mater. Sci. Ed. J.* 23 (2008): 125-129.
- [46] Modesti, M., Lorenzetti, A. Improvement on fire behaviour of water blown PIR-PUR foams: use of a halogen-free flame retardant. *Eur. Polym. J.* 39 (2003): 263-268.
- [47] Lorenzetti, A., Modesti, M., Zanella, L., Bertani, R., and Gleria, M. Thermally stable hybrid foams based on cyclophosphazenes and polyurethanes. *Polym. Degrad. Stabil.* 87 (2005): 287-292.

- [48] Murayama, S., Fukuda, K., Kimura, T., and Sasahara, T. Water-blown polyurethane rigid foam modified with maleate. *J. Cell. Plast.* 41 (2005): 373-378.
- [49] Modesti, M., Lorenzetti, A., Simioni, F., and Checchin, M. Influence of different flame retardants on fire behaviour of modified PIR/PUR polymers. *Polym. Degrad. Stabil.* 74 (2001): 475-479.
- [50] Barker, J. Analytical chemistry by open learning Mass Spectrometry. 2nd Edition. *John Wiley & Sons*, Chichester, England. (2000): 331-332.
- [51] Kurnoskin, A. V. Metalliferous epoxy chelate polymer: 1. Synthesis and properties. *Polymer.* 34 (1993): 1060-1067.
- [52] Kurnoskin, A. V. Metalliferous epoxy chelate polymer: 2. Influence of structural fragments on properties. *Polymer*, 34 (1993): 1068-1076.
- [53] Sardon, H., Irusta, L., and Fernández-Berridi, M.J. Synthesis of isophorone diisocyanate (IPDI) based waterborne polyurethanes: Comparison between zirconium and tin catalysts in the polymerization process. *Progress in Organic Coatings.* 66 (2009): 291-295.
- [54] Krishnan, K., Plane, R. A. Raman and Infrared Spectra of Complexes of Ethylenediamine with Zinc(II), Cadmium(II), and Mercury(II). *Inorg. Chem.* 5 (1966): 852-857.
- [55] Deacon, G. B., Phillip, R. J. Relationships between the carbon-oxygen stretching frequencies of carboxylato complexes and the type of carboxylate coordination. *Coord. Chem. Rev.*, 33 (1980): 227-251.
- [56] Martini, D., Pellei, M., Pettinari, C., Skelton, B. W., and White, A. H. Synthesis, spectroscopic and structural characterization of Cu(II) derivatives of tris(pyrazol-1-yl)methanes. *Inorg. Chim. Acta*, 333 (2002): 72-82.
- [57] Czakis-Sulikowska, D., Czyłkowska, A., and Malinowska, A. *J. Therm. Anal. Cal.*, 65 (2001): 505.
- [58] Czakis-Sulikowska, D., Czyłkowska, A. *J. Therm. Anal. Cal.*, 71 (2003): 395.

- [59] Mojumdar, S. C., Martiška, L., Valigura, D., and Melnk, M. *J. Therm. Anal. Cal.*, 74 (2003): 905.
- [60] Czakis-Sulikowska, D., Czyrkowska, A. *J. Therm. Anal. Cal.*, 76 (2004): 543.
- [61] Zelek, V., Gyryov, K., Mlynark, D. *Metal Based Drugs*, 8 (2002): 269.
- [62] Nara, M., Tasumi, M., Tanokura, M., Hiraoki, T., Yazawa, M., and Tsutsumi, A. Infrared studies of interaction between metal ions and Ca⁽²⁺⁾-binding proteins. Marker bands for identifying the types of coordination of the side-chain COO- groups to metal ions in pike parvalbumin (pI = 4.10). *FEBS Lett*, 349 (1994): 84.
- [63] Dean, L. K. L., DiDonato, G. C., Wood, T. D., and Busch, K. L. Cluster Ions in the Electron and Chemical Ionization Mass Spectra of Transition Metal Acetylacetonates, *Inorg. Chem.* 27 (1988): 4622-4627.
- [64] Geladi, P., Adams, F. The determination of cadmium, copper, iron, lead and zinc in aerosols by atomic absorption spectrometry, *Anal. Chim. Acta.* 96 (1978): 229-241.
- [65] Kam, S.I. Experimental Study of High-Temperature Foam for Acid Diversion. *Journal Petroleum Sci. Eng.* 58 (2007): 138–160.
- [66] Maris, R. V., Tamano, Y., Yoshimura, H., and Gray, K. Polyurethane catalysis by tertiary amines. *J. Cell. Plast.* 41 (2005): 305-322.
- [67] Mathew, S., Nair, C. G. R., and Ninan, K. N. *Thermochim Acta.* 181 (1991): 253.
- [68] Wendlandt, W. W. *J. Inorg. Nucl. Chem.* 25 (1963): 833.
- [69] Nair C. G. R., Mathew, S., and Ninan, K. N. *J. Thermal Anal.* 39(1991): 2325.
- [70] Langfelderová, H., Jorík, V. Červená, J. *J. Thermal Anal.* 39 (1993): 489.
- [71] Singh, G., Felix, S. P., and Pandey, D. K. *Thermochim. Acta*, 411 (2004): 61.
- [72] Singh, G., Pandey, D. K. *Propell. Explos. Pyrot.* 28 (2003): 231.
- [73] Donia, A.M. *Thermochim. Acta*, 320 (1998): 187.

- [74] Wrzeszcz, G., Dobrzanska, L. Spectroscopic, magnetic and thermal properties of new thiocyanato bridged complexes of the type $[M(\text{diamine})_2]_3[\text{Cr}(\text{NCS})_6]_2 \cdot n\text{H}_2\text{O}$, where $M = \text{Cu}(\text{II}), \text{Ni}(\text{II})$. *Pol. J. Chem.* 77 (2003): 1245.
- [75] Prabhumirashi, L.S., Khoje, J. K. TGA and DTA studies on en and tmn complexes of Cu(II) chloride, nitrate, sulphate, acetate and oxalate. *Thermochim. Acta*, 383 (2002):109.
- [76] Srivastava, P.C., Singh, B. N., Adhyam, S. D., and Banerji, K. C. *J. Thermal Anal.*, 27 (1983): 263.
- [77] Wood, G. *The ICI polyurethane book*. 2nd Edition. London: John Wiley & Sons, 1990.
- [78] Landrock, H. *Handbook of plastic foams*. USA: Noyes Publication, 1995.
- [79] Randall, D. and Lee, S. *The polyurethane book*. London: John Wiley & Sons, 2002.
- [80] Romero, R. R., Robert, A., Grigsby, J. R., Ernest, L., Rister, J. R., Rratt, J. K., and Ridgway, D. A study of the reaction kinetics of polyisocyanate foam formulations using real-time FTIR. *J. Cell. Plast.* 41 (2005): 339-359.
- [81] Elwell, M. J. and Ryan, A. J. An FTIR study of reaction kinetics and structure development in model flexible polyurethane foam system. *Polymer*. 37 (1996): 1353-1361.
- [82] Cateto, C.A., Barreiro, M. F. and Rodrigues, A. E. Monitoring of lignin-based polyurethane synthesis by IR-ATR. *Ind. Crop. Prod.* 27 (2008): 168-174.
- [83] Jones, S. A., Scott, K. W., Willoughby, B. G. and Sheard, E. A. Monitoring of polyurethane foam cure. *J. Cell. Plast.* 38 (2002): 285-299.
- [84] Raffel, B. and Loevenich, C. J. High throughput screening of rigid polyisocyanurate foam formulations: quantitative characterization of isocyanurate yield via the adiabatic temperature method. *J. Cell. Plast.* 42 (2006): 17-47.

- [85] Thomson, M. A., Melling, P. J., and Slepiski, A. M. Real time monitoring of isocyanate chemistry using a fiber-optic FTIR probe. *Polymer Preprints*. 42 (2001): 310-311.
- [86] Lorenzetti, A., Modisti, M., Zanella, L., Bertani, R., and Gleria, M. Thermally stable hybrid foams based on cyclophosphazenes and polyurethanes. *Polym. Degrad. Stabil.* 87 (2005): 287-292.

APPENDICES

Appendix A

NCO index and NCO conversion Calculations

NCO index calculation

#Example Calculate the parts by weight (pbw) of pure PMDI (MR-200), molar mass = 365.8, functionality = 2.7 at an isocyanate indexes of 100, 150, and 200 required to react with the following formulation:

Formulation (pbw)	Part by weight (g)
Raypol[®] 4221 (OHV = 440 mgKOH/ g, functionality = 4.3)	100.0
Catalysts	1.0
Surfactant	2.5
Blowing agent (water, Mw = 18 g/mole, functionality = 2)	3.0
PMDI (MR-200), NCO indexes of 100, 150, and 200	?

$$\text{Equivalent weight of raypol 4221} = \frac{56.1}{440} \times 1000 = 127.5$$

$$\text{Equivalent weight of water} = \frac{18}{2} = 9$$

Note: Surfactants and catalysts are neglected in stoichiometric calculations because they do not react with NCO groups.

$$\text{Number of equivalent in formulation} = \frac{\text{parts by weight (pbw)}}{\text{equivalent weight}}$$

Equivalent in the above formulation:

$$\text{Polyol (Raypol 4221)} = \frac{100}{127.5} = 0.784$$

$$\text{Water (blowing agent)} = \frac{4.0}{9.0} = 0.444$$

$$\text{Total equivalent weight} = 1.228$$

For stoichiometric equivalence, PMDI pbw is total equivalent x equivalent weight because PMDI reacts with polyol and water.

Thus:

$$\text{PMDI (pbw)} = 1.228 \times \frac{\text{PMDI molar mass}}{\text{functionality}} = 1.228 \times \frac{365.8}{2.7} = 166.37$$

Note: 166.4 defines the isocyanate quantity at 100 index

Where;

$$\text{Isocyanate index} = \frac{\text{actual amount of isocyanate}}{\text{theoretical amount of isocyanate}} \times 100$$

Thus:

Isocyanate index = 100;

$$\text{Isocyanate actual} = \frac{166.4}{100} \times 100 = 166.4 \text{ pbw}$$

Isocyanate index = 150;

$$\text{Isocyanate actual} = \frac{166.4}{100} \times 150 = 249.6 \text{ pbw}$$

Isocyanate index = 200;

$$\text{Isocyanate actual} = \frac{166.4}{100} \times 200 = 332.8 \text{ pbw}$$

Table A1 Isocyanate quantity at different NCO indexes in the above formulations

Formulation (pbw)	NCO indexes		
	100	150	200
Polyol (Raypol® 4221)	100	100	100
Catalysts	1.0	1.0	1.0
Surfactant	2.5	2.5	2.5
Blowing agent	4.0	4.0	4.0
PMDI (MR-200)	166.4	249.6	332.8

NCO conversion calculation

The NCO conversion can be calculated by FTIR method, defined as the ratio between isocyanate peak area at time t and isocyanate peak area at time 0, following equation:

$$\text{Isocyanate conversion (\%)} = \left[1 - \frac{\text{NCO}^f}{\text{NCO}^i} \right] \times 100$$

where;

NCO^f is the area of isocyanate absorbance peak area at time t

NCOⁱ is the area of isocyanate absorbance peak area at time 0

Quantity of free NCO in RPUR foams were normalized by aromatic ring absorption band at 1595 cm⁻¹.

Table A2 Free NCO absorbance peak area in PMDI (MR-200) from IR-ATR

PMDI (MR200) spectra	NCO Absorbance peak area Normalized @ 1.0 Ar-H peak area
1	79.378
2	81.635
3	78.262
4	79.499
5	79.491
Average (NCOⁱ); ATR-IR	79.65
NCOⁱ (FTIR)	98.0

Example Calculate the conversion of isocyanate (α) and PIR:PUR of rigid polyurethane foams catalyzed by $\text{Cu}(\text{OAc})_2(\text{en})_2:\text{Ni}(\text{OAc})_2(\text{en})_2$ catalyst at NCO index 150

Conversion of isocyanate (%)

Data at **Table A2**

Absorbance peak area of initial NCO = 79.65 = NCOⁱ

The data from **Table A4** at NCO index 100, absorbance peak area of free NCO was normalized by aromatic ring quantity:

Absorbance peak area of final NCO = 1.0850 = NCO^f

$$\begin{aligned} \text{Thus, conversion of isocyanate (\%)} &= \left[1 - \frac{\text{NCO}^f}{\text{NCO}^i} \right] \times 100 \\ &= \left[1 - \frac{1.0850}{79.65} \right] \times 100 \end{aligned}$$

$$\% \text{ NCO conversion} = 98.6$$

PIR:PUR

Absorbance peak area of PIR (polyisocyanurate) = 1.011

Absorbance peak area of PUR (polyurethane) = 5.466

$$\text{Thus, PIR:PUR} = \frac{1.011}{5.466} = 0.1849$$

Blowing agent = 3.0**Table A3** NCO conversion of RPUR foam catalyzed by DMCHA at different NCO indexes

NCO indexes	Peak Area					NCO conversion (%)	PIR/PUR
	NCO 2277 cm ⁻¹	Ar-H 1595 cm ⁻¹	PIR 1415 cm ⁻¹	PUR 1220 cm ⁻¹	NCO ^f (Ar-H=1.0)		
100	0.778	3.224	1.068	7.017	0.2413	99.8	0.1522
150	3.421	2.387	0.980	3.828	1.4332	98.5	0.2560
200	7.615	0.981	0.461	1.501	7.7625	92.1	0.3071

Table A4 NCO conversion of RPUR foam catalyzed by Cu(OAc)₂(en)₂:Ni(OAc)₂(en)₂ at different NCO indexes

NCO indexes	Peak Area					NCO conversion (%)	PIR/PUR
	NCO 2277 cm ⁻¹	Ar-H 1595 cm ⁻¹	PIR 1415 cm ⁻¹	PUR 1220 cm ⁻¹	NCO ^f (Ar-H=1.0)		
100	3.345	3.083	1.011	5.466	1.0850	98.6	0.1849
150	1.649	0.997	0.326	1.446	1.6540	98.3	0.2254
200	21.308	1.618	0.674	2.955	13.1693	86.6	0.2281

Table A5 NCO conversion of RPUR foam catalyzed by Cu(OAc)₂(en)₂:Zn(OAc)₂(en)₂ at different NCO indexes

NCO indexes	Peak Area					NCO conversion (%)	PIR/PUR
	NCO 2277 cm ⁻¹	Ar-H 1595 cm ⁻¹	PIR 1415 cm ⁻¹	PUR 1220 cm ⁻¹	NCO ^f (Ar-H=1.0)		
100	2.703	1.480	0.523	2.404	1.8264	98.1	0.2176
150	1.061	0.848	0.321	1.412	1.2515	98.7	0.2270

Table A6 NCO conversion of RPUR foam catalyzed by $\text{Cu}(\text{OAc})_2(\text{trien}):\text{Ni}(\text{OAc})_2(\text{trien})$ at different NCO indexes

NCO indexes	Peak Area					NCO conversion (%)	PIR/PUR
	NCO 2277 cm^{-1}	Ar-H 1595 cm^{-1}	PIR 1415 cm^{-1}	PUR 1220 cm^{-1}	NCO ^f (Ar-H=1.0)		
100	1.305	0.991	0.376	1.669	1.3169	98.7	0.2253
150	2.200	0.924	0.372	1.523	2.3810	97.6	0.2443
200	20.119	1.934	0.562	2.895	10.4028	89.4	0.1941

Table A7 NCO conversion of RPUR foam catalyzed by $\text{Cu}(\text{OAc})_2(\text{trien}):\text{Zn}(\text{OAc})_2(\text{trien})$ at different NCO indexes

NCO indexes	Peak Area					NCO conversion (%)	PIR/PUR
	NCO 2277 cm^{-1}	Ar-H 1595 cm^{-1}	PIR 1415 cm^{-1}	PUR 1220 cm^{-1}	NCO ^f (Ar-H=1.0)		
100	2.295	1.125	0.350	1.363	2.0400	97.9	0.2568
150	5.660	2.715	1.048	4.982	2.0847	97.9	0.2104
200	70.661	4.561	1.563	7.920	15.4924	84.2	0.1973

Table A8 NCO conversion of RPUR foam catalyzed by $\text{Cu}(\text{Sal})_2(\text{en})_2:\text{Ni}(\text{Sal})_2(\text{en})_2$ at different NCO indexes

NCO indexes	Peak Area					NCO conversion (%)	PIR/PUR
	NCO 2277 cm^{-1}	Ar-H 1595 cm^{-1}	PIR 1415 cm^{-1}	PUR 1220 cm^{-1}	NCO ^f (Ar-H=1.0)		
100	2.883	1.652	0.514	2.431	1.7452	98.2	0.2114
150	9.919	1.467	0.430	2.047	6.7614	93.1	0.2101
200	13.290	1.288	0.458	2.120	10.3183	89.5	0.2160

Table A9 NCO conversion of RPUR foam catalyzed by $\text{Cu}(\text{Sal})_2(\text{en})_2:\text{Zn}(\text{Sal})_2(\text{en})_2$ at different NCO indexes

NCO indexes	Peak Area					NCO conversion (%)	PIR/PUR
	NCO 2277 cm^{-1}	Ar-H 1595 cm^{-1}	PIR 1415 cm^{-1}	PUR 1220 cm^{-1}	NCO ^f (Ar-H=1.0)		
100	4.607	1.545	0.533	2.670	2.9819	97.0	0.1996
150	8.168	1.197	0.317	1.50	6.8237	93.0	0.2108
200	5.438	2.144	0.623	2.664	2.5364	97.4	0.2339

Table A10 NCO conversion of RPUR foam catalyzed by $\text{Cu}(\text{Sal})_2(\text{trien}):\text{Ni}(\text{Sal})_2(\text{trien})$ at different NCO indexes

NCO indexes	Peak Area					NCO conversion (%)	PIR/PUR
	NCO 2277 cm^{-1}	Ar-H 1595 cm^{-1}	PIR 1415 cm^{-1}	PUR 1220 cm^{-1}	NCO ^f (Ar-H=1.0)		
100	9.648	4.502	1.372	6.753	2.1430	97.8	0.2032
150	3.738	1.215	0.385	1.839	3.0765	96.9	0.2094
200	18.247	2.465	0.786	2.720	7.4024	92.4	0.2890

Table A11 NCO conversion of RPUR foam catalyzed by $\text{Cu}(\text{Sal})_2(\text{trien}):\text{Zn}(\text{Sal})_2(\text{trien})$ at different NCO indexes

NCO indexes	Peak Area					NCO conversion (%)	PIR/PUR
	NCO 2277 cm^{-1}	Ar-H 1595 cm^{-1}	PIR 1415 cm^{-1}	PUR 1220 cm^{-1}	NCO ^f (Ar-H=1.0)		
100	1.740	0.830	0.238	1.014	2.0964	97.9	0.2347
150	6.827	1.225	0.487	2.351	5.5731	94.3	0.2071
200	10.661	0.835	0.255	1.057	12.7677	87.0	0.2412

Blowing agent = 4.0**Table A12** NCO conversion of RPUR foam catalyzed by DMCHA at different NCO indexes

NCO indexes	Peak Area					NCO conversion (%)	PIR/PUR
	NCO 2277 cm ⁻¹	Ar-H 1595 cm ⁻¹	PIR 1415 cm ⁻¹	PUR 1220 cm ⁻¹	NCO ^f (Ar-H=1.0)		
100	0.839	1.247	0.497	2.449	0.6728	99.3	0.2029
150	0.732	0.666	0.926	1.345	1.0991	98.9	0.6885
200	1.691	1.159	0.988	2.313	1.4590	98.5	0.4272

Table A13 NCO conversion of RPUR foam catalyzed by Cu(OAc)₂(en)₂:Ni(OAc)₂(en)₂ at different NCO indexes

NCO indexes	Peak Area					NCO conversion (%)	PIR/PUR
	NCO 2277 cm ⁻¹	Ar-H 1595 cm ⁻¹	PIR 1415 cm ⁻¹	PUR 1220 cm ⁻¹	NCO ^f (Ar-H=1.0)		
100	1.800	1.676	0.601	2.603	1.0740	98.9	0.2309
150	0.850	1.314	0.489	2.142	0.6469	99.3	0.2283
200	3.194	1.671	0.595	2.626	1.9114	98.0	0.2266

Table A14 NCO conversion of RPUR foam catalyzed by Cu(OAc)₂(en)₂:Zn(OAc)₂(en)₂ at different NCO indexes

NCO indexes	Peak Area					NCO conversion (%)	PIR/PUR
	NCO 2277 cm ⁻¹	Ar-H 1595 cm ⁻¹	PIR 1415 cm ⁻¹	PUR 1220 cm ⁻¹	NCO ^f (Ar-H=1.0)		
100	3.065	3.527	1.235	5.958	0.8690	99.1	0.2073
150	3.424	2.073	0.694	3.085	1.6517	98.3	0.2250
200	1.933	0.881	0.922	1.709	2.1941	97.8	0.5395

Table A15 NCO conversion of RPUR foam catalyzed by
Cu(OAc)₂(trien):Ni(OAc)₂(trien) at different NCO indexes

NCO indexes	Peak Area					NCO conversion (%)	PIR/PUR
	NCO 2277 cm ⁻¹	Ar-H 1595 cm ⁻¹	PIR 1415 cm ⁻¹	PUR 1220 cm ⁻¹	NCO ^f (Ar-H=1.0)		
100	3.363	2.137	0.702	3.167	1.5737	98.4	0.2217
150	2.840	1.533	0.494	2.399	1.8526	98.1	0.2059

Table A16 NCO conversion of RPUR foam catalyzed by
Cu(OAc)₂(trien):Zn(OAc)₂(trien) at different NCO indexes

NCO indexes	Peak Area					NCO conversion (%)	PIR/PUR
	NCO 2277 cm ⁻¹	Ar-H 1595 cm ⁻¹	PIR 1415 cm ⁻¹	PUR 1220 cm ⁻¹	NCO ^f (Ar-H=1.0)		
100	2.619	2.753	0.867	3.717	0.9513	99.0	0.2333
150	2.708	1.920	0.613	2.578	1.4104	98.6	0.2378
200	35.336	2.875	0.984	4.673	12.2908	87.5	0.2106

Table A17 NCO conversion of RPUR foam catalyzed by Cu(Sal)₂(en)₂:Ni(Sal)₂(en)₂
at different NCO indexes

NCO indexes	Peak Area					NCO conversion (%)	PIR/PUR
	NCO 2277 cm ⁻¹	Ar-H 1595 cm ⁻¹	PIR 1415 cm ⁻¹	PUR 1220 cm ⁻¹	NCO ^f (Ar-H=1.0)		
100	21.884	6.696	2.254	11.557	3.2682	96.7	0.1950
150	25.962	3.374	1.121	5.746	7.6947	92.1	0.1951
200	29.660	3.388	1.148	5.660	8.7544	91.1	0.2028

Table A18 NCO conversion of RPUR foam catalyzed by $\text{Cu}(\text{Sal})_2(\text{en})_2:\text{Zn}(\text{Sal})_2(\text{en})_2$ at different NCO indexes

NCO indexes	Peak Area					NCO conversion (%)	PIR/PUR
	NCO 2277 cm^{-1}	Ar-H 1595 cm^{-1}	PIR 1415 cm^{-1}	PUR 1220 cm^{-1}	NCO ^f (Ar-H=1.0)		
100	7.881	3.670	1.217	5.907	2.1474	97.8	0.2060
150	4.661	0.802	0.254	1.095	5.8117	94.1	0.2320
200	4.263	0.756	0.249	0.929	5.6389	94.2	0.2680

Table A19 NCO conversion of RPUR foam catalyzed by $\text{Cu}(\text{Sal})_2(\text{trien}):\text{Ni}(\text{Sal})_2(\text{trien})$ at different NCO indexes

NCO indexes	Peak Area					NCO conversion (%)	PIR/PUR
	NCO 2277 cm^{-1}	Ar-H 1595 cm^{-1}	PIR 1415 cm^{-1}	PUR 1220 cm^{-1}	NCO ^f (Ar-H=1.0)		
100	1.447	1.099	0.330	1.485	1.3167	98.7	0.2222
150	2.582	0.943	0.309	1.326	2.7381	97.2	0.2330
200	6.330	0.982	0.297	1.230	6.4460	93.4	0.2415

Table A20 NCO conversion of RPUR foam catalyzed by $\text{Cu}(\text{Sal})_2(\text{trien}):\text{Zn}(\text{Sal})_2(\text{trien})$ at different NCO indexes

NCO indexes	Peak Area					NCO conversion (%)	PIR/PUR
	NCO 2277 cm^{-1}	Ar-H 1595 cm^{-1}	PIR 1415 cm^{-1}	PUR 1220 cm^{-1}	NCO ^f (Ar-H=1.0)		
100	10.835	3.605	1.233	6.267	3.0055	96.9	0.1967
150	13.207	3.222	1.158	5.769	4.0990	95.8	0.2007
200	6.432	1.440	0.497	2.317	4.4667	95.4	0.2145

Appendix B
Reaction Time and Compression Data

Table B1 Reaction profiles of RPUR foam catalyzed by
Ni(OAc)₂:M₂(OAc)₂:ethylenediamine at index 100

Chemicals	DMCHA	Ni(OAc) ₂ (en) ₂ :Ca(OAc) ₂ (en) ₂	Ni(OAc) ₂ (en) ₂ :Ba(OAc) ₂ (en) ₂	Ni(OAc) ₂ (en) ₂ :Co(OAc) ₂ (en) ₂	Ni(OAc) ₂ (en) ₂ :Cu(OAc) ₂ (en) ₂	Ni(OAc) ₂ (en) ₂ :Zn(OAc) ₂ (en) ₂
Raypol[®] 4221	100	100	100	100	100	100
Catalysts	1.0	1.0	1.0	1.0	1.0	1.0
B8460	2.5	2.5	2.5	2.5	2.5	2.5
H₂O	4.0	4.0	4.0	4.0	4.0	4.0
MR-200	166	166	166	166	166	166
Cream time (s)	0:25	0:27	0:26	0:26	0:26	0:28
Gel time (s)	0:33	1:23	0:57	1:19	0:43	0:59
Tack free time (s)	3:42	11:52	7:05	10:57	2:37	6:23
Volume (V)	7/8V	5/8V	7/8V	5/8V	7/8V	7/8V
Density (Kg/m³)	33.8	46.6	37.8	46.0	43.7	34.4

Table B2 Reaction profiles of RPUR foam catalyzed by $M_1(\text{OAc})_2:M_2(\text{OAc})_2:\text{amine}$ with different $M_1(\text{OAc})_2:\text{amine}$ ratios at index 150

Reaction Time (min)	DMCHA	$\text{Cu}(\text{OAc})_2:\text{Zn}(\text{OAc})_2:(\text{en})_x$			$\text{Cu}(\text{OAc})_2:\text{Zn}(\text{OAc})_2:(\text{trien})_x$		
		0.5:0.5:0.5	0.5:0.5:1	0.5:0.5:2	0.5:0.5:0.5	0.5:0.5:1	0.5:0.5:2
		Cream time	0:25	0:41	0:38	0:31	0:42
Gel time	0:37	1:15	0:58	0:48	1:13	1:18	1:36
Tack free time	3:26	3:30	2:45	2:26	3:17	3:17	4:12
Rise time	2:00	3:56	3:26	3:03	3:54	3:54	4:58
Volume (V)	8/8V	8/8V	8/8V	8/8V	8/8V	8/8V	8/8V
Density (Kg/m^3)	44.6	47.8	49.1	44.6	48.4	48.7	48.7

Table B3 Summary of formulations, reaction times, physical and mechanical properties of PUR foams catalyzed by mixed complexes (metal ratio = 0.7:0.3) and amines as catalysts.

Formulations (pbw)	Catalysts at different NCO index									
	DMCHA (Ref.)		Cu(en) ₂ :Zn(en) ₂		Cu(trien):Zn(trien)		Ni(en) ₂ :Cu(en) ₂		Ni(trien):Cu(trien)	
	100	150	100	150	100	150	100	150	100	150
Raypol [®] 4221	100	100	100	100	100	100	100	100	100	100
Catalysts	1.0	1.0	1.0	1.0	1.0	1.0	1.0	1.0	1.0	1.0
B8460	2.5	2.5	2.5	2.5	2.5	2.5	2.5	2.5	2.5	2.5
H ₂ O	4.0	4.0	4.0	4.0	4.0	4.0	4.0	4.0	4.0	4.0
MR-200	166	250	166	250	166	250	166	250	166	250
Reaction times										
Cream time (min)	0:22	0:25	0:24	0:31	0:37	0:52	0:39	0:54	0:32	0:43
Gel time (min)	0:33	0:37	0:35	0:48	1:01	1:17	1:11	1:34	1:30	1:54
Tack free time (min)	3:00	3:26	1:40	2:26	2:40	3:36	4:42	5:15	6:21	8:23
Rise time (min)	1:10	2:00	2:24	3:03	2:40	3:43	4:13	6:06	5:27	7:30
Volume(V)	8/8V	8/8V	8/8V	8/8V	8/8V	8/8V	7/8V	7/8V	6/8V	7/8V
Density (Kg/m³)	33.8	44.7	35.4	44.6	37.0	44.3	42.0	55.7	42.8	56.3

Table B4 Summary of formulations, reaction times, physical and mechanical properties of PUR foams catalyzed by mixed transition complexes (matal ratio = 0.5:0.5) and amines as catalysts.

Formulations (pbw)	Catalysts at different NCO index									
	DMCHA (Ref.)		Cu(en) ₂ :Zn(en) ₂		Cu(trien):Zn(trien)		Ni(en) ₂ :Cu(en) ₂		Ni(trien):Cu(trien)	
	100	150	100	150	100	150	100	150	100	150
Raypol [®] 4221	100	100	100	100	100	100	100	100	100	100
Catalysts	1.0	1.0	0.5	0.5	0.5	0.5	1.0	1.0	1.0	1.0
B8460	2.5	2.5	2.5	2.5	2.5	2.5	2.5	2.5	2.5	2.5
H ₂ O	4.0	4.0	4.0	4.0	4.0	4.0	4.0	4.0	4.0	4.0
MR-200	166	250	166	250	166	250	166	250	166	250
Reaction times										
Cream time (min)	0:22	0:25	0:31	0:30	0:34	0:37	0:32	0:38	0:32	0:50
Gel time (min)	0:33	0:37	0:56	0:55	1:00	1:23	0:56	1:17	1:28	1:51
Tack free time (min)	3:00	3:26	3:10	3:47	3:45	4:53	3:29	4:43	6:11	8:05
Rise time (min)	1:10	2:00	2:47	4:10	3:32	5:09	2:45	3:25	-	-
Volume(V)	8/8V	8/8V	8/8V	8/8V	7/8V	7/8V	7/8V	7/8V	7/8V	7/8V
Density (Kg/m³)	33.8	44.7	40.3	48.2	40.5	46.9	39.5	52.4	41.9	52.3

Table B5 Summary of formulations, reaction times, physical and mechanical properties of PUR foams catalyzed by mixed transition complexes (matal ratio = 0.3:0.7) and amines as catalysts.

Formulations (pbw)	Catalysts at different NCO index									
	DMCHA (Ref.)		Cu(en) ₂ :Zn(en) ₂		Cu(trien):Zn(trien)		Ni(en) ₂ :Cu(en) ₂		Ni(trien):Cu(trien)	
	100	150	100	150	100	150	100	150	100	150
Raypol [®] 4221	100	100	100	100	100	100	100	100	100	100
Catalysts	1.0	1.0	1.0	1.0	1.0	1.0	1.0	1.0	1.0	1.0
B8460	2.5	2.5	2.5	2.5	2.5	2.5	2.5	2.5	2.5	2.5
H ₂ O	4.0	4.0	4.0	4.0	4.0	4.0	4.0	4.0	4.0	4.0
MR-200	166	250	166	250	166	250	166	250	166	250
Reaction times										
Cream time (min)	0:22	0:25	0:31	0:32	0:39	0:50	0:34	0:44	0:33	0:42
Gel time (min)	0:33	0:37	0:42	1:03	1:09	1:39	0:54	1:06	1:13	1:45
Tack free time (min)	3:00	3:26	3:46	4:45	4:10	5:40	3:14	3:30	6:01	7:53
Rise time (min)	1:10	2:00	3:57	4:34	4:25	5:14	3:30	3:45	5:18	8:28
Volume(V)	8/8V	8/8V	8/8V	8/8V	8/8V	8/8V	7/8V	7/8V	6/8V	7/8V
Density (Kg/m³)	33.8	44.7	43.8	47.4	37.9	46.8	40.0	54.2	40.9	59.7

Table B6 Summary of formulations, reaction times, physical and mechanical properties of PUR foams catalyzed by Cu : Zn : amines as catalysts.

Formulations (pbw)	Catalysts at NCO index = 150						
	DMCHA 150	Cu(trien):Zn(trien) 0.3:0.7:1	Cu(trien):Zn(trien) 0.5:0.5:1	Cu(trien):Zn(trien) 0.7:0.3:1	Cu(en) ₂ :Zn(en) ₂ 0.3:0.7:2	Cu(en) ₂ :Zn(en) ₂ 0.5:0.5:2	Cu(en) ₂ :Zn(en) ₂ 0.7:0.3:2
Raypol [®] 4221	100	100	100	100	100	100	100
Catalysts	1.0	1.0	1.0	1.0	1.0	1.0	1.0
B8460	2.5	2.5	2.5	2.5	2.5	2.5	2.5
H ₂ O	4.0	4.0	4.0	4.0	4.0	4.0	4.0
MR-200	250	250	250	250	250	250	250
Reaction times							
Cream time (min)	0:25	0:50	0:37	0:52	0:54	0:42	0:40
Gel time (min)	0:37	1:39	1:23	1:17	1:36	1:13	1:21
Tack free time (min)	3:26	5:40	4:53	3:36	4:12	3:15	4:21
Rise time (min)	3:28	5:14	5:09	3:43	4:58	3:55	4:40
Volume(V)	8/8V	8/8V	7/8V	8/8V	8/8V	8/8V	8/8V
Density (Kg/m³)	44.7	46.8	46.9	44.3	48.7	48.4	51.7
Mechanical properties							
Compressive strength (kPa)	415.9	264.0	343.7	329.6	203.8	258.5	260.8
Compressive modulus (MPa)	6.68	4.84	4.73	6.40	4.31	6.21	6.03

Table B7 Summary of formulations, reaction times, physical and mechanical properties of PUR foams catalyzed by mixed transition complexes and amines as catalysts

Formulations (pbw)	Catalysts at different NCO index										
	DMCHA (Ref.)		Cu(en) ₂ :Zn(en) ₂		Cu(trien):Zn(trien)		Cu(en) ₂ :Ni(en) ₂		Cu(trien):Ni(trien)		
	100	150	100	150	100	150	100	150	100	150	
Raypol 4221	100	100	100	100	100	100	100	100	100	100	100
Catalysts	1.0	1.0	1.0	1.0	1.0	1.0	1.0	1.0	1.0	1.0	1.0
B8460	2.5	2.5	2.5	2.5	2.5	2.5	2.5	2.5	2.5	2.5	2.5
H ₂ O	3.0	3.0	3.0	3.0	3.0	3.0	3.0	3.0	3.0	3.0	3.0
MR-200	151	227	151	227	151	227	151	227	151	227	227
Reaction times											
Cream time (min)	0:30	0:35	0:28	0:29	0:27	0:31	0:28	0:34	0:32	0:37	0:37
Gel time (min)	0:35	0:39	0:32	0:38	0:46	0:54	0:38	0:47	0:56	1:26	1:26
Tack free time (min)	4:45	5:49	1:30	1:53	2:39	3:02	2:47	3:30	4:47	6:00	6:00
Density (Kg/m³)											
	39.6	50.3	38.9	45.9	43.7	48.1	42.8	50.1	42.8	50.3	50.3
Mechanical properties											
Compressive strength (kPa)	198.2	321.5	255.9	308.8	271.0	391.2	262.7	365.2	-	-	-
Compressive modulus (MPa)	3.54	4.92	5.11	5.82	4.43	5.88	4.96	6.15	-	-	-

Table B8 Summary of formulations, reaction times, physical and mechanical properties of PUR foams catalyzed by mixed metal : amines : salicylic as catalysts

(H₂O=4.0)

Formulation (pbw)	NCO Index 100				NCO Index 150			
	Ni(en) ₂ Sal ₂ :Cu(en) ₂ Sal ₂	Ni(trien)Sal ₂ : Cu(trien)Sal ₂	Cu(en) ₂ Sal ₂ :Zn(en) ₂ Sal ₂	Cu(trien)Sal ₂ :Zn(trien)Sal ₂	Ni(en) ₂ Sal ₂ :Cu(en) ₂ Sal ₂	Ni(trien)Sal ₂ : Cu(trien)Sal ₂	Cu(en) ₂ Sal ₂ :Zn(en) ₂ Sal ₂	Cu(trien)Sal ₂ :Zn(trien)Sal ₂
<i>Reaction times</i>								
Cream time (min)	0:25	0:27	0:30	0:28	0:35	0:34	0:38	0:35
Gel time (min)	0:54	1:12	1:06	1:02	1:44	1:54	1:25	1:20
Tack free time (min)	8:50	7:14	6:48	3:34	6:35	8:12	8:25	5:49
Rise time (min)	6:22	5:56	5:56	3:00	6:35	7:40	7:31	5:15
<i>Density (Kg/m³)</i>	44.1	43.8	40.8	40.3	50.0	51.3	49.8	51.2
<i>Volume(V)</i>	6/8V	6/8V	7/8V	7/8V	7/8V	7/8V	7/8V	7/8V

Appendix C

Mass spectrometry

Isotope Ratio Data

Isotopes are variants of atoms of a particular chemical element, which have differing numbers of neutrons. Atoms of a particular element by definition must contain the same number of protons but may have a distinct number of neutrons which differs from atom to atom, without changing the designation of the atom as a particular element. The abundance of a chemical element measures how relatively common (or rare) the element is, or how much of the element is present in a given environment by comparison to all other elements. The table C1 shows the abundance of elements in Earth's crust.

Table C1 Natural abundances of common elements and their isotopes

Element	Isotopes	Relative atomic mass	Abundance (%)
Ni	⁵⁸ Ni	57.935348(2)	68.077(9)
	⁶⁰ Ni	59.930791(2)	26.223(8)
	⁶¹ Ni	60.931060(2)	1.140(1)
	⁶² Ni	61.928349(2)	3.634(2)
	⁶⁴ Ni	63.927970(2)	0.926(1)
Cu	⁶³ Cu	62.929601(2)	69.17(3)
	⁶⁵ Cu	64.927794(2)	30.83(3)
Zn	⁶⁴ Zn	63.929147(2)	48.6(3)
	⁶⁶ Zn	65.926037(2)	27.9(2)
	⁶⁷ Zn	66.927131(2)	4.1(1)
	⁶⁸ Zn	67.924848(2)	18.8(4)
	⁷⁰ Zn	69.925325(4)	0.6(1)

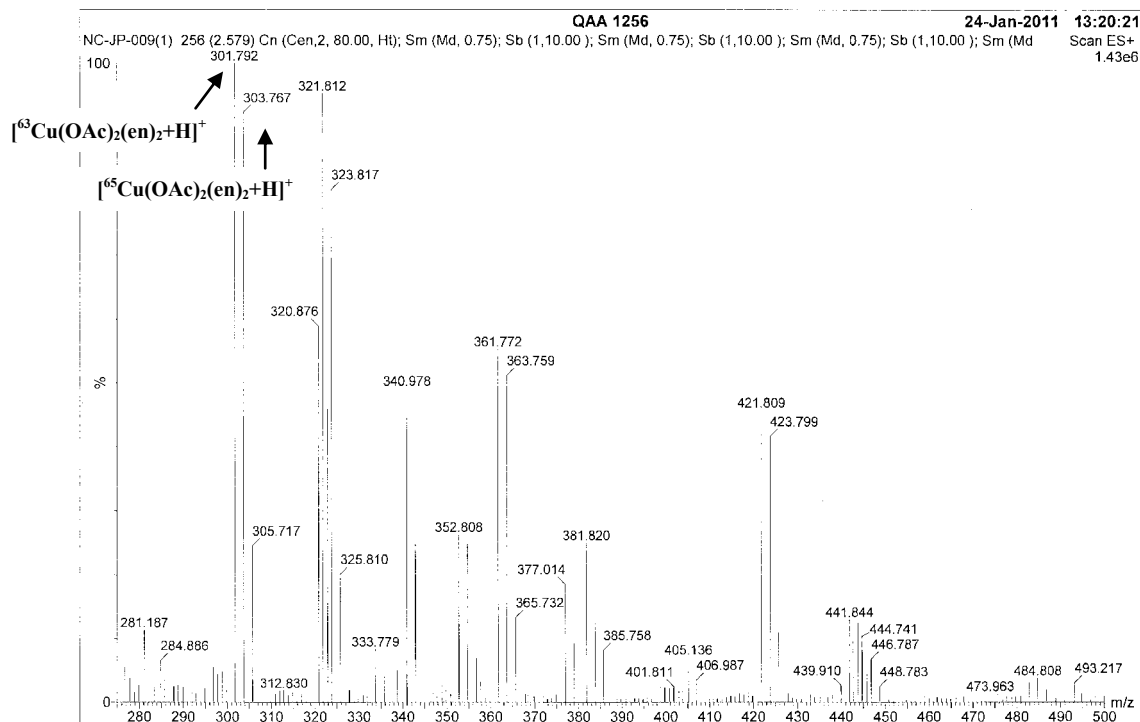


Figure C1 positive ESI mass spectra of $\text{Cu}(\text{OAc})_2(\text{en})_2$

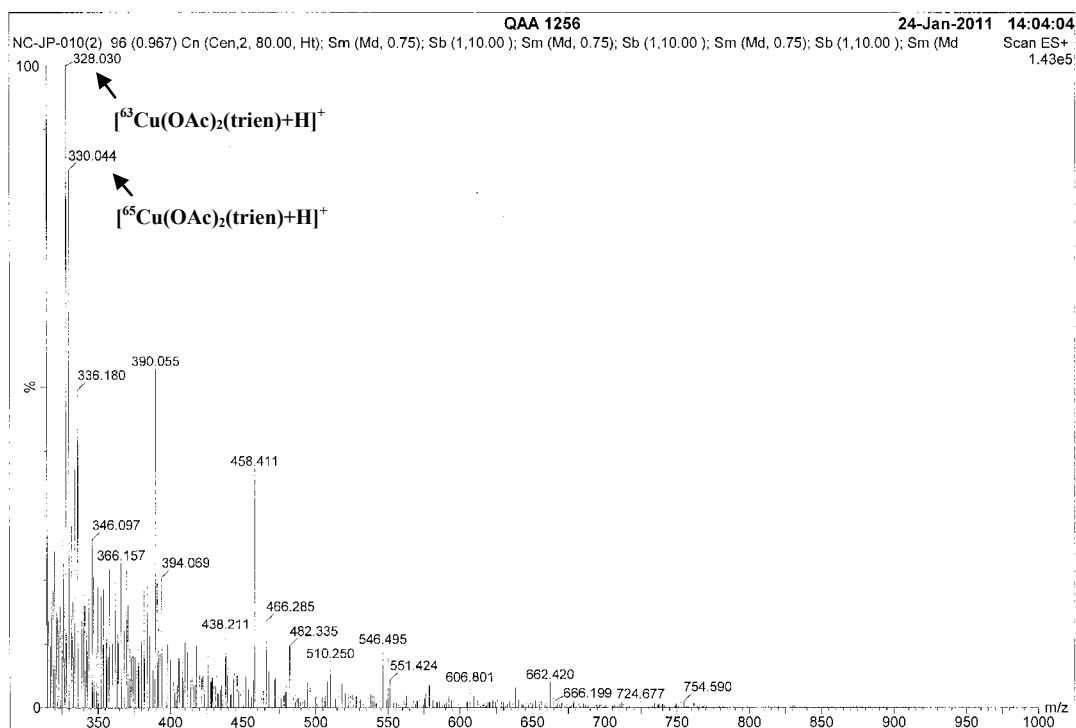


Figure C2 positive ESI mass spectra of $\text{Cu}(\text{OAc})_2(\text{trien})$

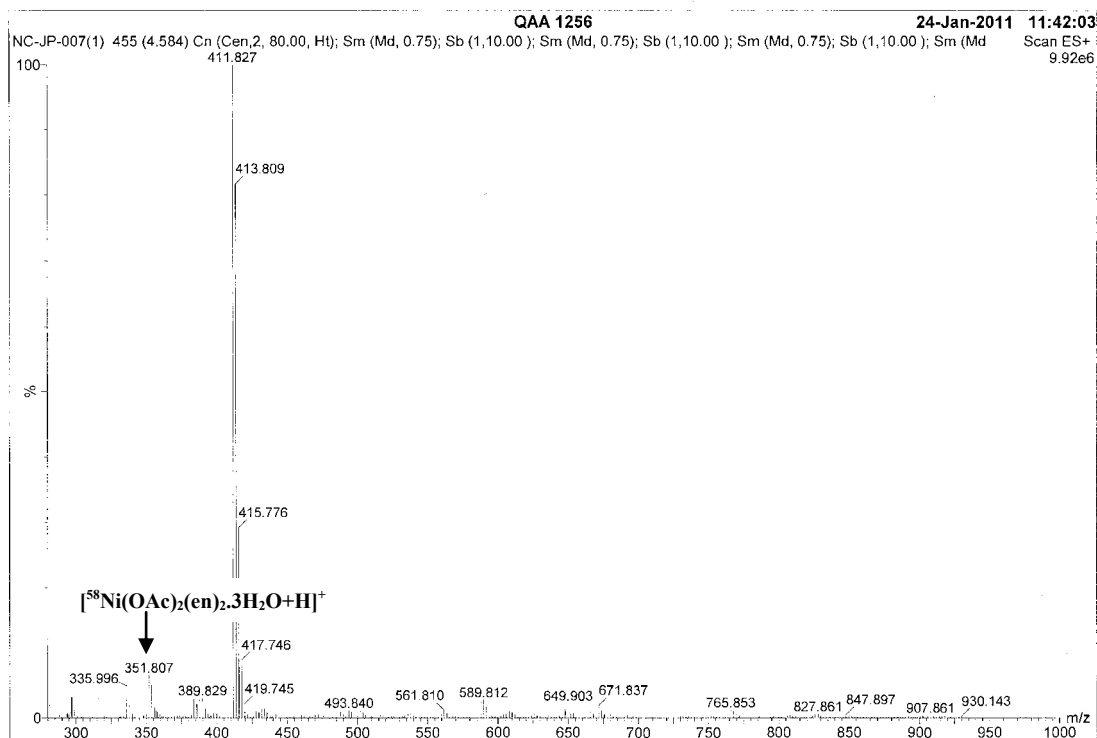


Figure C3 positive ESI mass spectra of $\text{Ni}(\text{OAc})_2(\text{en})_2$

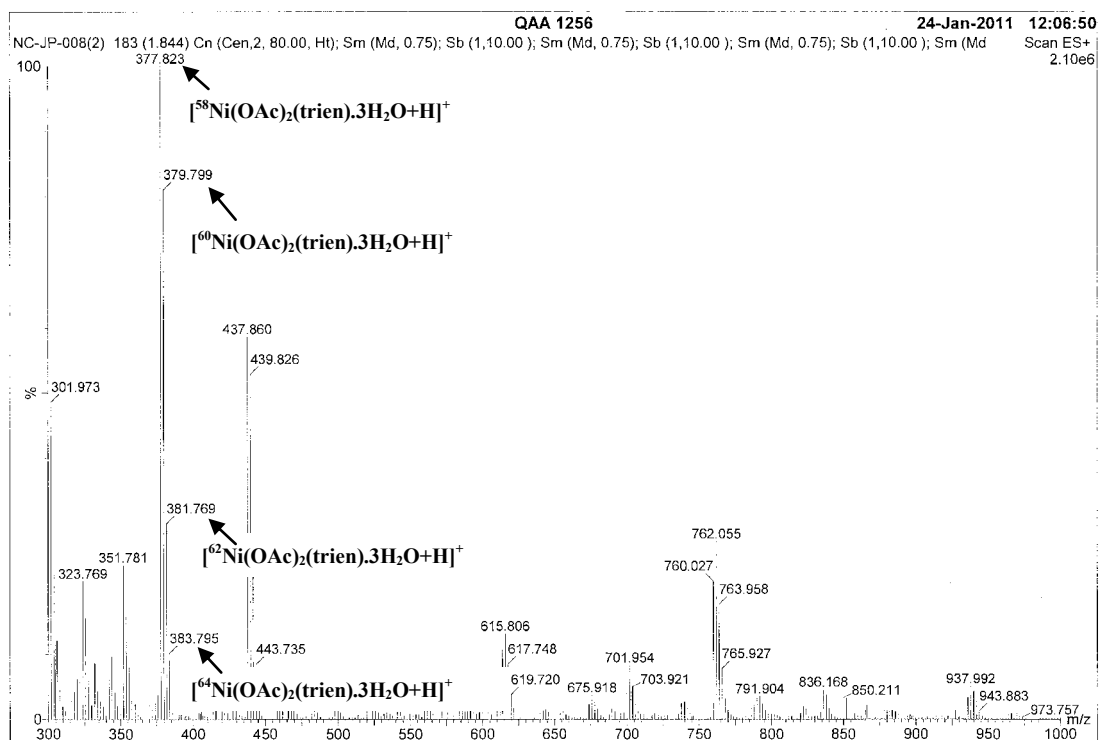


Figure C4 positive ESI mass spectra of $\text{Ni}(\text{OAc})_2(\text{trien})$

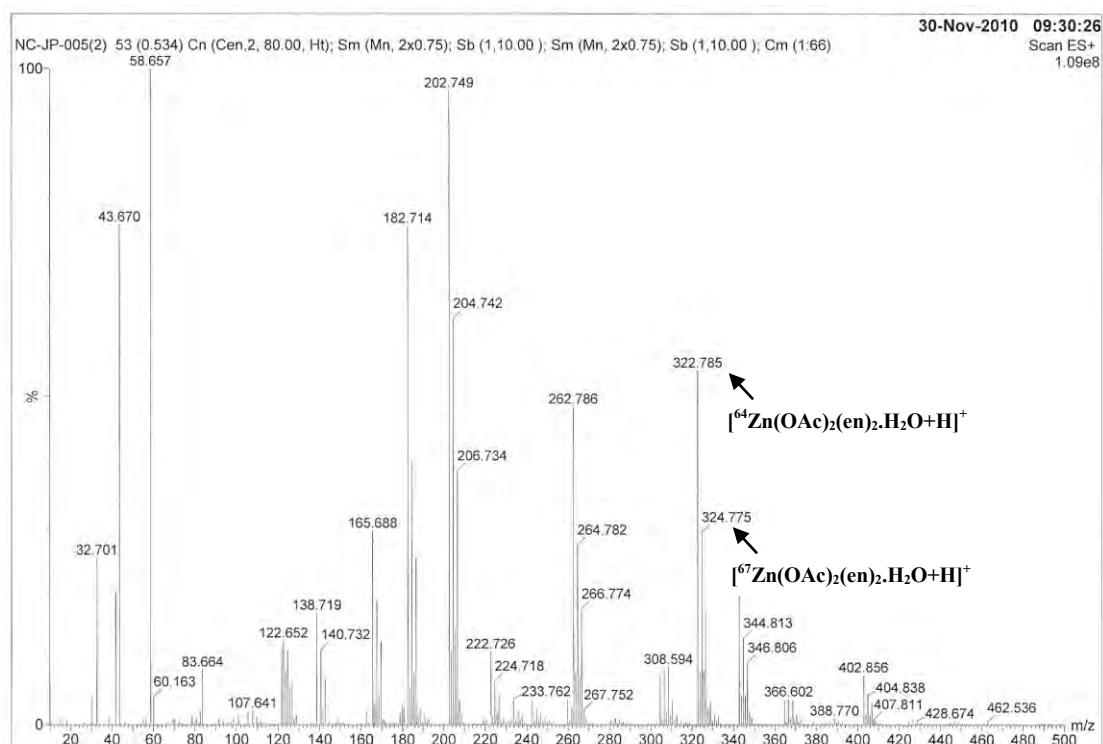


Figure C5 positive ESI mass spectra of Zn(OAc)₂(en)₂

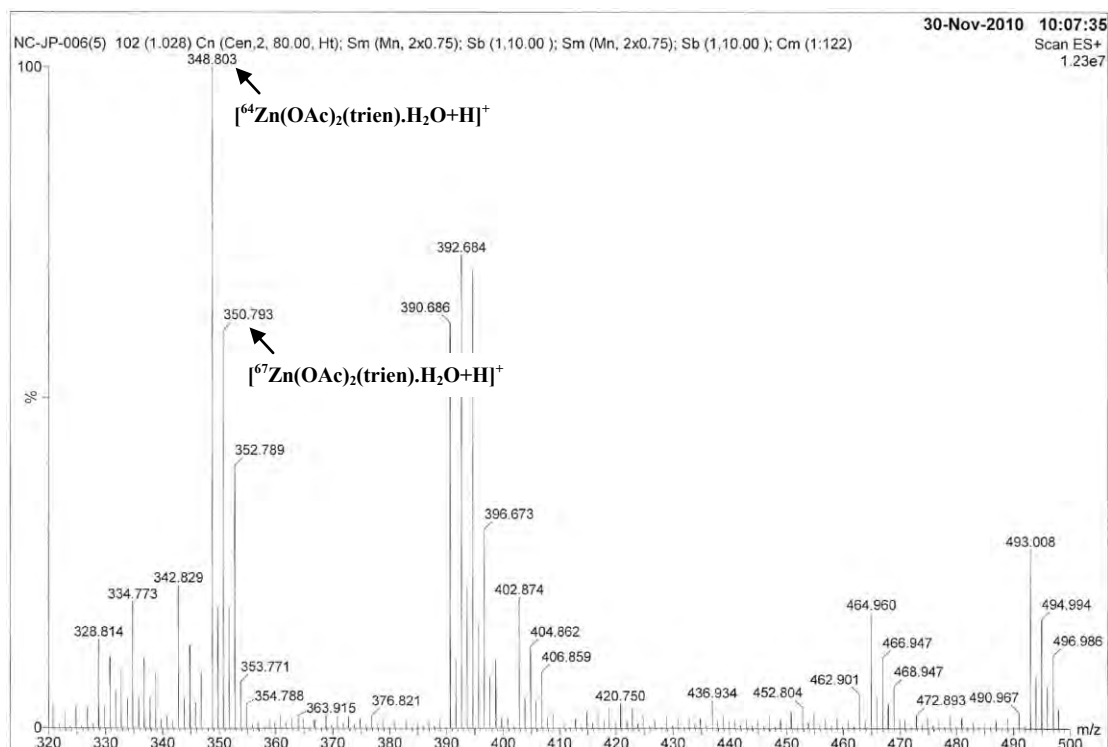


Figure C6 positive ESI mass spectra of Zn(OAc)₂(trien)

Table C2 Positive ESI mass spectra of M(OAc)₂(en)₂ and M(OAc)₂(trien) complexes

Molecular ion	Calculated	Found
* [⁶³ Cu(OAc) ₂ (en) ₂] ⁺	301.214	301.792
[⁶⁵ Cu(OAc) ₂ (en) ₂] ⁺	303.199	303.767
* [⁶³ Cu(OAc) ₂ (en) ₂ .2H ₂ O+Na] ⁺	360.822	-
* [⁶³ Cu(OAc) ₂ (en) ₃] ⁺	361.890	361.801
[⁶⁵ Cu(OAc) ₂ (en) ₃] ⁺	363.297	363.789
* [⁶³ Cu(OAc) ₂ (en) ₃ .2H ₂ O+Na] ⁺	420.920	421.838
* [⁶³ Cu(OAc) ₂ (trien)+H] ⁺	328.259	328.030
[⁶⁵ Cu(OAc) ₂ (trien)+H] ⁺	330.257	330.044
* [⁵⁸ Ni(OAc) ₂ (en) ₂ +H] ⁺	297.227	298.734
* [⁵⁸ Ni(OAc) ₂ (en) ₂ .3H ₂ O+H] ⁺	351.273	351.807
* [⁵⁸ Ni(OAc) ₂ (trien).3H ₂ O+H] ⁺	377.311	377.823
[⁶⁰ Ni(OAc) ₂ (trien).3H ₂ O+H] ⁺	379.306	379.799
[⁶² Ni(OAc) ₂ (trien).3H ₂ O+H] ⁺	381.304	381.769
[⁶⁴ Ni(OAc) ₂ (trien).3H ₂ O+H] ⁺	383.303	383.795
* [⁶⁴ Zn(OAc) ₂ (en) ₂] ⁺	302.214	-
* [⁶⁴ Zn(OAc) ₂ (en) ₂ +H] ⁺	303.222	303.800
* [⁶⁴ Zn(OAc) ₂ (en) ₂ .2H ₂ O+Na] ⁺	362.310	363.789
* [⁶⁴ Zn(OAc) ₂ (en) ₂ .H ₂ O+H] ⁺	321.237	322.785
[⁶⁷ Zn(OAc) ₂ (en) ₂ .H ₂ O+H] ⁺	324.235	324.775
* [⁶⁴ Zn(OAc) ₂ (en) ₃ +H] ⁺	363.315	363.789
* [⁶⁴ Zn(OAc) ₂ (en) ₃ .2H ₂ O+Na] ⁺	422.408	423.832
* [⁶⁴ Zn(OAc) ₂ (trien).H ₂ O+H] ⁺	347.274	348.803
[⁶⁷ Zn(OAc) ₂ (trien).H ₂ O+H] ⁺	350.272	350.793

*Most abundant isotope

VITAE

Name : Miss Jariyaporn Pomsook
Date of birth : February 10, 1987
Nationality : Thai
Address : 102/1 M.3 Pongsawai, Muang, Ratchaburi, 70000.
University Education : Bachelor's Degree from Department of Chemistry,
Faculty of Science, Srinakarinwirot University, 2006-
2009.
Conference attendance : Poster presentation "Rigid Polyurethane Foam by using
Mixed Metal Complexes and Ethylenediamine as
Catalysts" at The 20th Thaksin University Annual
Conference: Thai Society Development with Creative
Research in J.B. Hotel Hat-Yai, Songkhla 90110,
Thailand.